Atomistic Simulations of PuO_2 Ageing and Fuel Residues

By Nathan Palmer

Monday, 14th November 2016

DISTINCTIVE

UNIVERSITY OF BIRMINGHAM

Contents

- The Potential Model
- Potential Evaluation
- Defect Calculations
- Helium in PuO_2
- Defect Migration
- MOX Fuel Modelling
- Surface Simulations
- Current and Future Work

The Potential Model

The Born model ⇒ suitable for ionic solids of point charges

$$V(r_{ij}) = \underbrace{\frac{q_i q_j e^2}{4\pi\varepsilon_0 r_{ij}}}_{\text{Electrostatic interaction}} + \underbrace{\phi(r_{ij})}_{\text{Short-range interaction}}$$

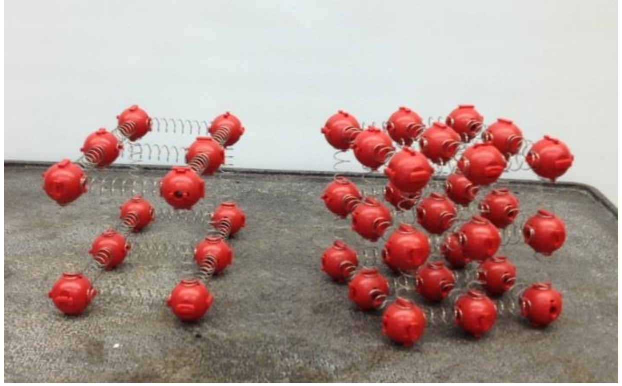

Buckingham potential ⇒ short -range potential

$$\phi(r_{ij})_{Buck} = \underbrace{A_{ij} \exp\left(\frac{-r_{ij}}{\rho_{ij}}\right)}_{\text{Electron repulsion}} - \underbrace{\frac{C_{ij}}{r_{ij}^6}}_{\text{Transient dipole attraction}}$$

The core-shell model ⇒ model polarisation of ions

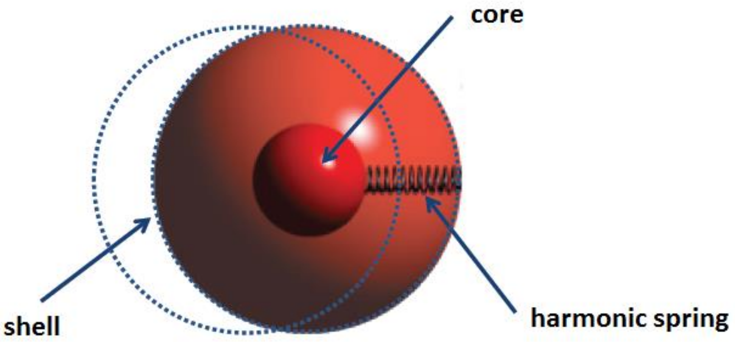

$$V_{cs}(r_{cs}) = \underbrace{\frac{1}{2}k_2 r_{cs}^2}_{\text{Harmonic interaction}} + \underbrace{\frac{1}{24}k_4 r_{cs}^4}_{\text{Anharmonic interaction}}$$

$$\alpha = \underbrace{\frac{q_s^2}{k_{cs}}}_{\text{Atomic polarizability}}$$

Picture credit: Dr Mark S. D. Read

Pu-O Interatomic Potential Used

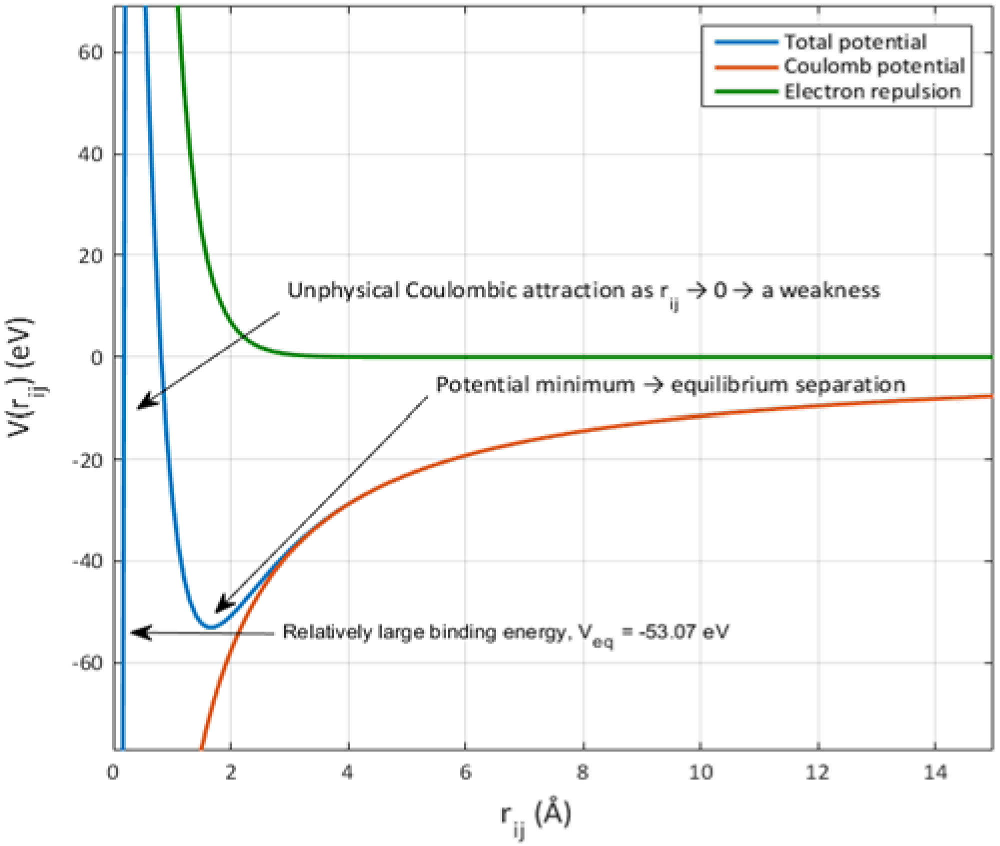

Potentials Ref: Read MSD, Walker SR, Jackson RA. *Derivation of enhanced potentials for plutonium dioxide and the calculation of lattice and intrinsic defect properties*. Journal of Nuclear Materials. 2014;**448(1–3)**:20-5.

Potential Evaluation for PuO_2

Property	Calculated	Experimental	Δ %
a_0 (Å)	5.39812	5.39819[a]	-0.001
Pu^{4+} -Pu^{4+} (Å)	3.8171	3.8171[a]	0.000
Pu^{4+}-O^{2-} (Å)	2.3375	2.3375[a]	0.000
O^{2} -O^{2-} (Å)	2.6991	2.6991[a]	0.000
C_{11} (GPa)	408.6	430.6[b]	-5.1
C_{12} (GPa)	130.2	128.4[b]	1.4
C_{44} (GPa)	67.3	67.3[b]	0.0
B (GPa)	223.0	-	-
Y (GPa)	345.6	-	-
K (Gpa)	84.8	-	-
ε_0	15.92	19.27[b]	-17.38
ε_∞	3.2	3.0[c]	6.7

Ref a- Belin et al. J Appl Crystallogr. 2004; **37(6)**:1034–7.
Ref b- Meis et al. Materials Science and Engineering: B. 1998; **57(1)**:52-61.
Ref c- R.G. Haire, Advance in Plutonium Chemistry 1967–2000, American Nuclear Society, 2000.

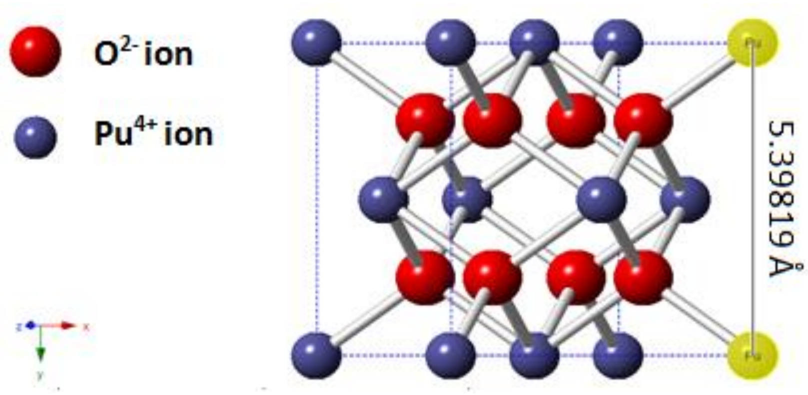

Unit cell of fluorite PuO_2

- As shown, the potentials used in particular provide excellent agreement with crystallographic data and elastic constants.

Defect Energy Calculations

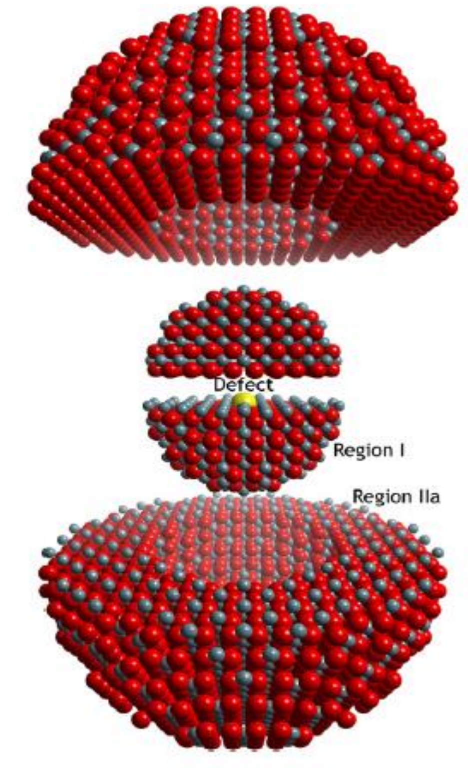

Two region strategy for calculation of defect energy.

Ref: Read MSD, Jackson RA. Journal of Nuclear Materials. 2010;**406(3)**:293-303.

The Mott-Littleton Method

- For a charged point defect, it is positioned in the centre of two spherical regions of the crystal: region I and II (inner and outer regions respectively).
- Region II consists of region IIa and IIb, where region IIa is a spherical shell between region I and region IIb, which in theory extends to infinity.
- Ions in region I are explicitly relaxed to equilibrium, whilst in region Iia, ions respond harmonically to the defect itself.
- For ions in region IIb only the Coulomb interaction with the defect is calculated.
- To ensure energy convergence, in the simulations presented, region radii, r_{I} and $\mathrm{r}_{\mathrm{IIa}}$ are 14 Å and 28 Å, containing ~ 1600 and ~ 12,000 ions respectively.

Ref: Mott NF, Littleton MJ. Trans Faraday Soc. 1938:**485**.

Oxygen Interstitial

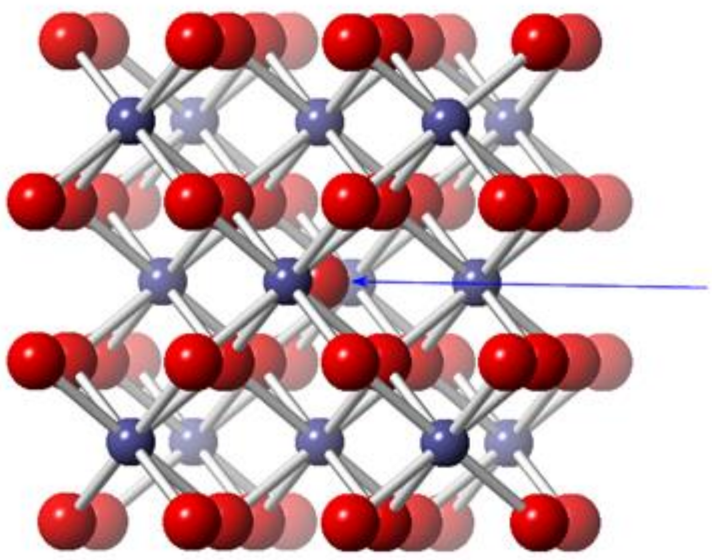
Unrelaxed Structure

Oxygen interstitial

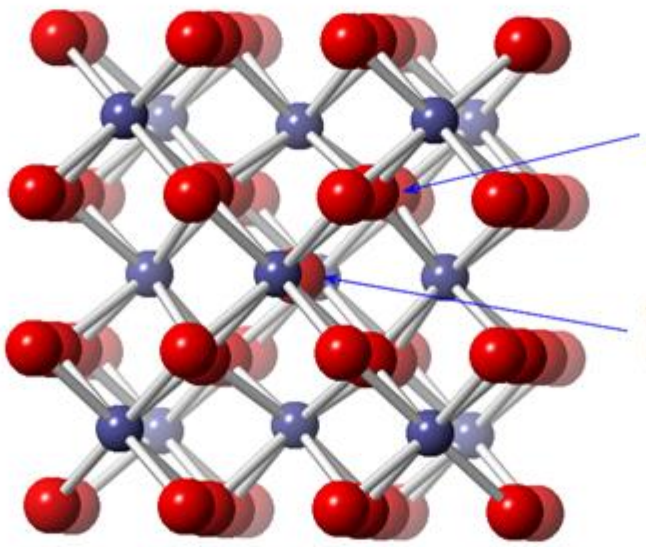
Relaxed Structure

Lattice distortion

Oxygen interstitial

Defect visualisation code credit: Dr Mark S. D. Read

Intrinsic Defect Energies

Bound defect	Formation reaction	E^{form}_{defect} (eV)	E^{bind}_{defect} (eV)	Reported E^{form}_{defect} (eV)
Schottky defect	$\mathrm{Pu}^{\times}_{\mathrm{Pu}} + 2\mathrm{O}^{\times}_{\mathrm{O}} \rightleftharpoons \left\{\mathrm{V}^{////}_{\mathrm{Pu}} + 2\mathrm{V}^{\bullet\bullet}_{\mathrm{O}}\right\}^{\times} + \mathrm{PuO}_{2\,(\mathrm{surface})}$	5.79-6.33	-4.84 to -4.32	-
Oxygen Frenkel pair	$\mathrm{O}^{\times}_{\mathrm{O}} \rightleftharpoons \left\{\mathrm{V}^{\bullet\bullet}_{\mathrm{O}} + \mathrm{O}^{//}_{\mathrm{i}}\right\}^{\times}$	4.08-4.32	-1.25 to -1.00	2.72-2.92[a], 3.48[b]
Plutonium Frenkel pair	$\mathrm{Pu}^{\times}_{\mathrm{Pu}} \rightleftharpoons \left\{\mathrm{V}^{////}_{\mathrm{Pu}} + \mathrm{Pu}^{\bullet\bullet\bullet\bullet}_{\mathrm{i}}\right\}^{\times}$	15.74	-4.32	15.19[b]

Ref a- Murch G, Catlow C. J Chem Soc, Faraday Trans II. 1987; **83(7)**:1157-69.
Ref b- Lu Y, Yang Y, Zhang P. Journal of Alloys and Compounds. 2015; **649**:544-52.

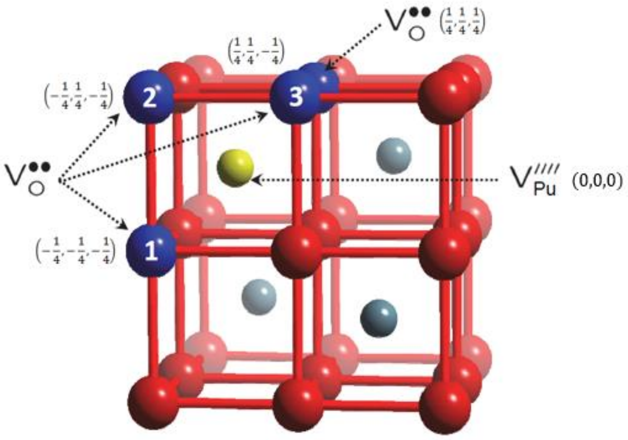

3 Schottky defect configurations

Ref: Read MSD, Jackson RA. Journal of Nuclear Materials. 2010;**406(3)**:293-303.

Point defect	E^{form}_{defect} (eV)
Oxygen vacancy	17.08
Plutonium vacancy	80.04
Oxygen interstitial at octahedral site	-11.76
Plutonium interstitial at octahedral site	-59.98

He-Pu Interatomic Potential Used

Lennard-Jones potential

$$V(r_{ij}) = \underbrace{\frac{A_{ij}}{r_{ij}^{12}}}_{\text{Electron repulsion}} - \overbrace{\frac{B_{ij}}{r_{ij}^{6}}}^{\text{Transient dipole attraction}}$$

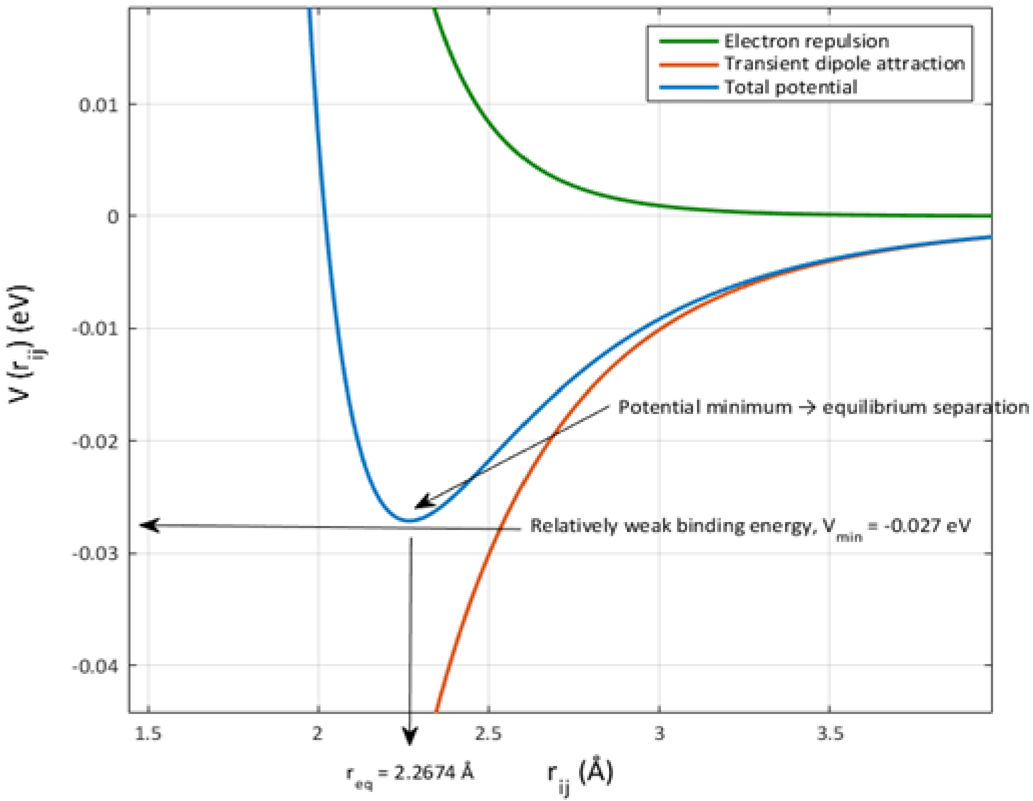

Potentials Ref: Grimes, R.W., R.H. Miller, and C.R.A. Catlow. Journal of Nuclear Materials, 1990. **172(1)**: p. 123-125.

Helium Accommodation in Bulk PuO_2: Octahedral Sites

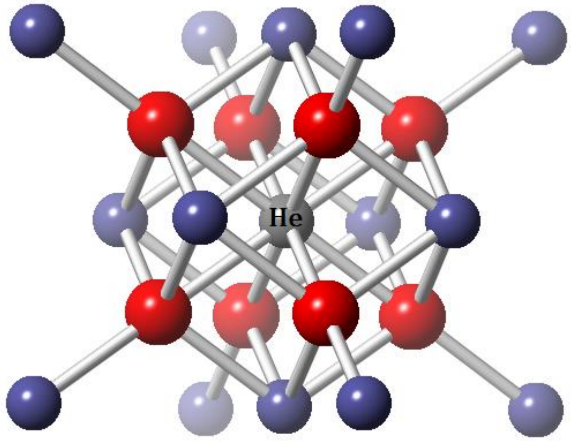

Number of helium in octahedral site	E_{He}^{incorp} per helium atom (eV)	E_{He}^{bind} per helium atom (eV)
1	**0.65**	**-**
2	**1.42**	**0.77**
3	**2.08**	**1.43**

- Small endothermic (positive) defect incorporation energy of 0.65 eV implies helium accommodation at octahedral sites requires small energy input so possible.

- Helium atom clustering not energetically favoured in octahedral sites due to positive binding energies.

Helium Migration and Accommodation in Bulk PuO_2 : Schottky Defect

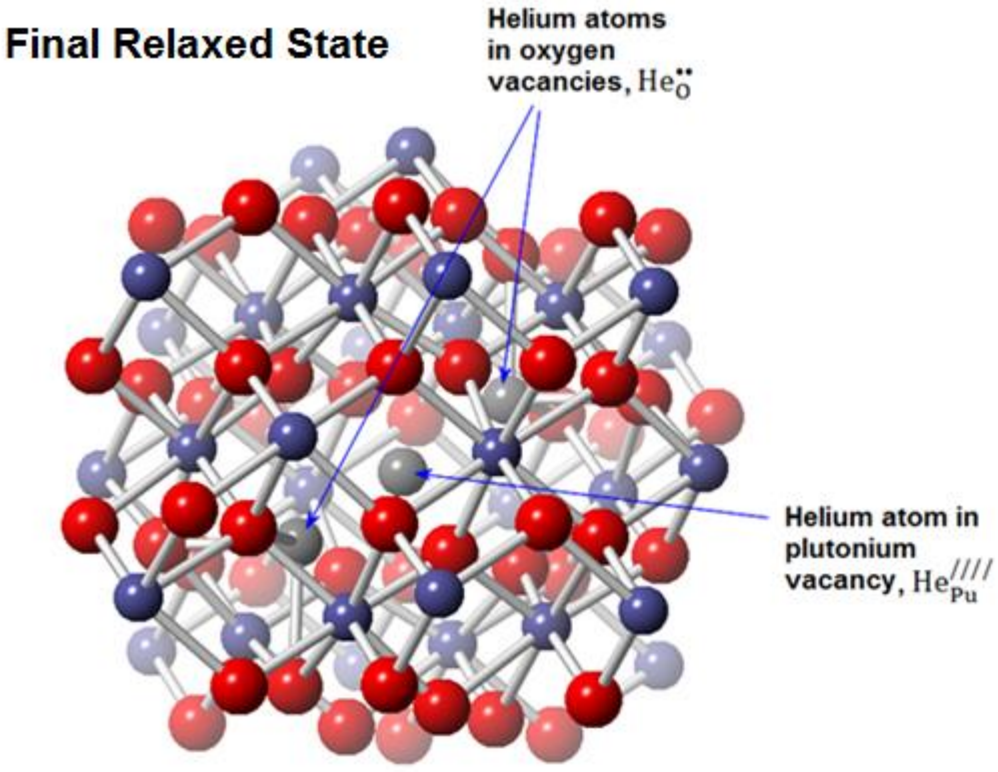

Model the migration paths of three helium atoms initially all packed in an octahedral site to nearby oxygen and plutonium vacancies.

- Two helium atoms migrate to the nearest oxygen and plutonium vacancy and remain there.
- The third helium atom migrates to an oxygen vacancy further away in Schottky defect.
- From the octahedral site, this helium atom moves half-way between two oxygen ions, with a corresponding transition state energy of $\mathbf{E}_{\mathbf{He}}^{\mathbf{act,\,TS}}$ = **1.74 eV.**
- Finally, this helium atom occupies the oxygen vacancy.
- For overall process for all helium atoms, $\Delta\mathbf{H}_{\mathbf{He}}^{\mathbf{mig}}$ = **-1.67 eV** per helium atom.
- Exothermic, hence, an energetically favourable process, provided activation barriers are overcome.

Defect visualisation code credit: Dr Mark S. D. Read

Oxygen Migration in Bulk PuO_2 : Oxygen Frenkel Pair

Oxygen Interstitial Unrelaxed Pathway

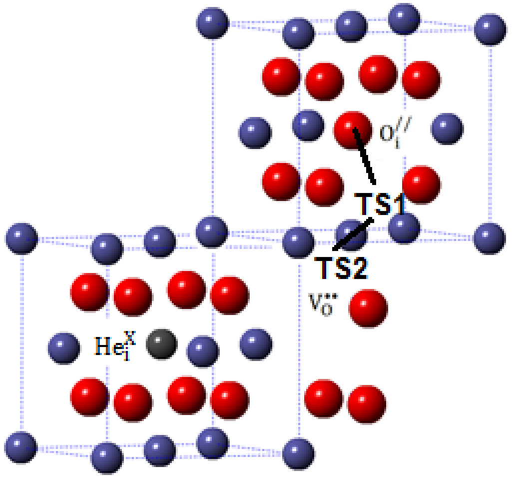

Final Unrelaxed State

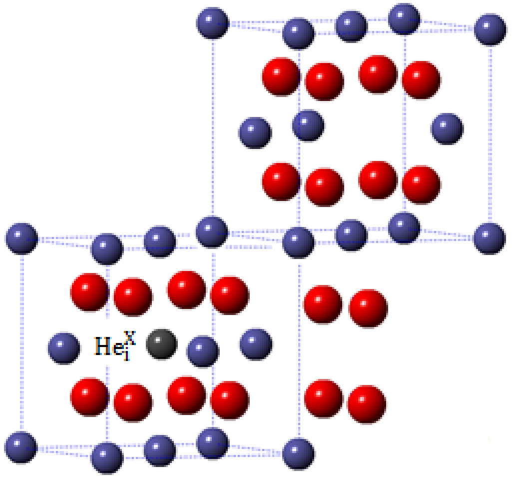

Model the migration path of an oxygen interstitial in a Frenkel pair, initially in an octahedral site to the oxygen vacancy in the presence of a (fixed) helium interstitial.

- Oxygen ion migrates to position half-way between to oxygen ions, corresponding to a transition state energy of $E_O^{act, TS1}$ **= 3.60 eV**.
- Then it moves to a position very close to a corner plutonium ion, corresponding to a transition state energy of $E_O^{act, TS2}$ **= 2.54 eV.**
- Finally, this oxygen ion occupies the oxygen vacancy (recombination).
- For overall path, enthalpy change is ΔH_o^{mig} **= -3.37 eV.**
- Exothermic, hence an energetically favourable process, provided activation barriers are overcome.
- Regarding the helium atom, there is no Coulomb attraction to the vacancy and the enthalpy change to occupy it is slightly unfavourable with ΔH_o^{mig} **= 0.2 eV**, providing the oxygen interstitial is fixed.

MOX Fuel Modelling

Mixed Oxide (MOX) fuel is a solid solution of UO_2 and PuO_2. Uranium and plutonium in used nuclear fuel can be re-used in nuclear reactors by production of MOX fuel. It is a key option for using the plutonium stockpile. To model this, two methods are used:

Mean Field Approach

- Involves assigning to each cation site a mixed occupancy factor, $0 < x \leq 1$ for U and Pu ions such that $\mathrm{MOX} = \mathrm{Pu}_x\mathrm{U}_{1-x}\mathrm{O}_2$.
- Hence, the concentration of Pu can hence be varied and MOX properties calculated.
- This is feasible for MOX as the UO_2 and PuO_2 potentials are very similar physical and chemical properties.

Supercell Method

- Involves setting up a supercell of UO_2 and substitutional doping of Pu ions at U ion sites (done homogeneously here before energy optimisation).
- Hence, the concentration of Pu can be varied and MOX properties calculated.

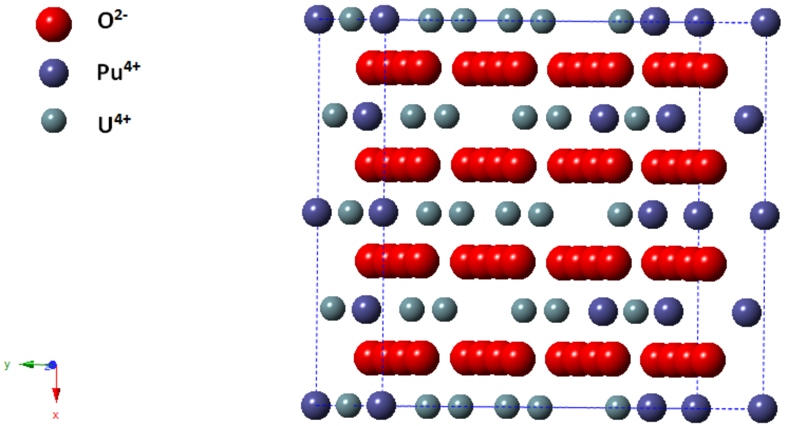

222 supercell of $\mathbf{Pu_{0.25}U_{0.75}O_2}$

MOX Fuel Bulk Properties: Lattice Parameter, a_0

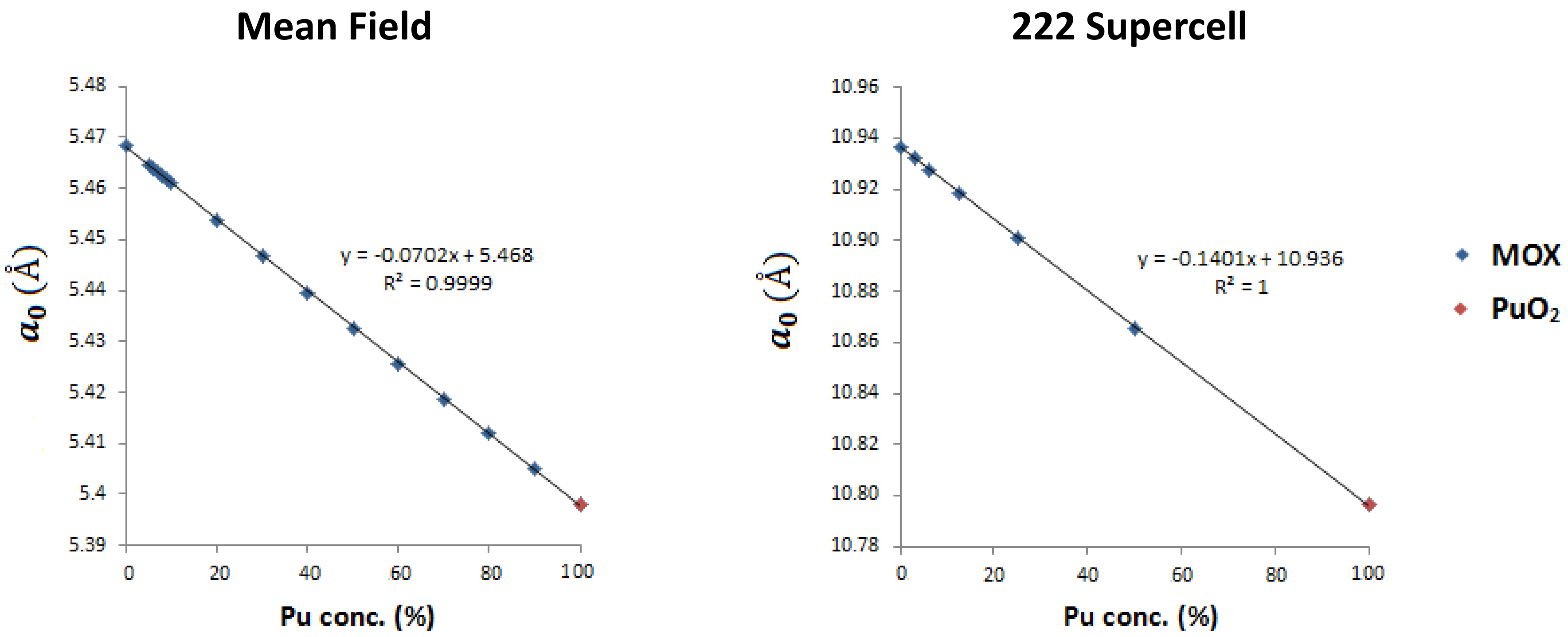
Mean Field

222 Supercell

- The linear trends indicate that Vegard's Law is being followed.
- Both methods agree very well.

MOX Fuel Bulk Properties: Bulk Modulus, *B*

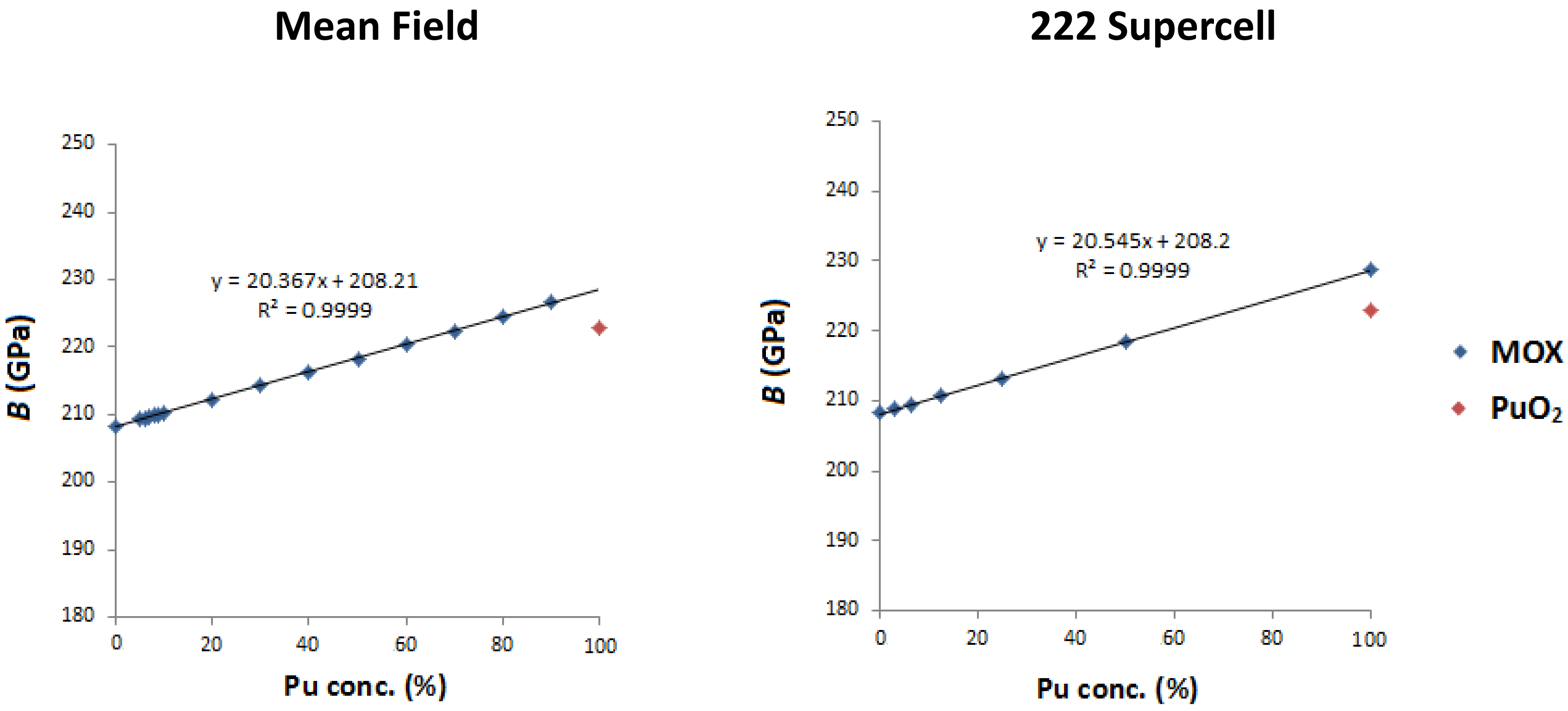
Mean Field

222 Supercell

- The linear trends indicate that Vegard’s Law is being followed.
- Both methods agree very well.

Surface Simulations of Pure PuO$_2$

Surface	E^{Unrel}_{Surf} (Jm^{-2})	$E^{Relaxed}_{Surf}$ (Jm^{-2})	ΔE_{Surf} (Jm^{-2})
(100)	2.42	-	-
(110)	3.32	2.07	-1.24
(111)	1.65	1.32	-0.32
(210)	11.64	3.06	-8.58
(211)	8.21	-	-
(221)	2.41	1.63	-0.78
(310)	18.28	3.09	-15.19
(311)	8.95	2.62	-6.32
(331)	2.61	1.74	-0.87

Surface	% relaxation
(110)	37.50
(111)	19.70
(210)	73.68
(221)	32.45
(310)	83.09
(311)	70.68
(331)	33.36

- Greater relaxation for initially less stable surfaces.
- Energetically preferred surfaces are the (111), (221) and (331) surfaces.
- Least favourable for polar (100) surface (didn't optimise), (210) and (310) surfaces.
- Hence, the simulations indicate that the {nn1} set of surfaces are most energetically stable, with generally the {n10} set least stable.
- Both sets of surfaces become less stable for higher n.

Unrelaxed **Relaxed**

(111) surface

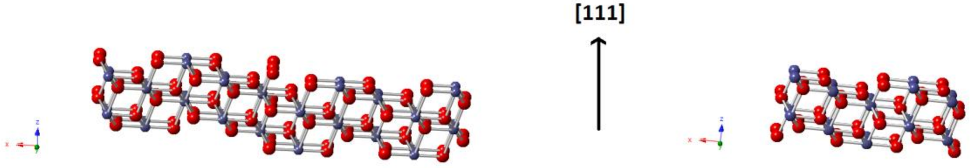

$E_{Surf}^{Relaxed}$ = **1.32 Jm^{-2}**

(221) surface

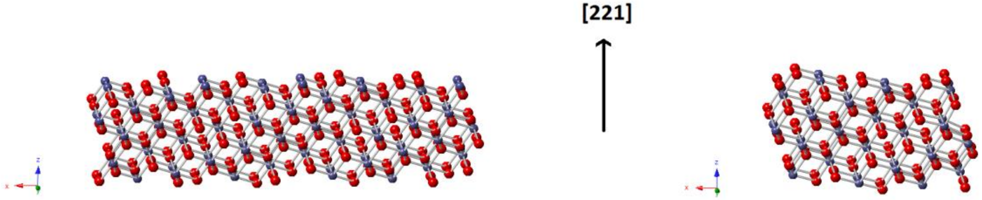

$E_{Surf}^{Relaxed}$ = **1.63 Jm^{-2}**

(331) surface

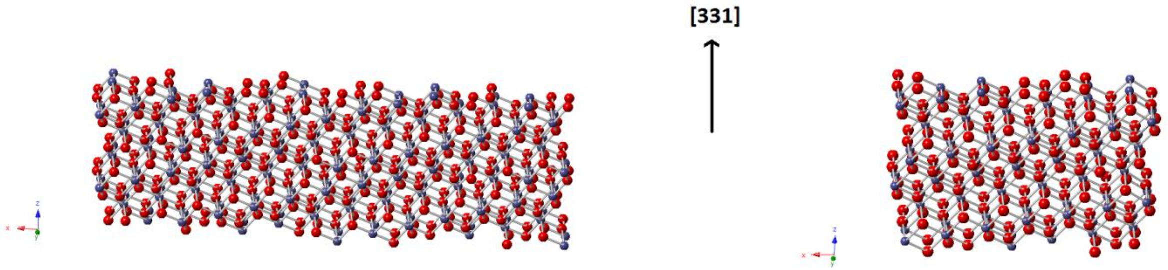

$E_{Surf}^{Relaxed}$ = **1.74 Jm^{-2}**

Current Work

- Modelling helium and oxygen defects and their migration in bulk PuO_2.
- Simulations of pure PuO_2 surfaces.

Future Work

- Modelling of extended defects e.g. grain boundaries and surfaces in more detail.
- Atomistic simulations of $\alpha\text{-}\mathrm{Pu_2O_3}$ similar as for PuO_2.
- Applying molecular dynamics simulations to model diffusion and migration of species.

Acknowledgements

Dr Mark S. D. Read- University of Birmingham

Professor Steve Parker- University of Bath

Robin Orr (NNL) and Helen Steele (SL)

The BlueBEAR High Performance Computing Service

NNL, SL and the EPSRC

EPSRC
Engineering and Physical Sciences
Research Council

Thank you
Any Questions?

DISTINCTIVE

Ceramic and glass-ceramic wasteforms for actinide disposition

Shi-Kuan Sun, Claire Corkhill, Martin Stennett and Neil Hyatt

Immobilisation Science Laboratory,
Department of Materials Science and Engineering,
The University of Sheffield

DISTINCTIVE – Theme 2 meetings
Monday 14th Nov.
The Rheged Centre, Penrith, UK

Zirconolite glass-ceramic

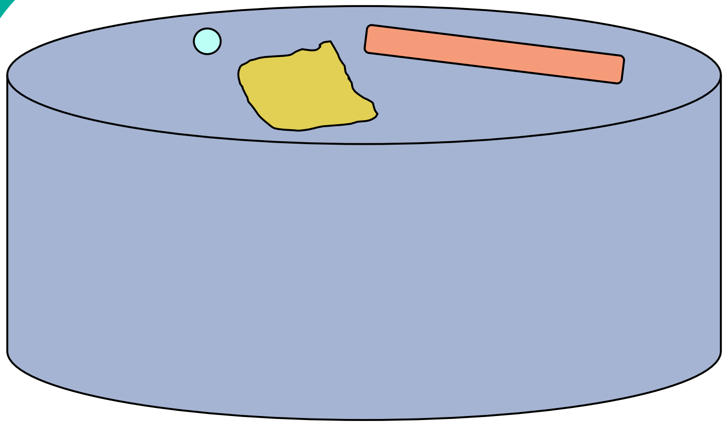

Glass-ceramics

Dual barrier system:

Crystalline phase: Actinides

Glass phase: The remaining wastes

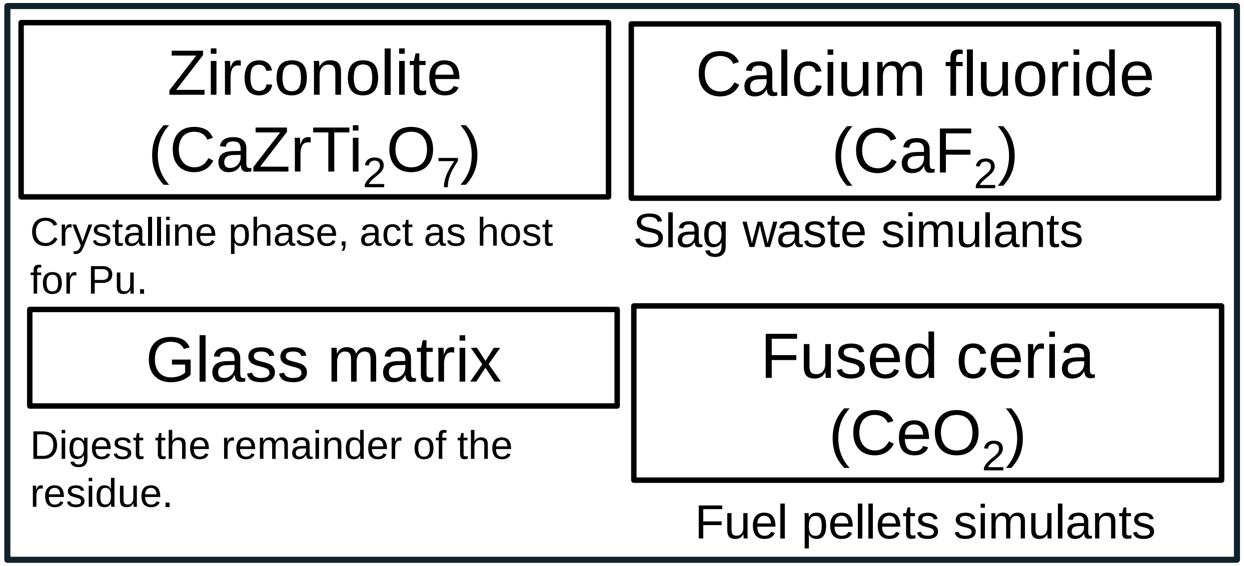

Zirconolite ($CaZrTi_2O_7$)

Crystalline phase, act as host for Pu.

Calcium fluoride (CaF_2)

Slag waste simulants

Glass matrix

Digest the remainder of the residue.

Fused ceria (CeO_2)

Fuel pellets simulants

Experimental - Zirconolite glass-ceramic

GLASS CERAMIC	
SiO_2	28.3
Al_2O_3	25.6
B_2O_3	5.6
Na_2O	6.4
CaO	6.9
CaF_2	5.3
TiO_2	10.5
ZrO_2	11.5

19 wt% fluorspar
1 wt% CeO_2 powder
80 wt% glass ceramic prec.

Mixing

2 x 575 g attrition milled
20 minutes @ 250 rpm
c. 15 kg 9.5 mm balls
Product granulated

Size reduction

1150 °C, 100 MPa, 2 hours
Granules fed into double dumbbell can

HIP

Finished by NNL

Finished HIP cans by NNL

To study the radiation resistance properties:

Ion implantation induced damages

2 MeV Au-ion 3 × 10^{15} labelled as **A**
2 MeV Au-ion 5 × 10^{15} labelled as **B**
5 MeV Au-ion 3 × 10^{15} **C**
5 MeV Au-ion 5 × 10^{15} **D**

Uniform irradiation

2 MeV Au-ion 5 × 10^{15}
2 MeV Au-ion 1 × 10^{16}

Gaussian irradiation

HIP: Hot isostatic pressing

Pristine phase

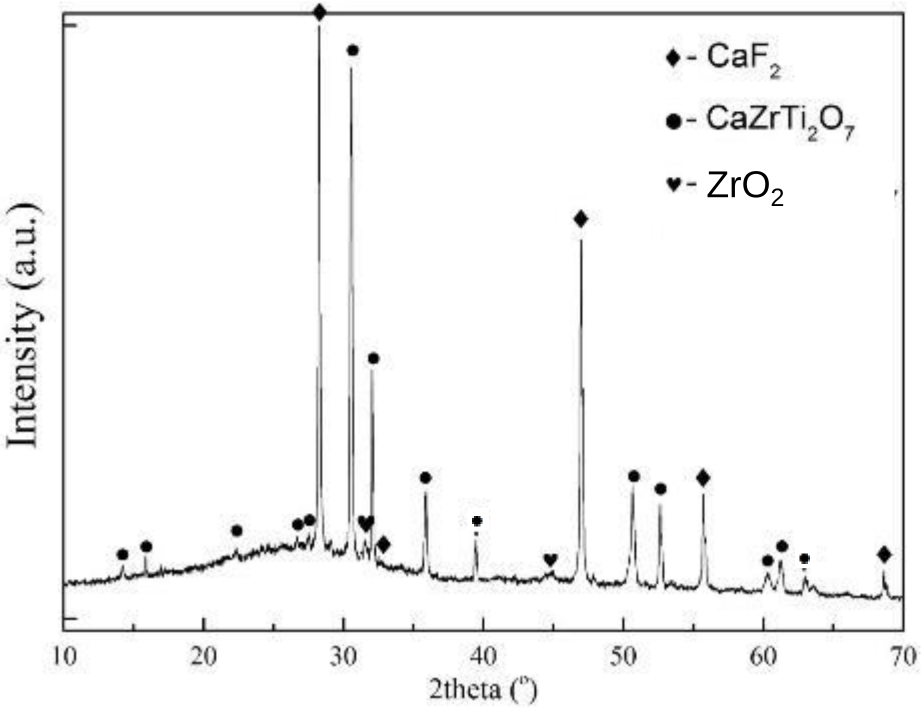

1. Major phase: CaF_2 and Zirconolite;
2. Minor phase: ZrO_2;
3. Glass phase: Diffuse scattering

QPA (Refinement)	Weight fraction (%)
CaF_2	21.8 ± 0.2
Zirconolite	21.9 ± 0.2
ZrO_2	1.8 ± 0.1
Glass phase	54.3

Using MgO as the internal standard
*R*wp= 11.59% *R*p=7.98% χ^2=9.171

Calculation from raw materials	Weight fraction (%)
CaF_2	23.2
Zirconolite	23.1
CeO_2	1.0
Glass phase	52.7

Calculated based on the raw materials

Microstructure

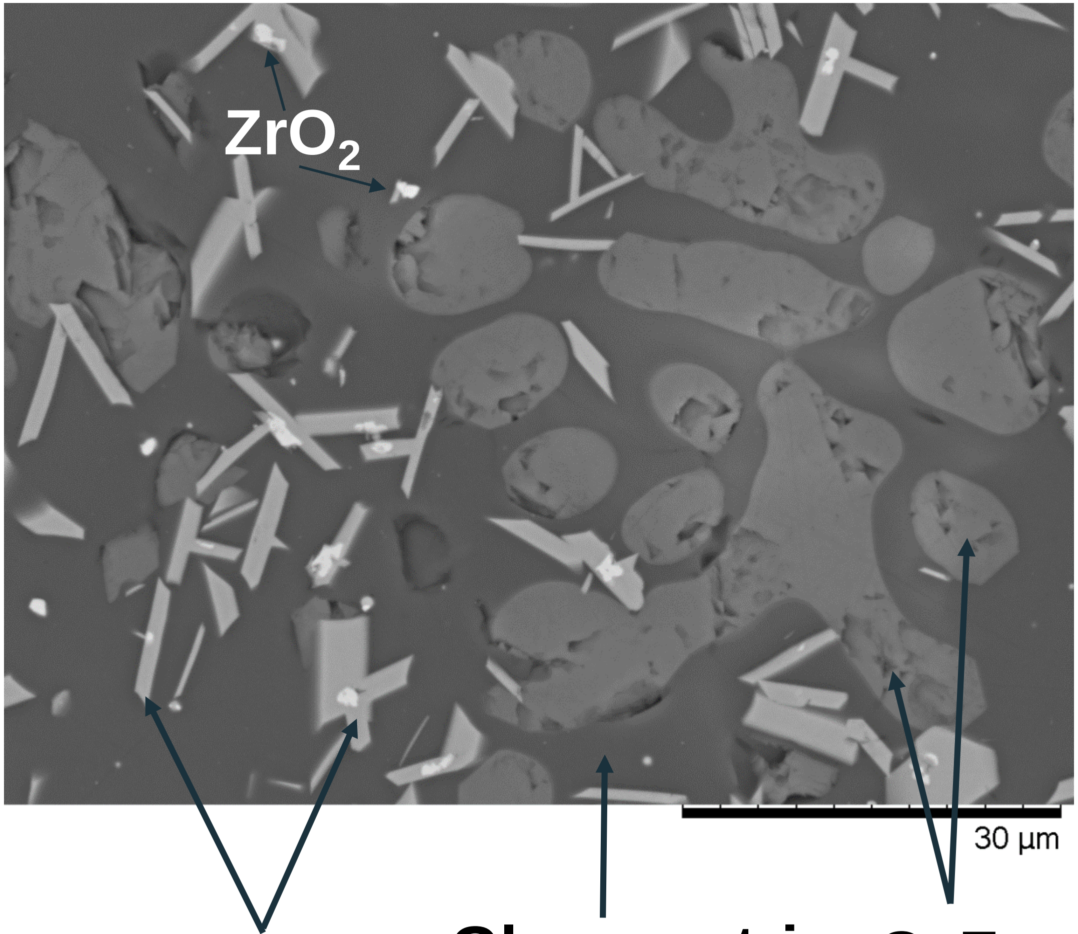

$CaZrTi_2O_7$

Light grey laths

Glass matrix

CaF_2

Irregular grain

AFM: Pristine sample

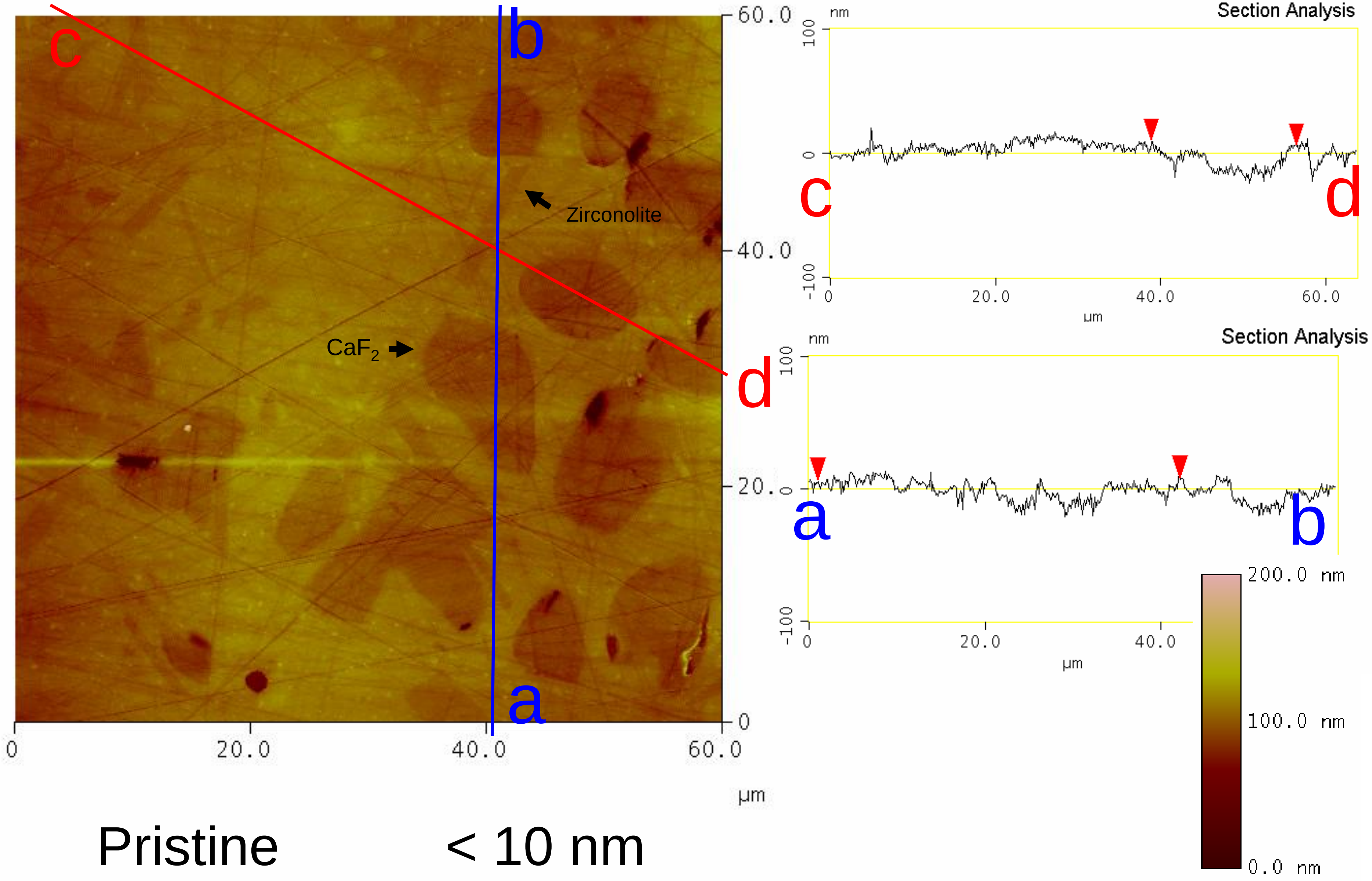

Pristine < 10 nm

SRIM estimation of damage

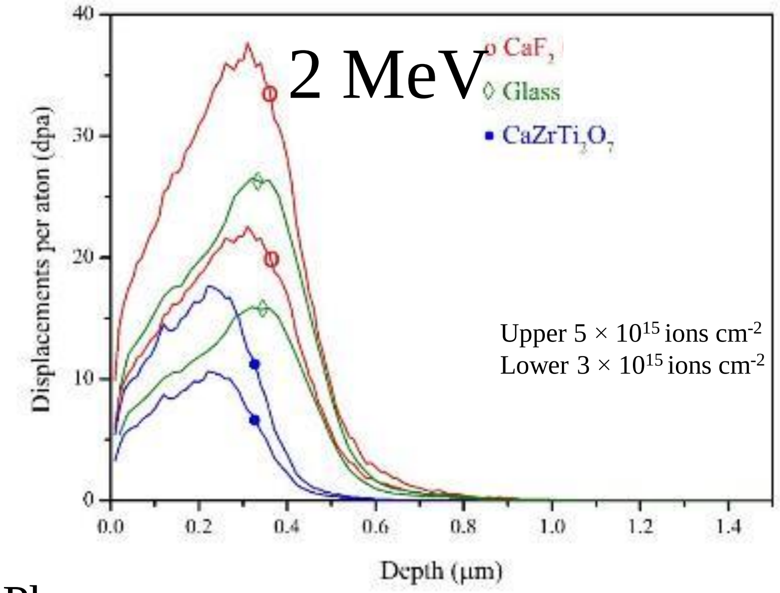

Upper 5 × 10^{15} ions cm^{-2}
Lower 3 × 10^{15} ions cm^{-2}

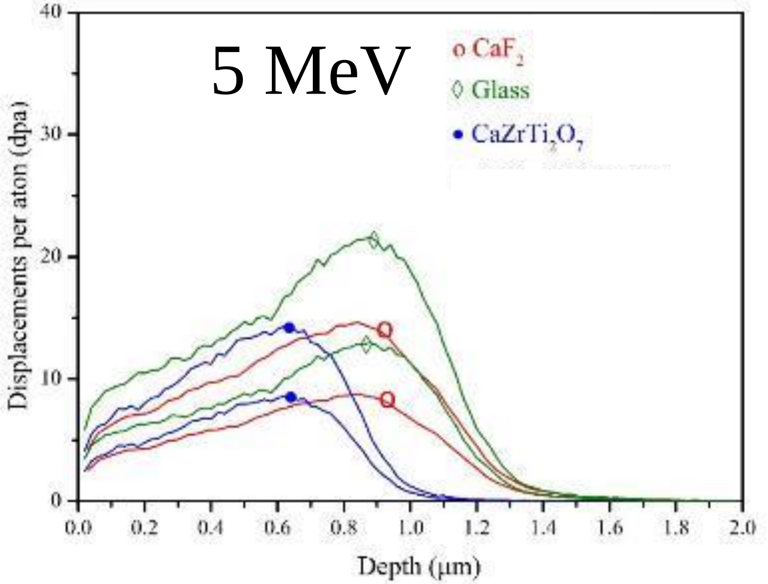

Phases:

- Zirconolite
- Calcium fluoride
- Glass ($Na_{1.28}Al_{3.12}B_1Si_{2.93}O_{13.68}$)

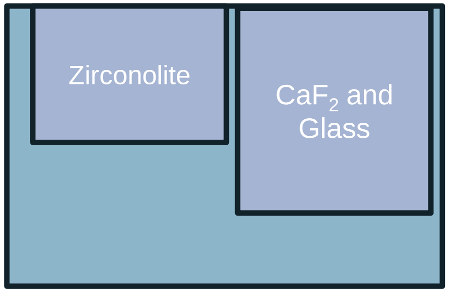

GIXRD: Amorphisation

Grazing incidence X-ray diffraction (GIXRD), uses small incident angles for the incoming X-ray beam, so that diffraction can be made surface sensitive.

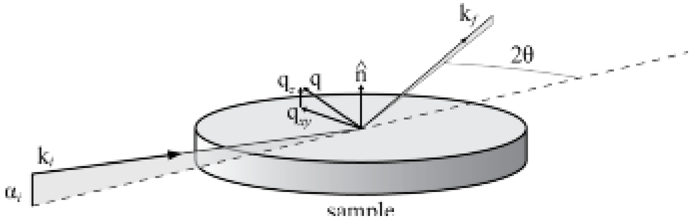

GI = 0.5°

Amorphisation on the surface.

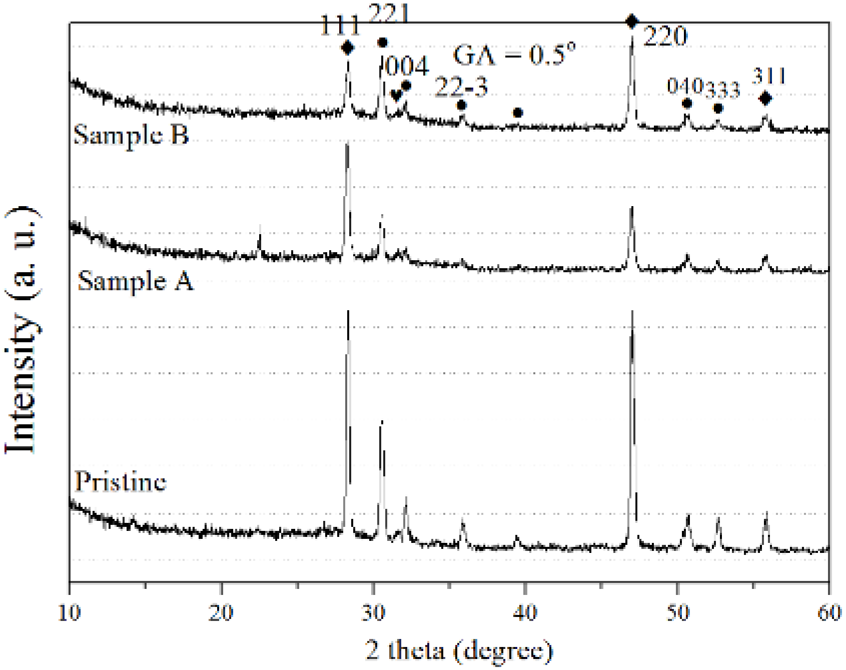

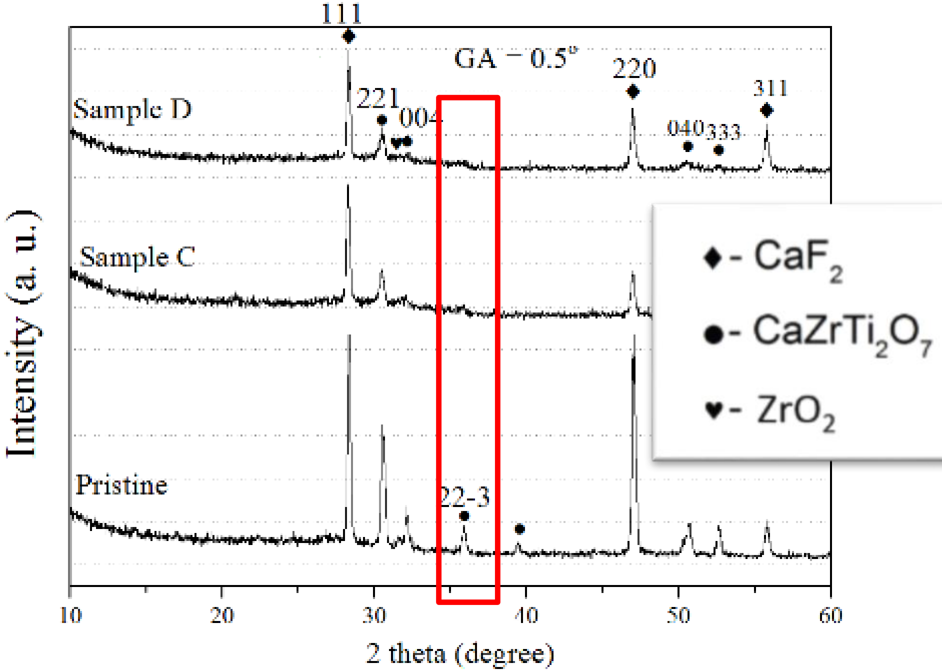

Attenuation depths of Cu Ka at different Glancing Angle

Glancing Angle	$CaZrTi_2O_7$	CaF_2
0.5°	375 nm	643 nm
1°	717 nm	1.24 um

DISTINCTIVE

Irradiated surface

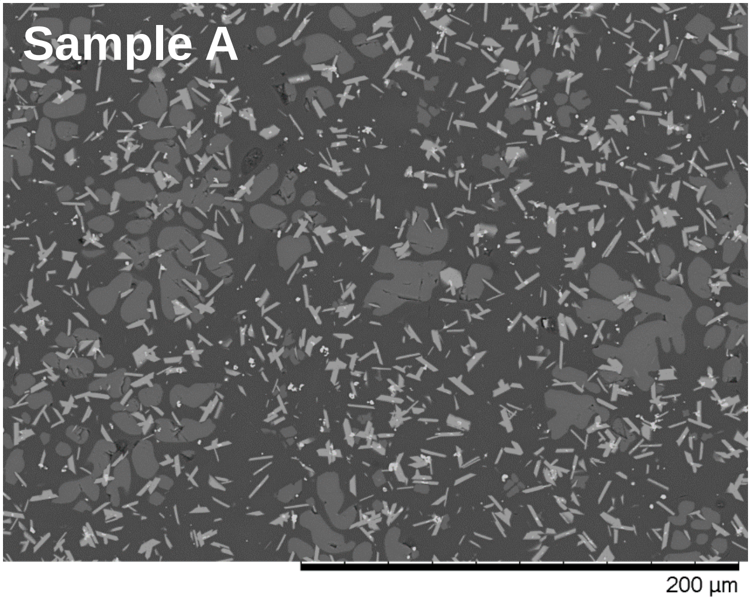

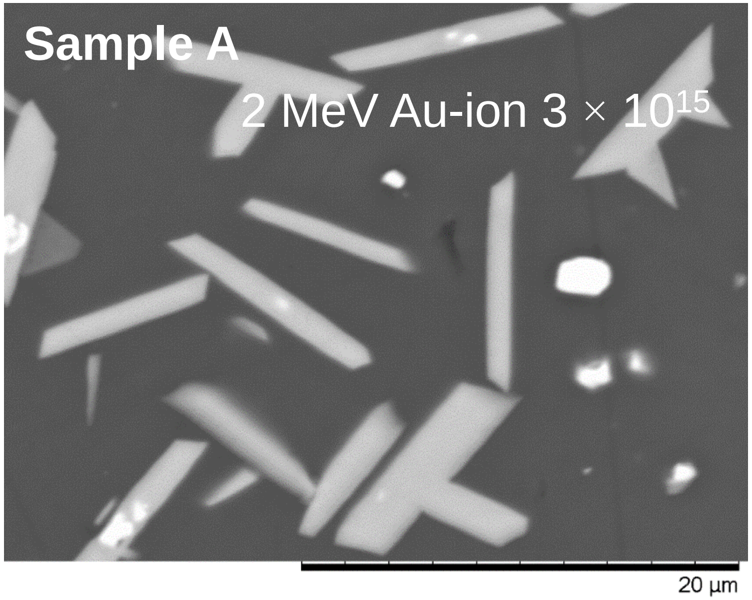

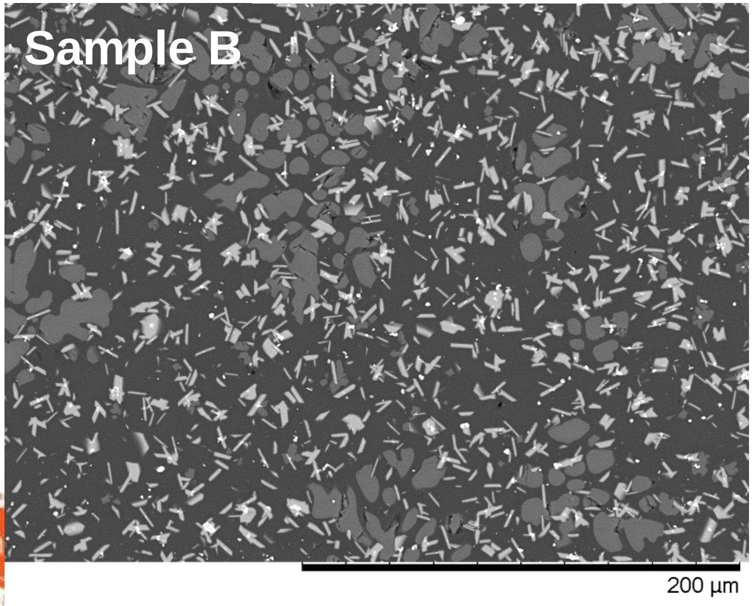

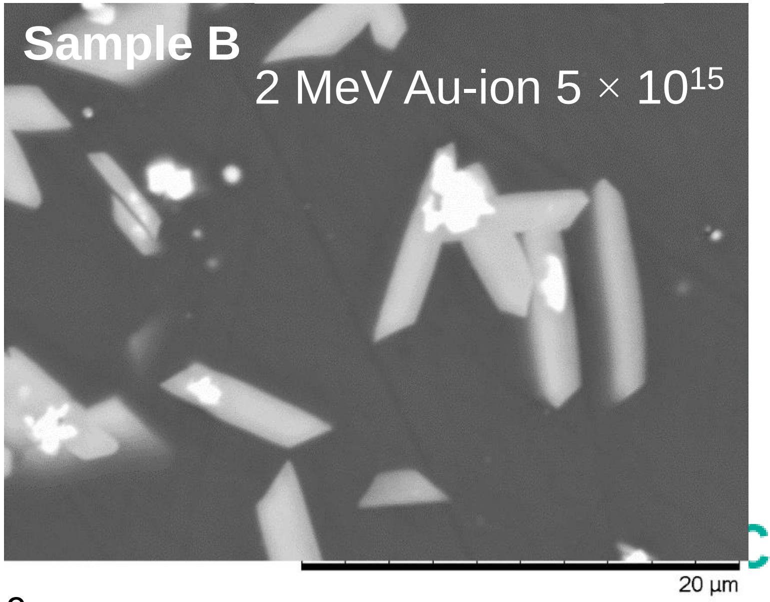

Deformation

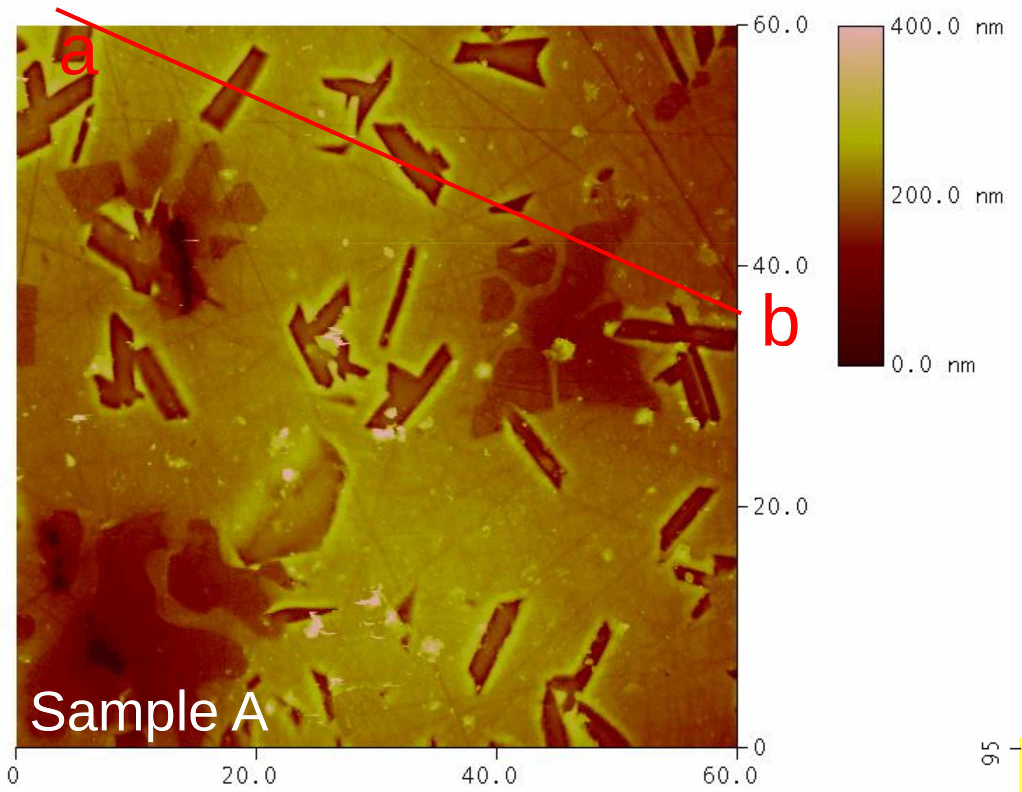

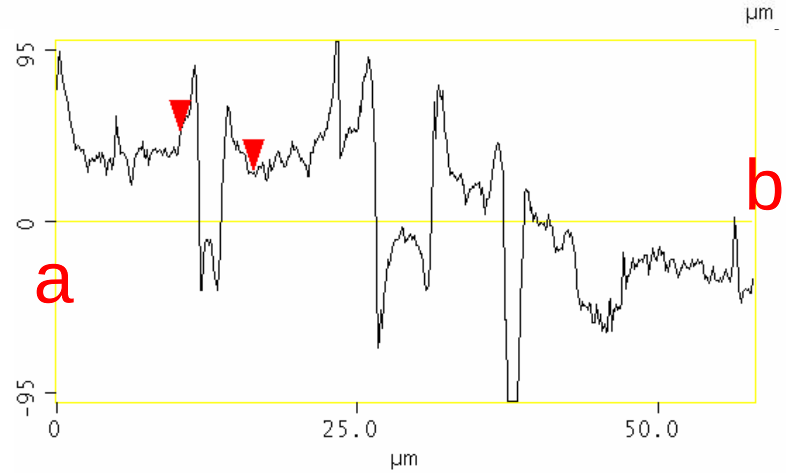

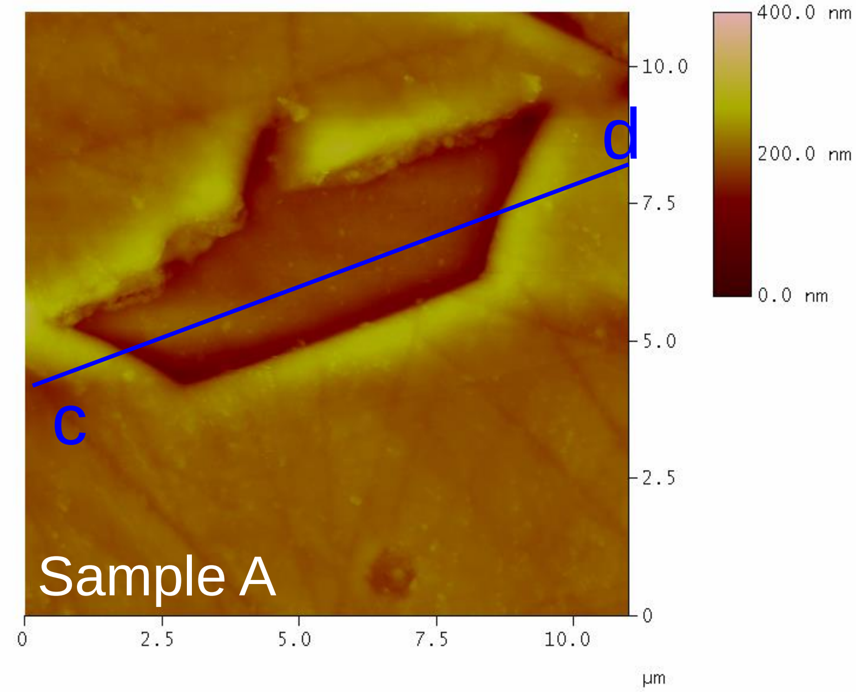

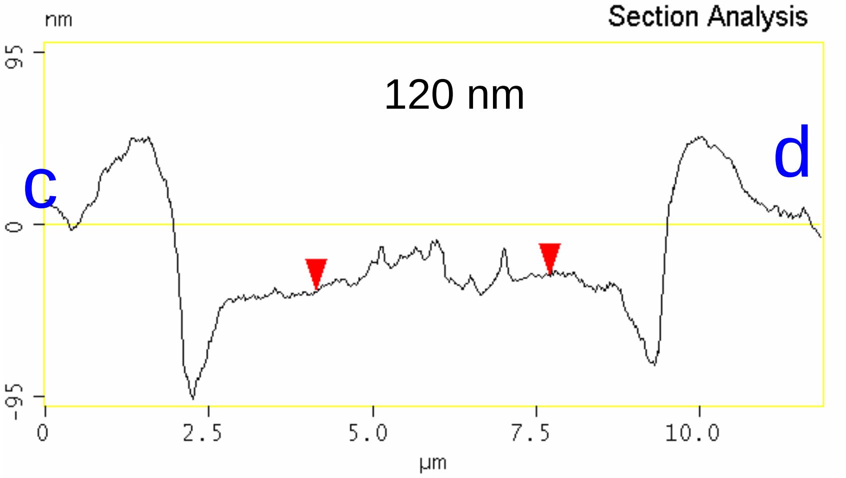

Similar situation in Sample B.

Micro-cracking!

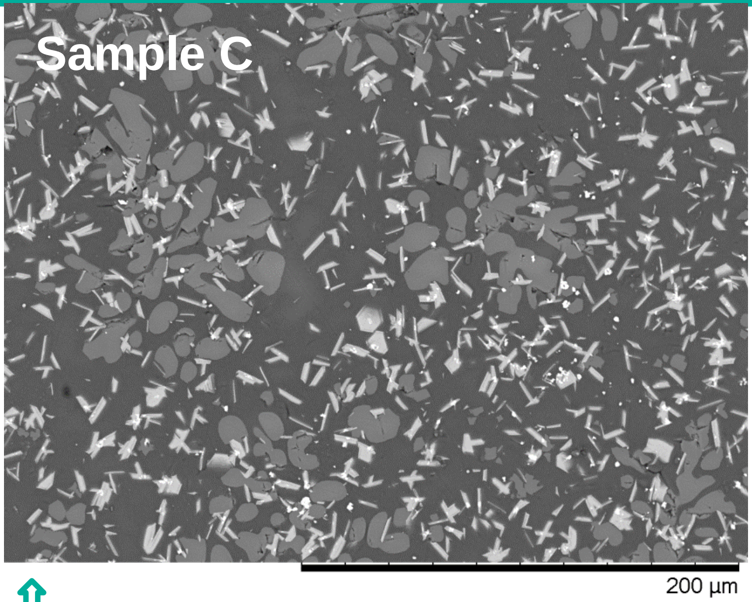

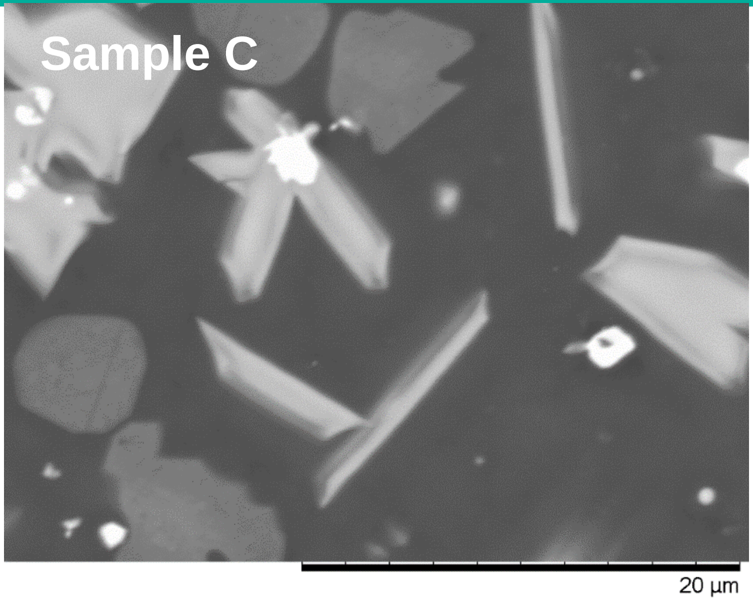

5 MeV Au-ion 3 × 10^{15}

5 MeV Au-ion 5 × 10^{15}

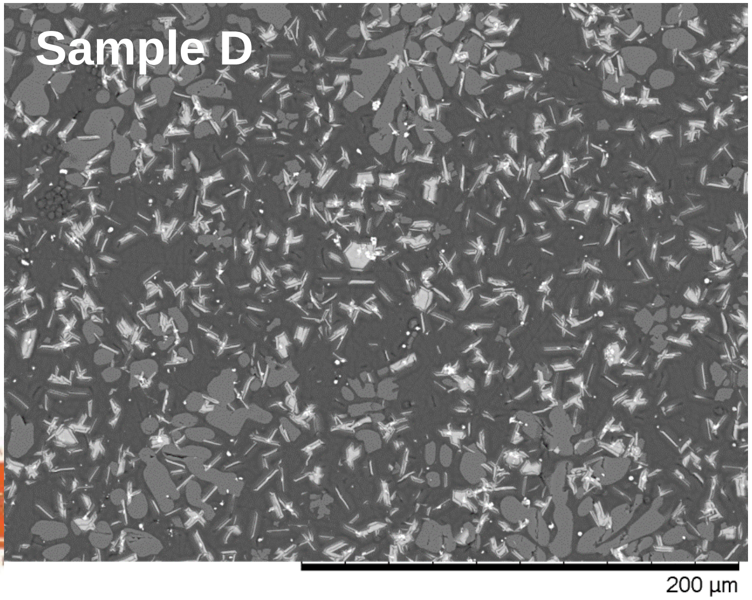

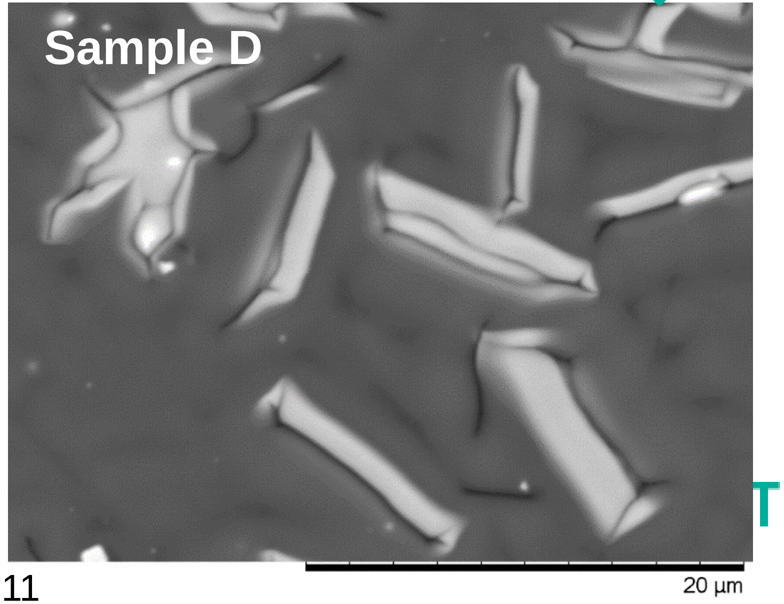

Swelling feature

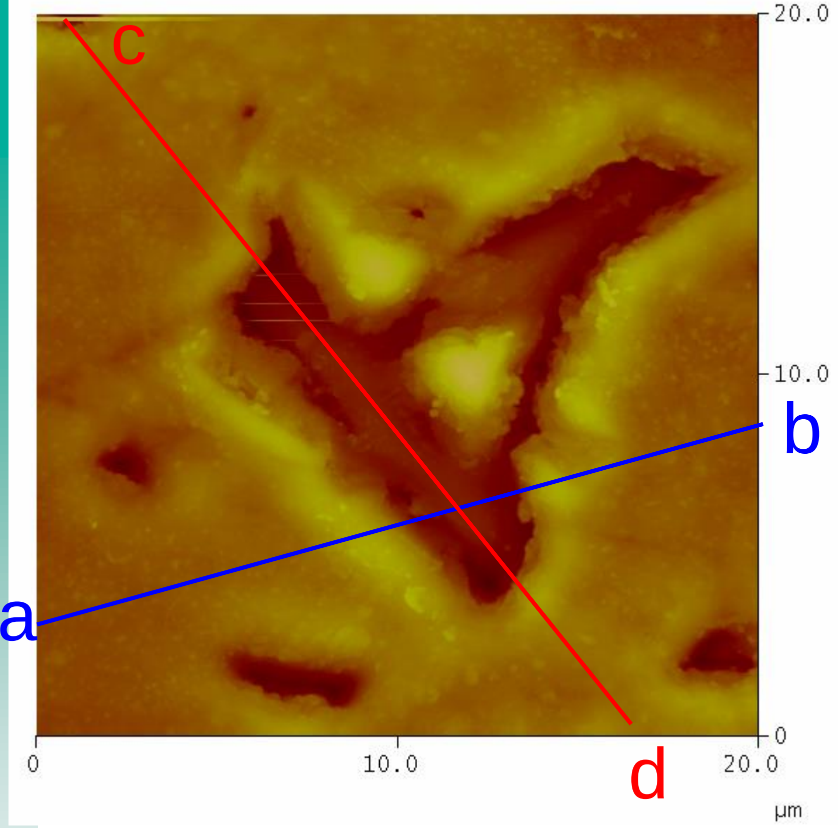

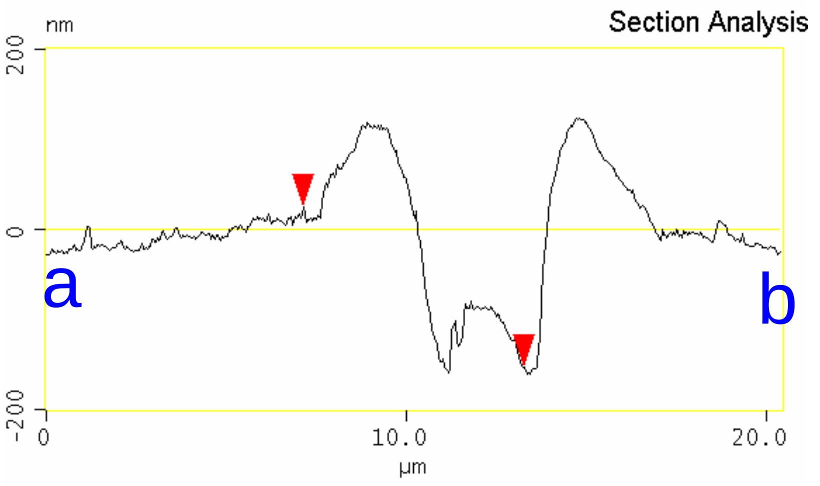

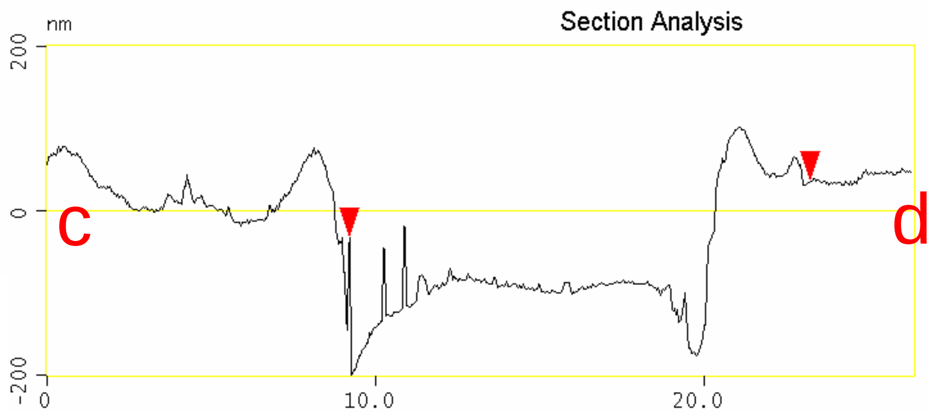

Sample C

~ 250 nm

Cliff-like feature

Cracking – not observed

Swelling feature

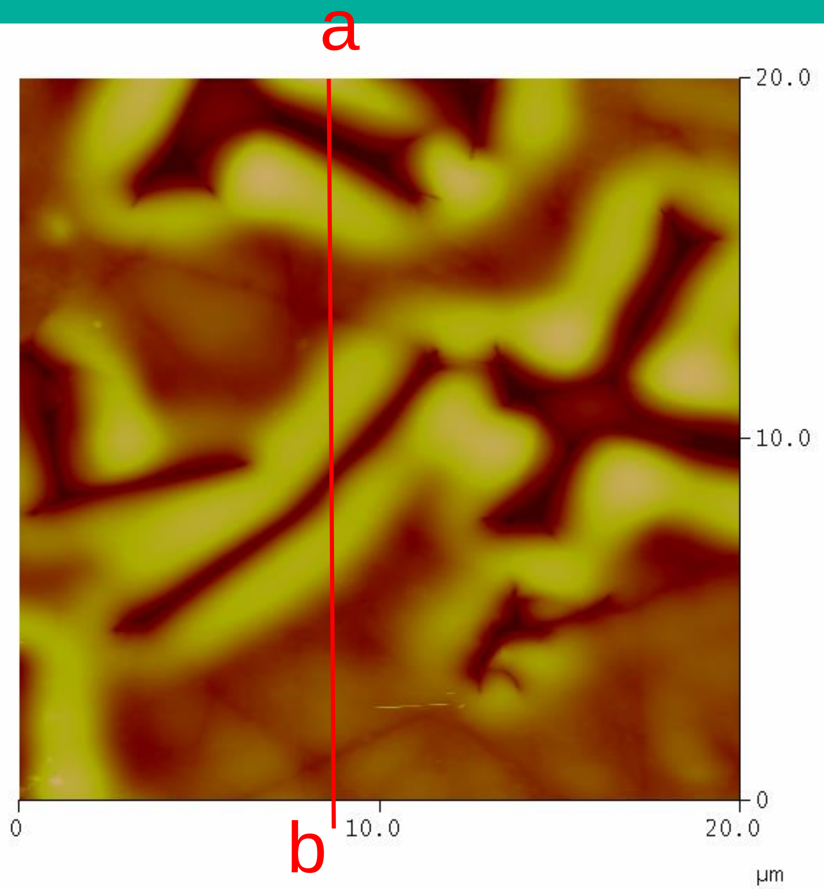

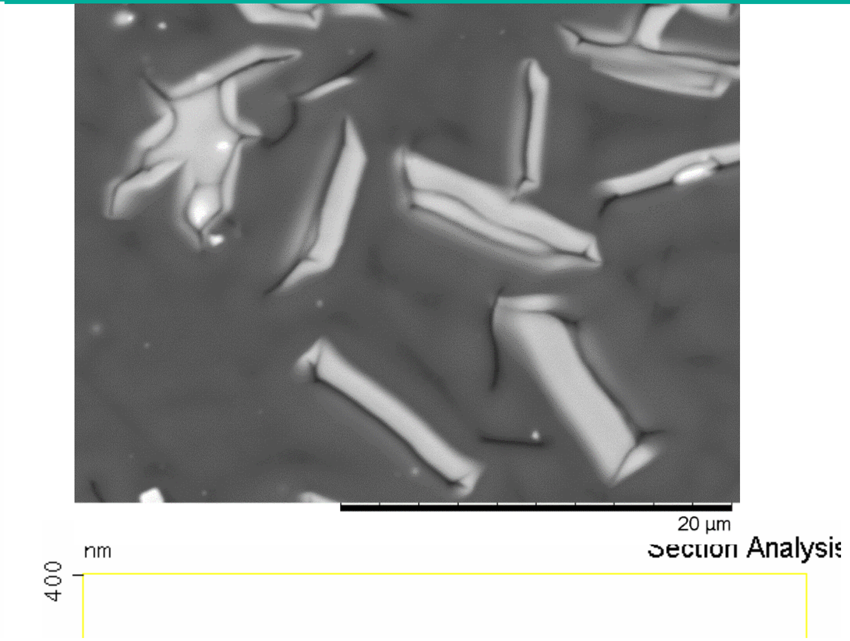

~ 500 nm

Sample D

Cracking – disappear?

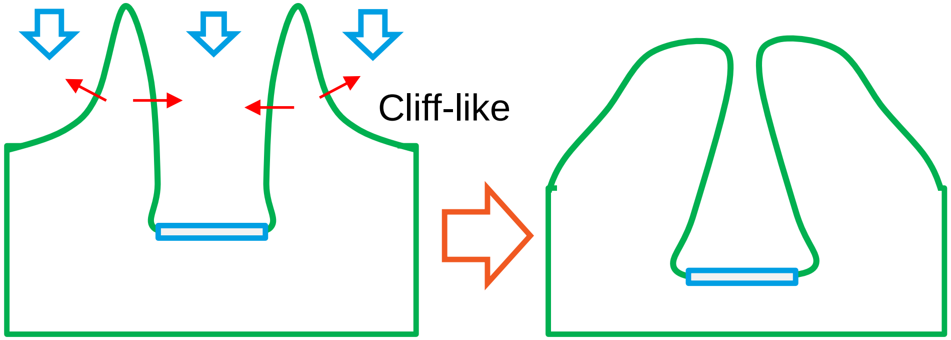

Glass matrix swelling feature

on the top of zirconolite grain

Gaussian Profile Irradiation

Formation procedure of a large-area uniform beam

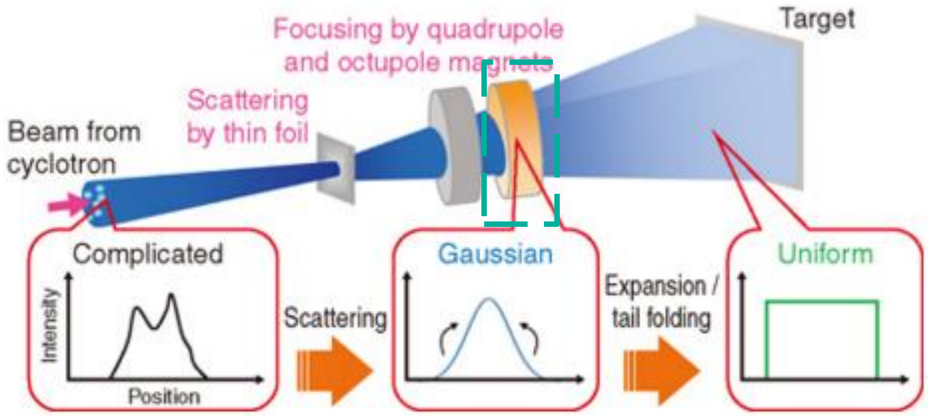

2 MeV Au-ion 5 × 10^{15} ions/cm^2

2 MeV Au-ion 1 × 10^{16} ions/cm^2

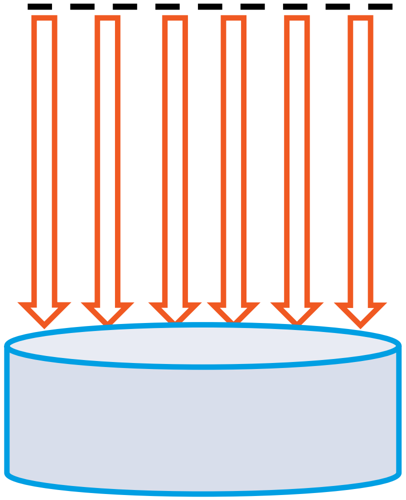

Uniform beam

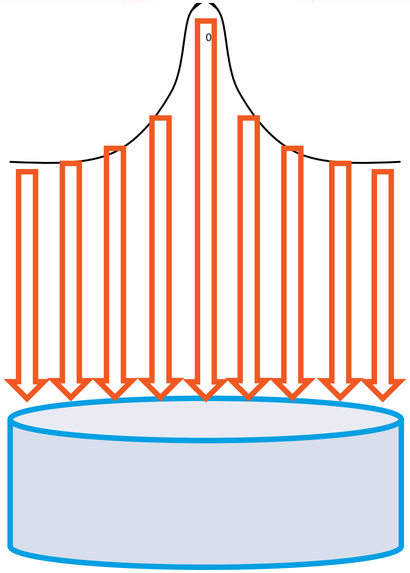

Gaussian-profile beam

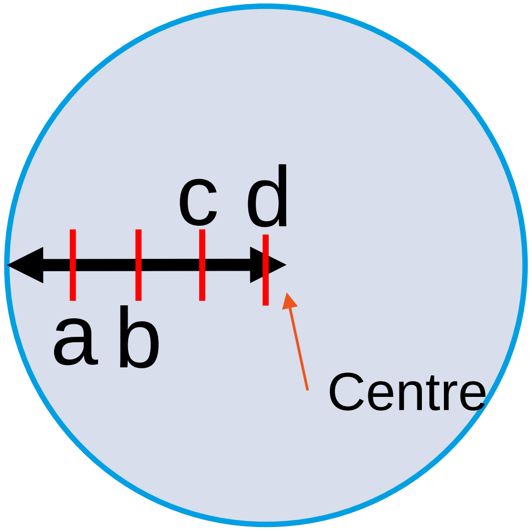

$$y = \frac{1}{\sigma\sqrt{2\pi}} e^{-\frac{(x-\mu)^2}{2\sigma^2}}$$

$\mu =$ Mean
$\sigma =$ Standard Deviation
$\pi \approx 3.14159\cdots$
$e \approx 2.71828\cdots$

Image from: http://jolisfukyu.tokai-sc.jaea.go.jp/fukyu/mirai-en/2015/5_15.html

2MeV 5e15 ions/cm^2 Gaussian irradiation

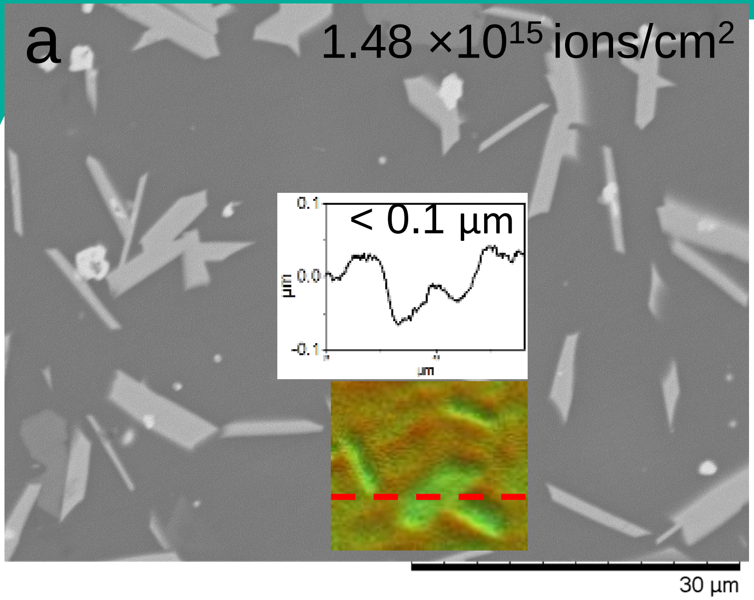

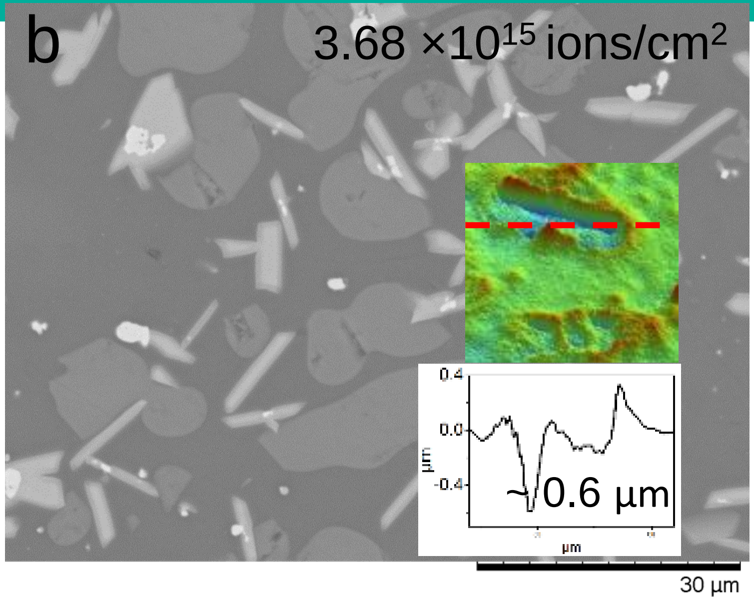

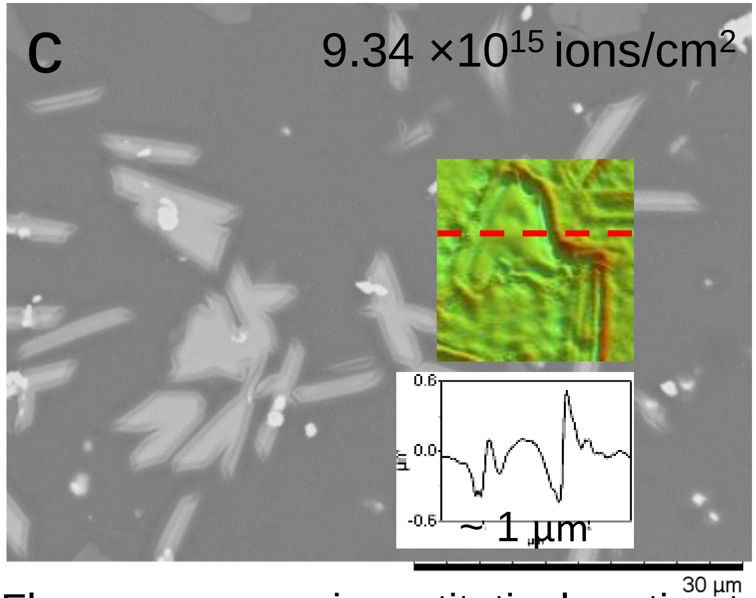

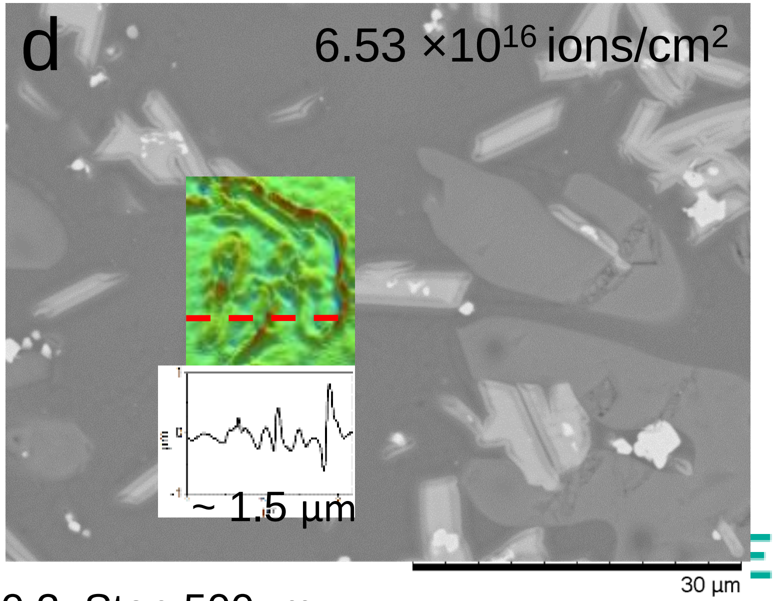

Fluence was semiquantitatively estimated, giving SD=0.3, Step 500µm.

Need further confirmation with the beam scientist.

2MeV 1e16 Gaussian irradiation

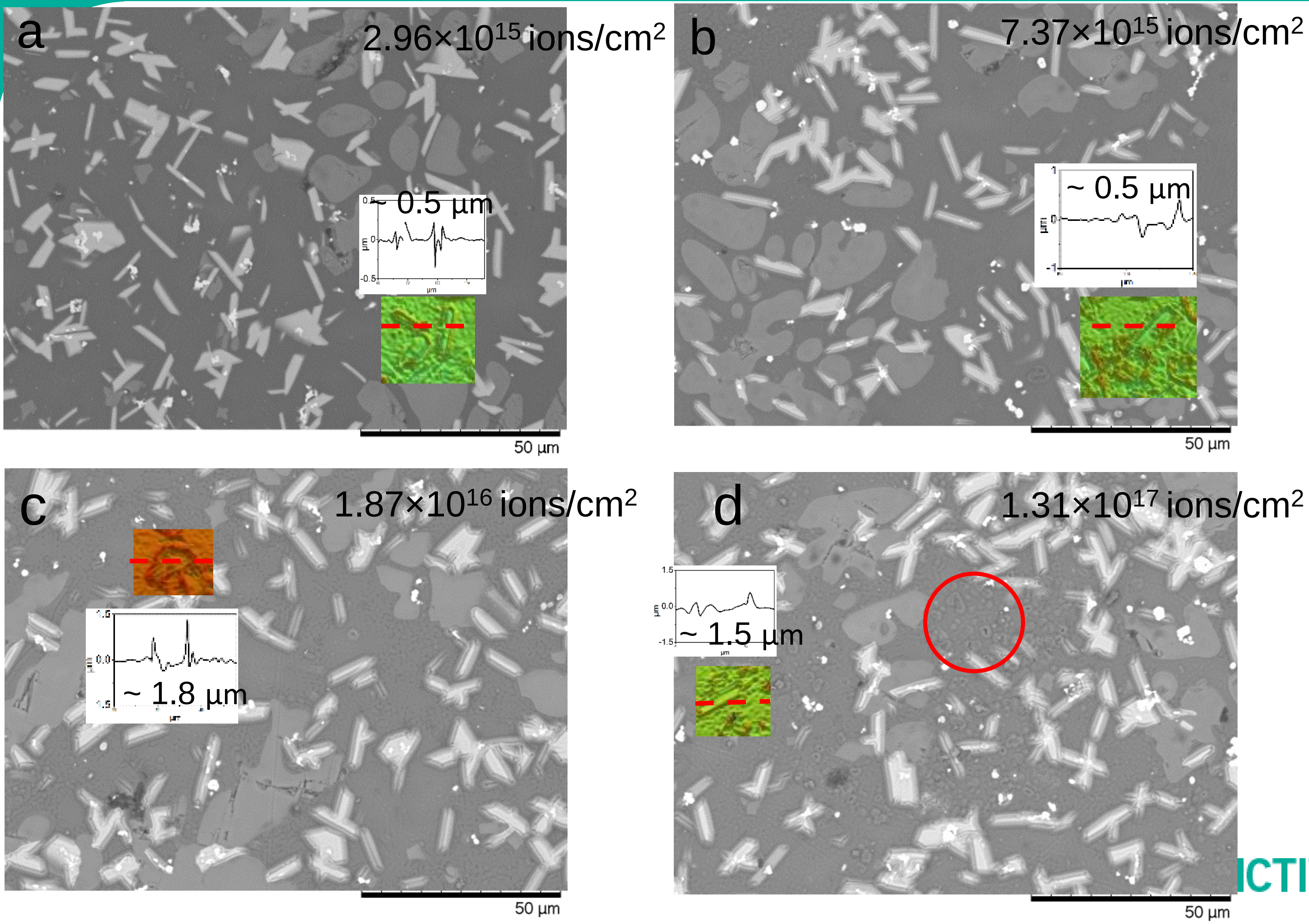

Leaching test

- 90^{o}C, water
- 90^{o}C, pH = 2.0

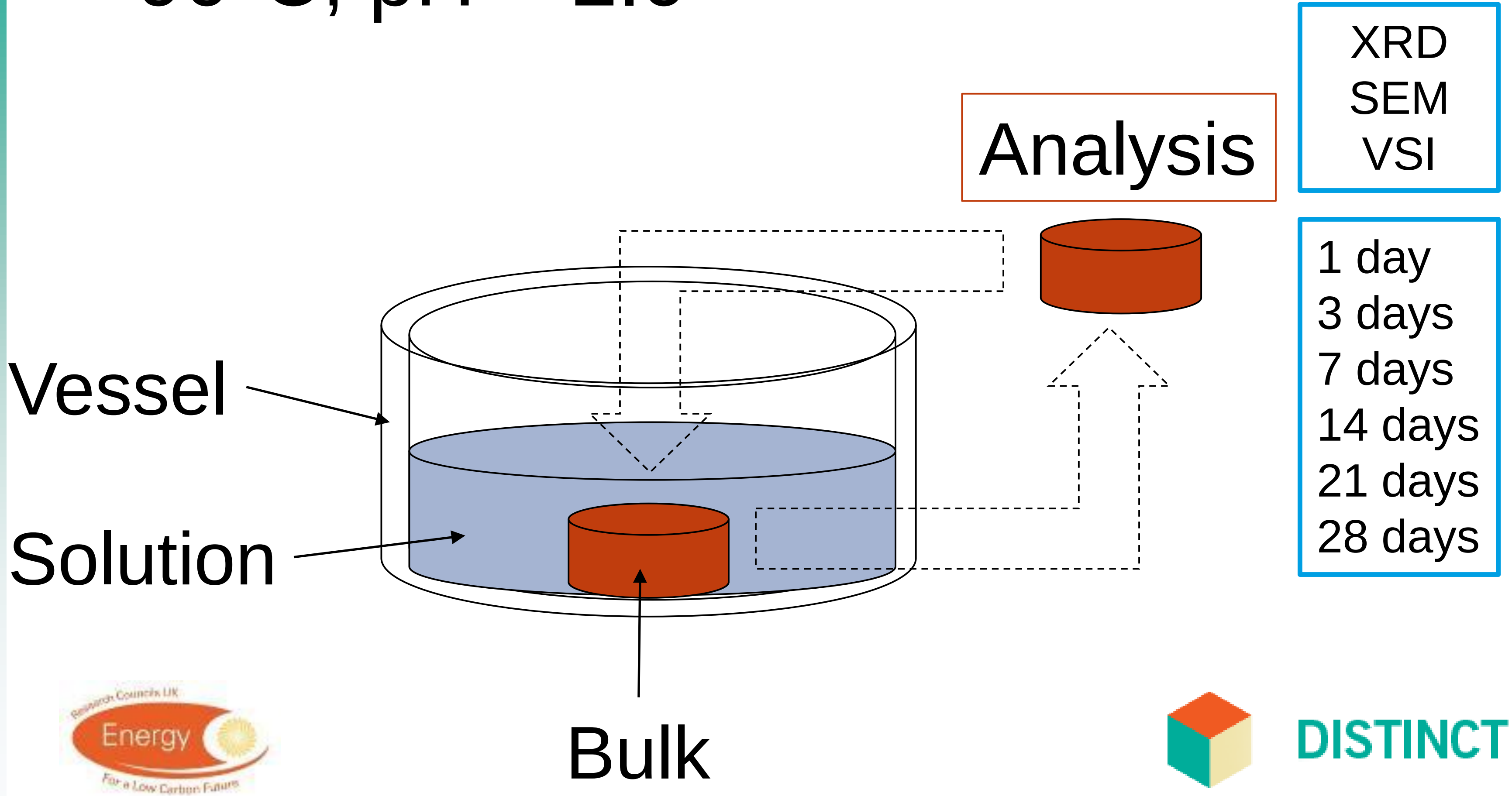

Analysis

XRD
SEM
VSI

1 day
3 days
7 days
14 days
21 days
28 days

Vessel

Solution

Bulk

Research Councils UK
Energy
For a Low Carbon Future

DISTINCTIVE

Leaching (90°C water): XRD

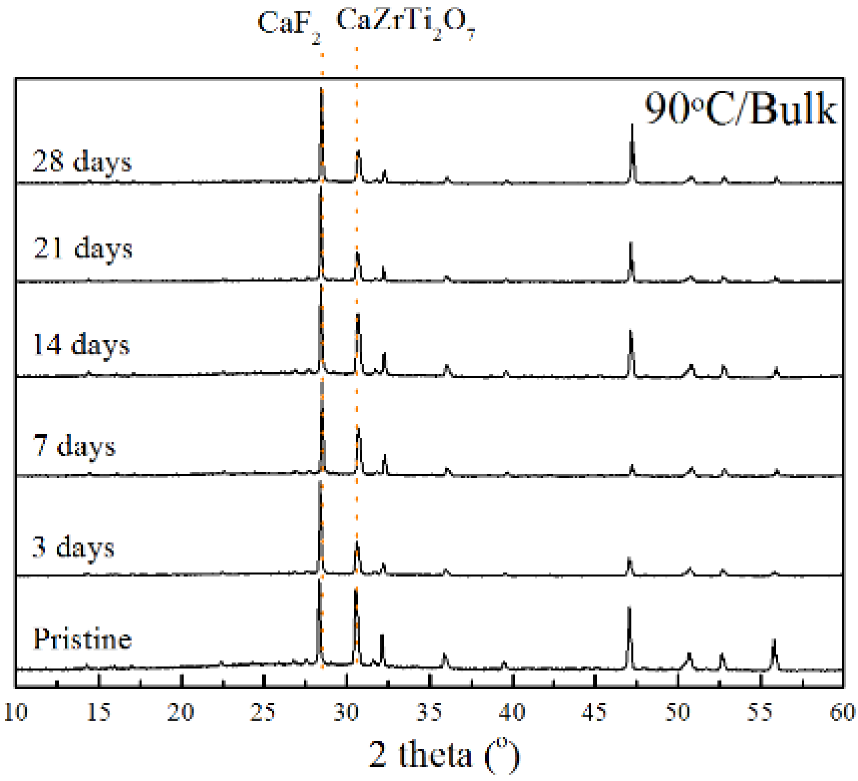

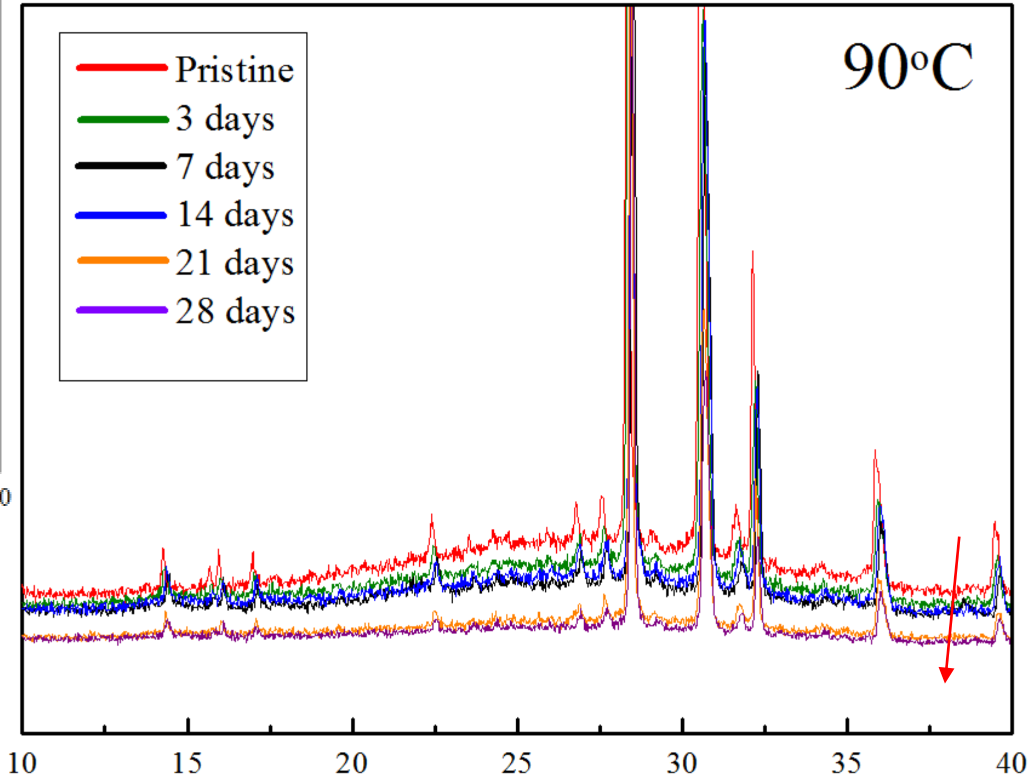

Phase: no obvious change.

Diffuse scattering decreased.

Leaching (90ºC water): SEM Overall

Pristine

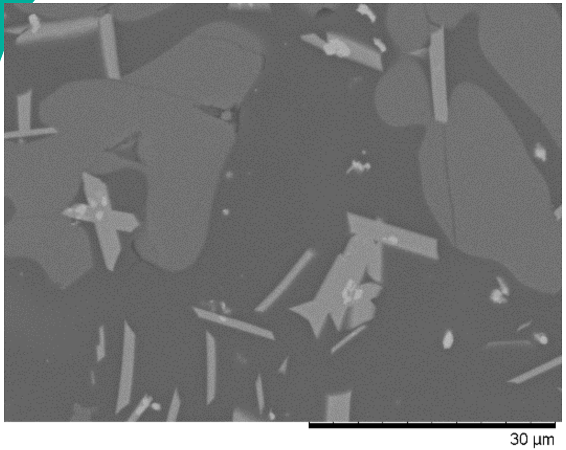

28 days

1 day

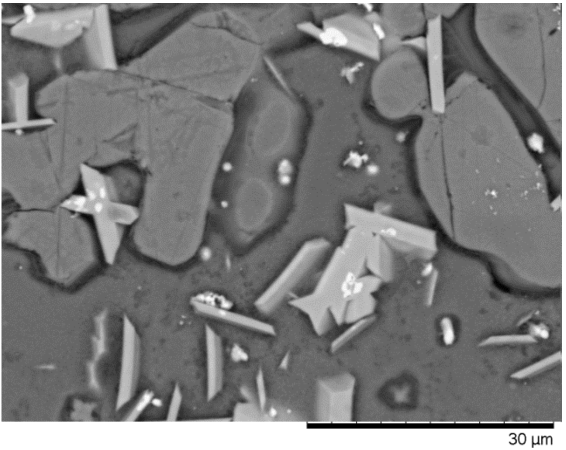

3 days

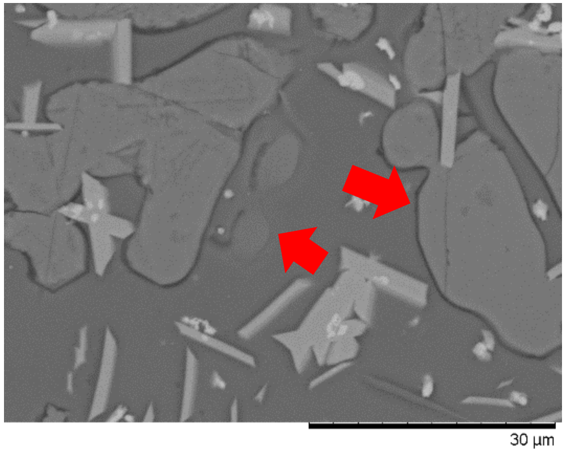

7 days

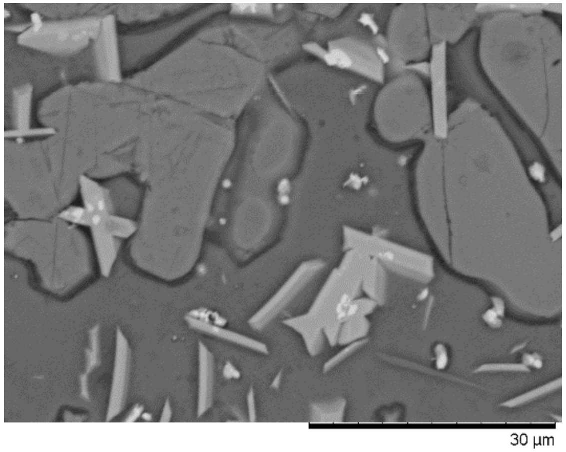

14 days

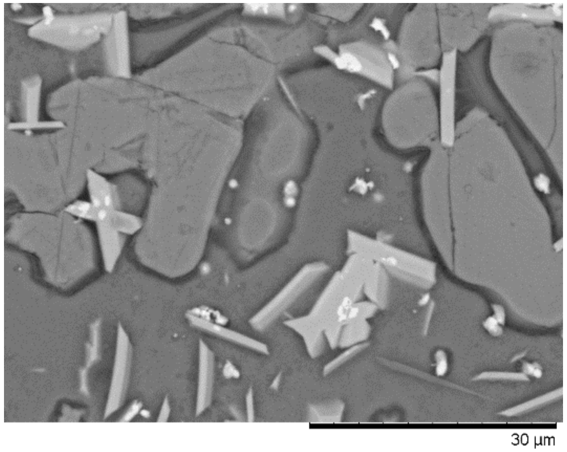

21 days

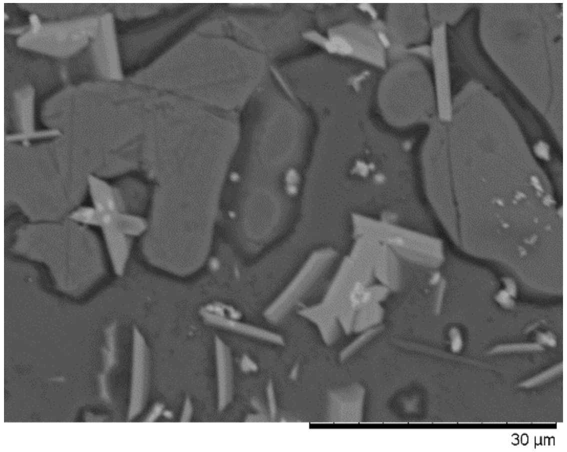

Research Councils UK Energy For a Low Carbon Future

DISTINCTIVE

Leaching (90ºC water): SEM

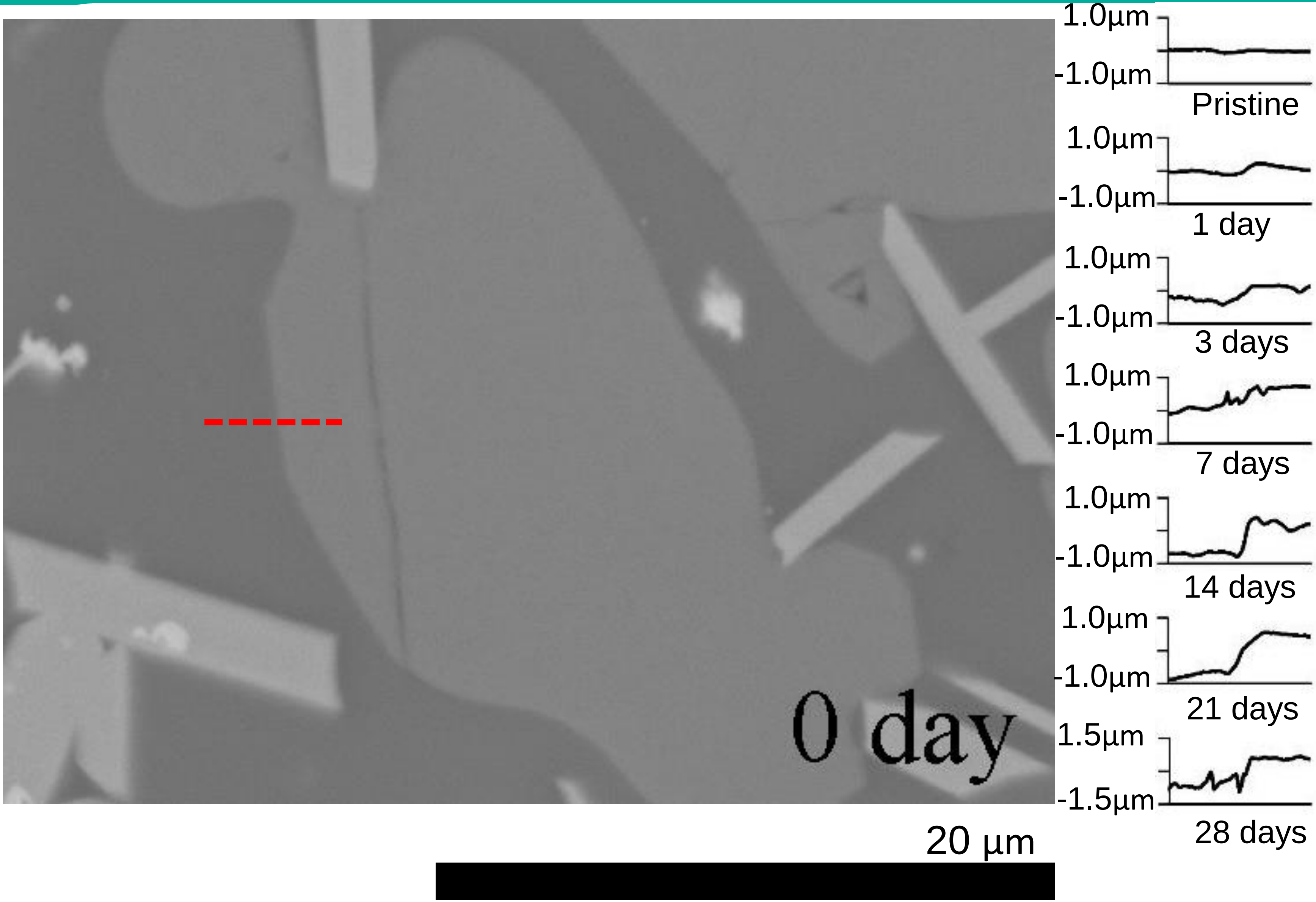

Leaching (90^{o}C water): VSI

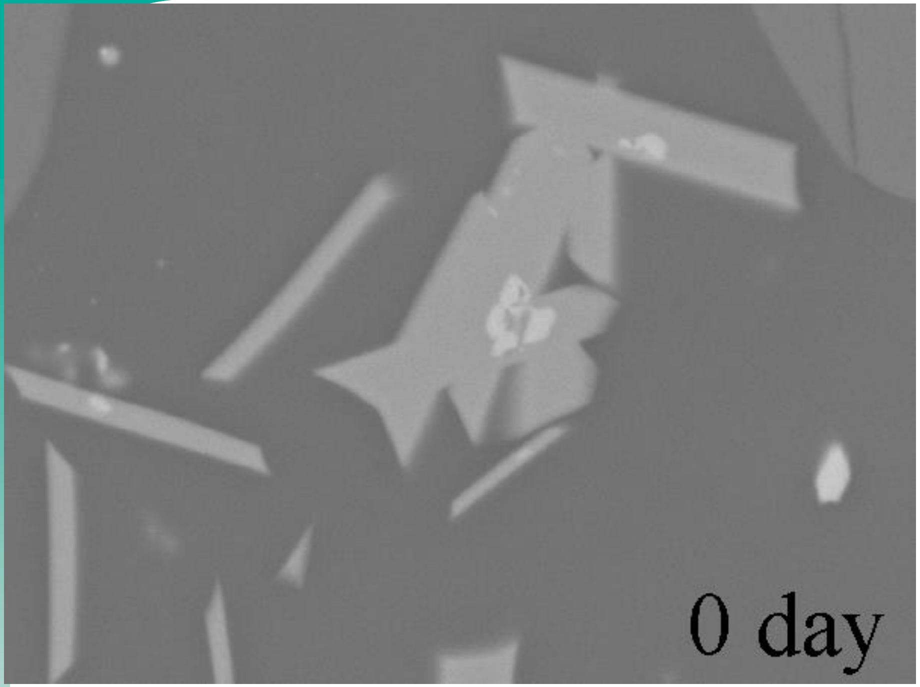

0 day

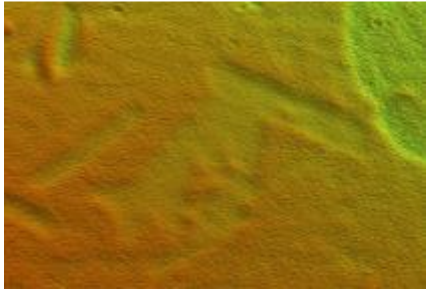

1 day

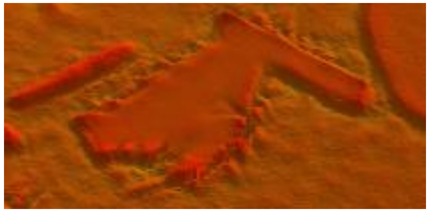

3 days

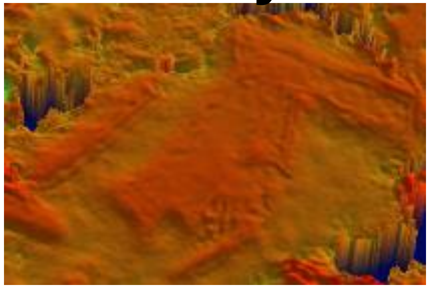

7 days

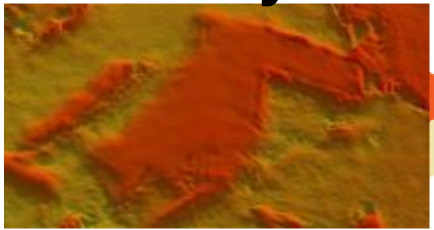

14 days

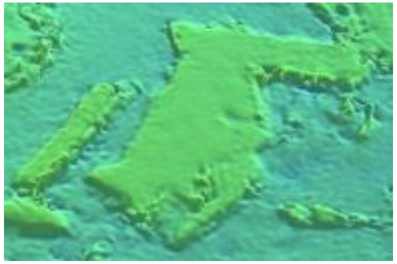

21 days

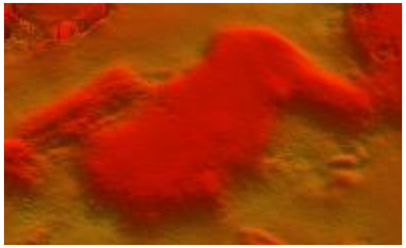

28 days

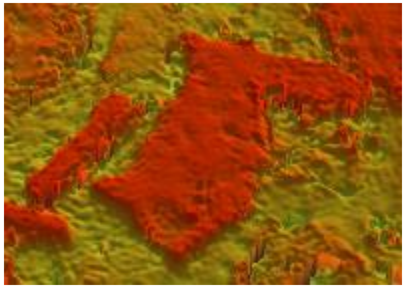

Leaching (90ºC pH=2.0): XRD

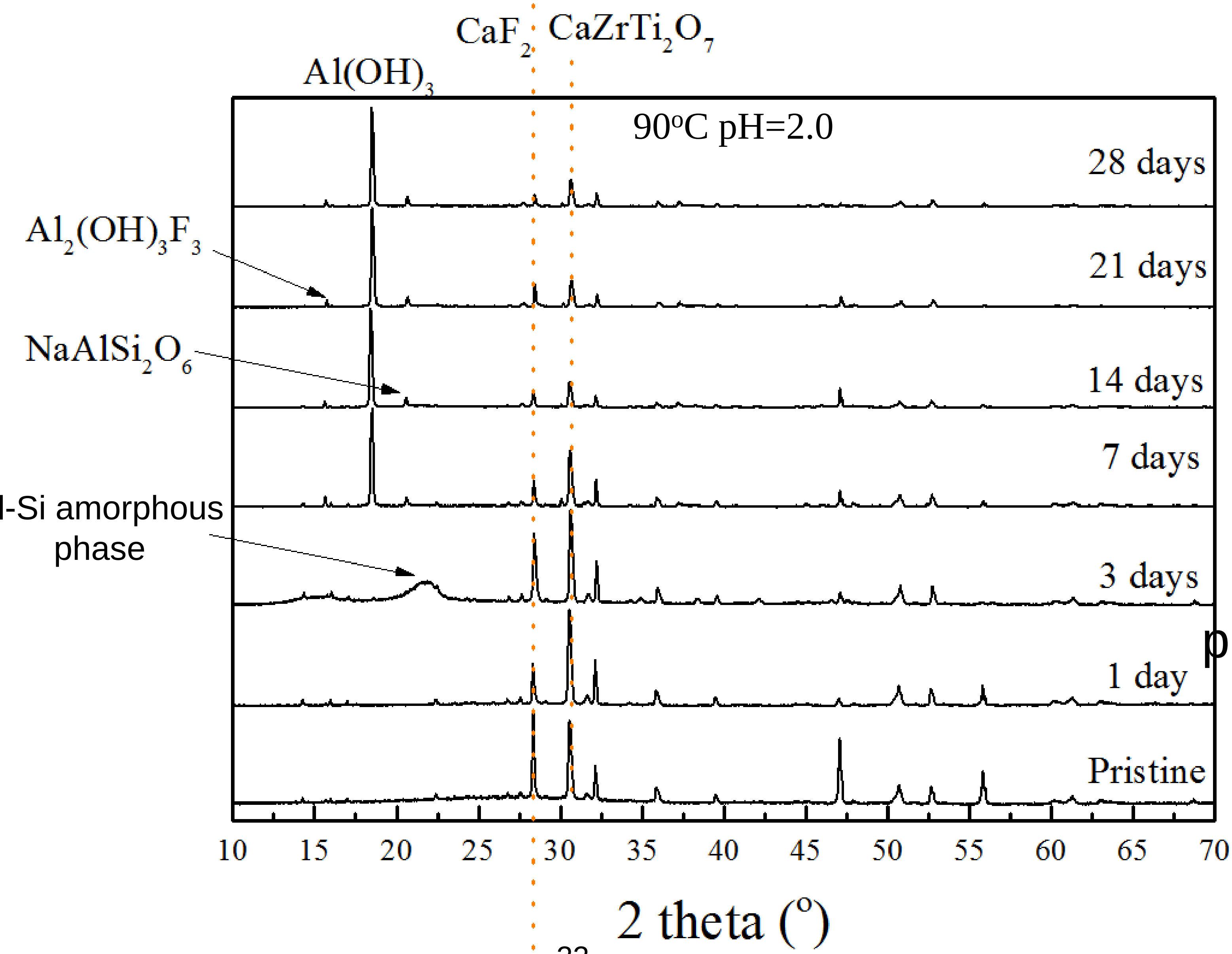

$NaAlSi_3O_8$

⇩ H^+

$Al_2Si_2O_5(OH)_4$

⇩ Ca^{2+}

$Al_3(OH)_3$ &

$CaSiO_3$ ↓

pH=2.0 → 5.8

Leaching 90^{o}C pH=2.0

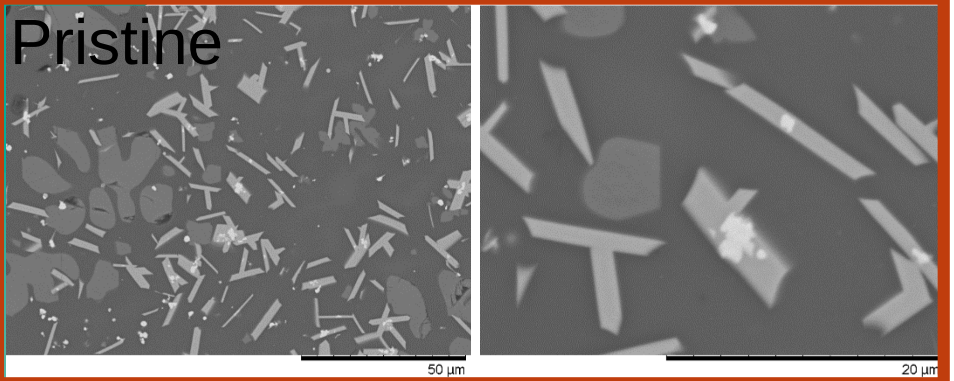
Pristine

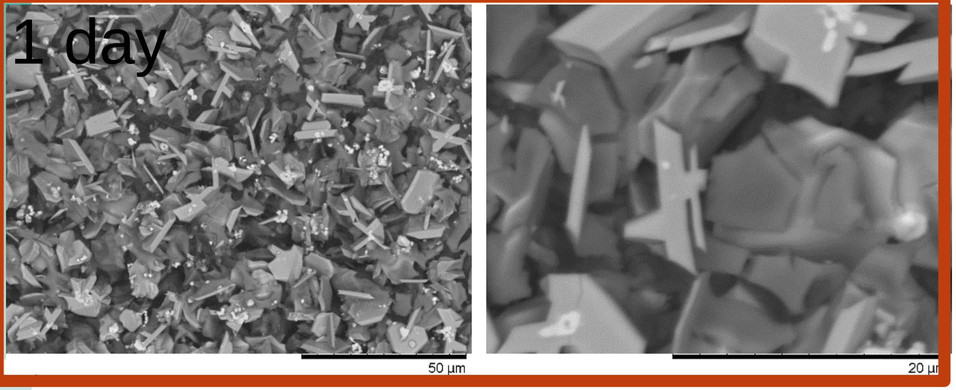
1 day

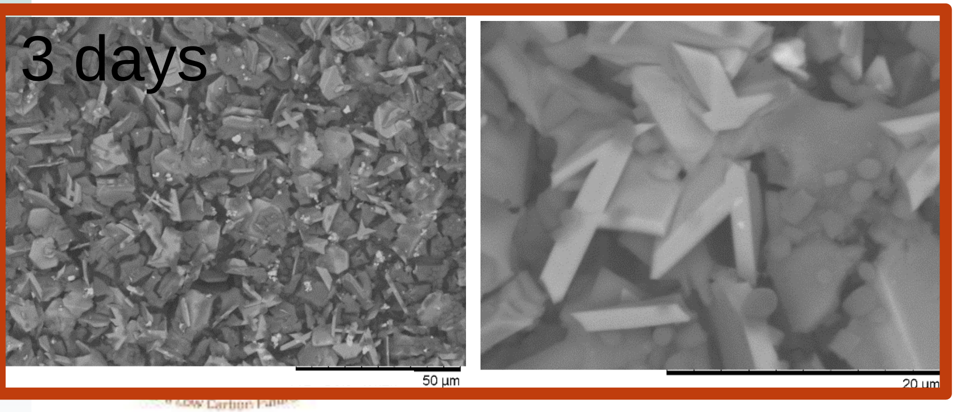
3 days

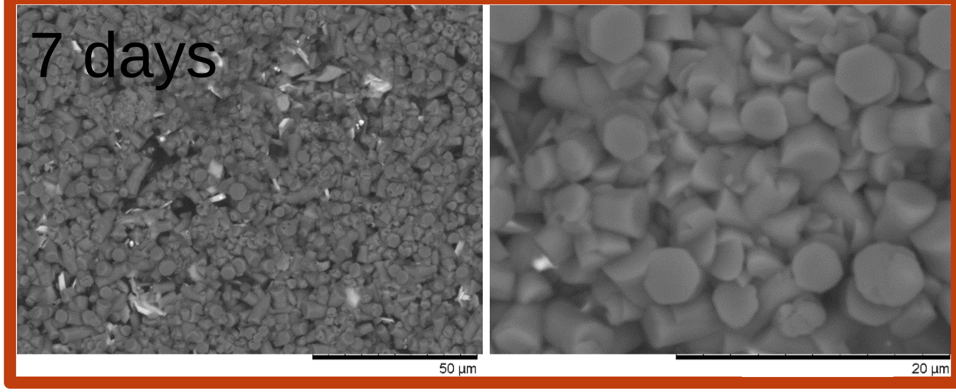
7 days

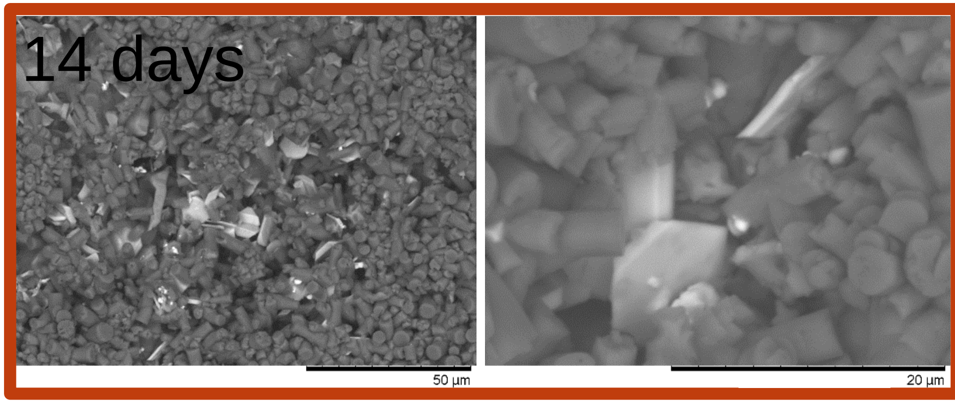
14 days

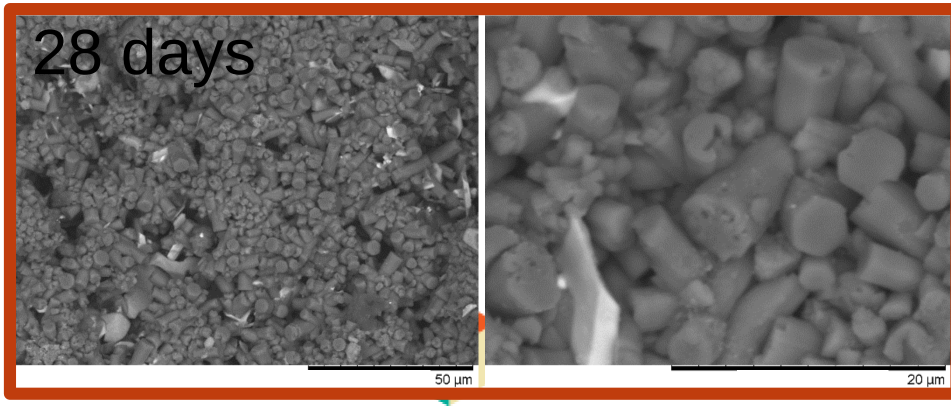
28 days

Conclusion

- Glass matrix swelling feature was observed on the irradiated zirconolite glass-ceramic.
- Glass partially dissolved after 3 days at 90^{o}C/water. A layer of $Al(OH)_3$ formed after 7 days at 90^{o}C/pH=2.0.
- The neutral solution condition inhibited the formation of $Al(OH)_3$ and the dissolution of CaF_2 phase.

Acknowledgements

DISTINCTIVE

Decommissioning, Immobilisation and Storage
soluTIons for NuClear wasTe InVEntories

EPSRC
Engineering and Physical Sciences
Research Council

EP/L014041/1

The
University
Of
Sheffield.

midas

Materials for **I**nnovative **D**isposition from **A**dvanced **S**eparations
support from the Department for Energy and Climate Change

ISL

Immobilisation Science Laboratory

NATIONAL NUCLEAR
LABORATORY

Dr. Ewan Maddrell (NNL)
Dr. Martin Stennett
Dr. Claire Corkhill
Prof. Neil Hyatt

Research Councils UK
Energy
For a Low Carbon Future

DISTINCTIVE

Thank you!

Research Councils UK
Energy
For a Low Carbon Future

DISTINCTIVE

Glass-Ceramics for Pu Disposition: Where are we now?

Stephanie Thornber

Supervisors: Prof Neil Hyatt[1] Dr Martin Stennett[1] Dr Ewan Maddrell[2]

[1] Immobilisation Science Laboratory, Department of Materials Science & Engineering, The University of Sheffield

[2] National Nuclear Laboratory, Sellafield, Seascale, Cumbria, CA20 1PG

sthornber1@Sheffield.ac.uk

DISTINCTIVE consortium annual conference
5-6th April 2017, York, UK

Background

- The UK stores over 120 tonnes of civil separated PuO_2.
- The current policy is to reuse the PuO_2 as MOx fuel. As part of the safety case for this decision, R&D into alternative immobilisation options is underway in-case of any need to dispose of the stockpile in the future.
- Some material is not economically viable for fuel fabrication.

Pu-residues

- Pu-residues are classified as higher activity waste.
- Chemically heterogeneous and physically variable.

Powders

High purity

Fuel pellets

Glass formers

Fuel pins

Sludges

ZrO_2

Cl

Low purity

Solids

Image courtesy of NNL

Previous work developed glass-ceramics for impure Pu-residues and full ceramics for pure waste-streams consolidated by hot isostatic pressing.

Background

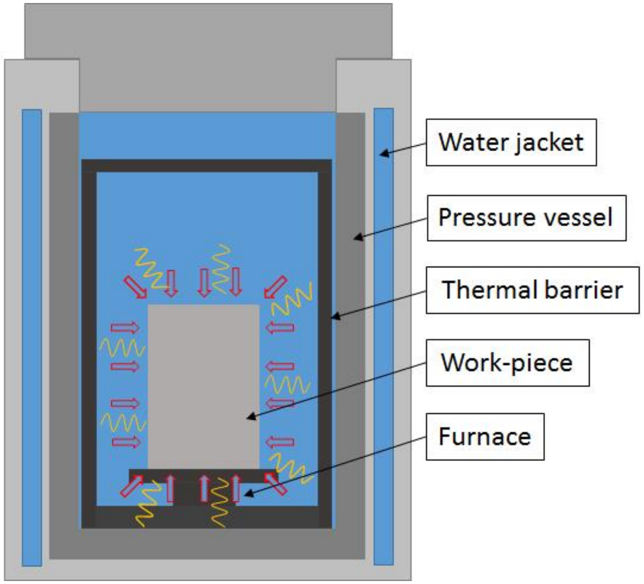

Advantages:
Batch process
Flexible to waste feed and material
Range of processing conditions
Hermetically sealed wasteforms
Significant volume reduction
Uniform incorporation of radionuclides
No off-gas production
No limitations on the wasteform
No secondary waste produced
Significant cost saving

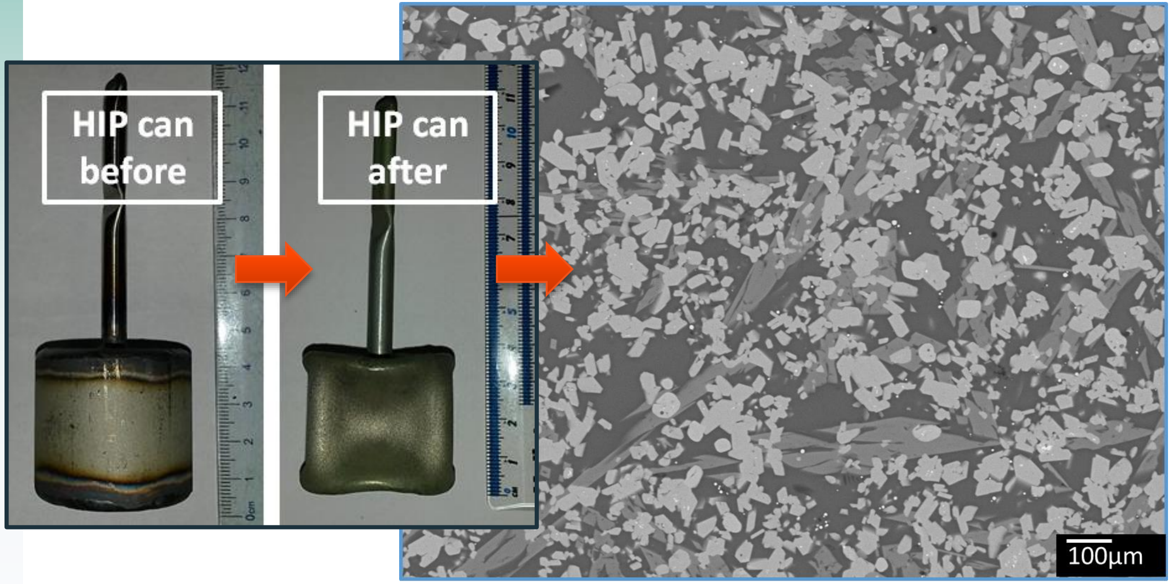

Main advantages:
Proliferation resistance
Chemical durability
Chemical flexibility
Waste loading capacity
Ease of processing
Natural analogues

Process Optimisation

An ex-situ calcination prior to packing the canisters was shown to achieve reproducible high quality samples and increased sample throughput by $^2/_3$.

Sample	**Heat Treatment**	
	Calcine (°C)	Bake out (°C)
A	0	300 °C
B	0	600 °C
C	**600 °C**	**300 °C**
D	600 °C	0

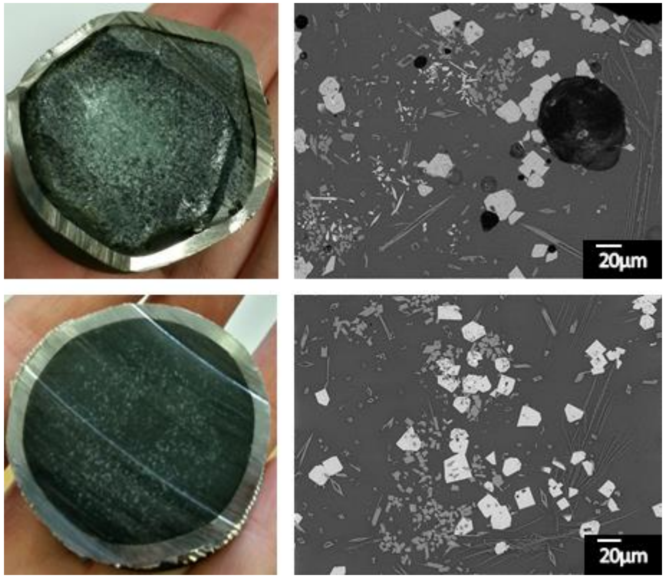

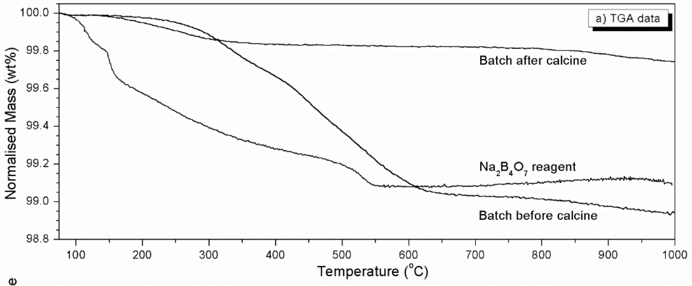

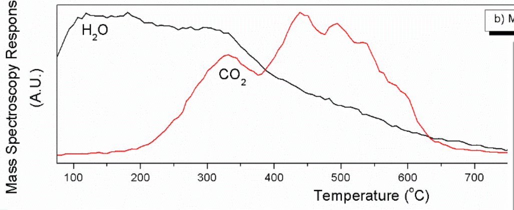

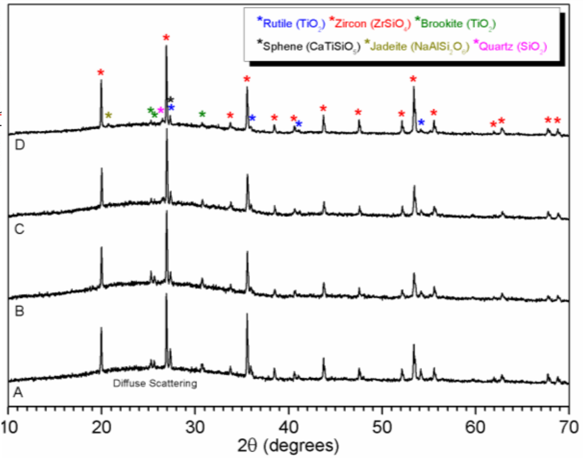

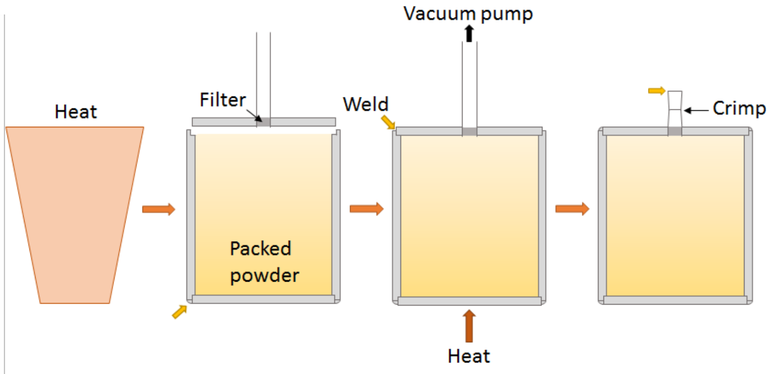

Thornber *et* al. J. Nucl. Mat. 2017

Formulation development

Previous work developed a formulation based on residues containing high CaF_{2}.

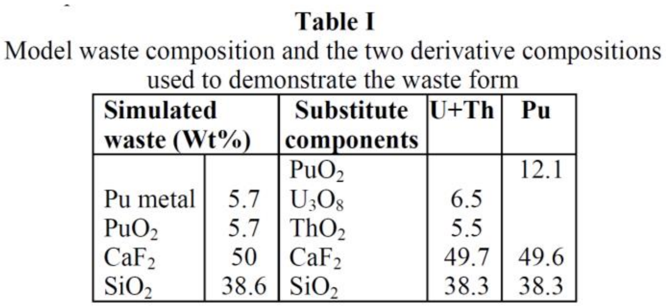

Table I
Model waste composition and the two derivative compositions used to demonstrate the waste form

Simulated waste (Wt%)		**Substitute components**	**U+Th**	**Pu**
		PuO_2		12.1
Pu metal	5.7	U_3O_8	6.5	
PuO_2	5.7	ThO_2	5.5	
CaF_2	50	CaF_2	49.7	49.6
SiO_2	38.6	SiO_2	38.3	38.3

Day *et* al. 2005

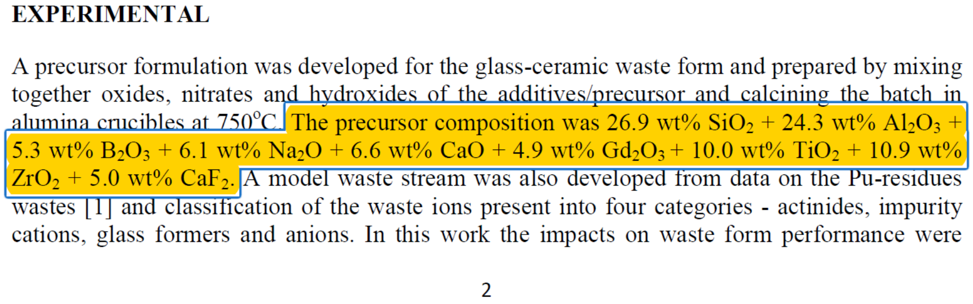

EXPERIMENTAL

A precursor formulation was developed for the glass-ceramic waste form and prepared by mixing together oxides, nitrates and hydroxides of the additives/precursor and calcining the batch in alumina crucibles at 750°C. The precursor composition was 26.9 wt% SiO_2 + 24.3 wt% Al_2O_3 + 5.3 wt% B_2O_3 + 6.1 wt% Na_2O + 6.6 wt% CaO + 4.9 wt% Gd_2O_3 + 10.0 wt% TiO_2 + 10.9 wt% ZrO_2 + 5.0 wt% CaF_2. A model waste stream was also developed from data on the Pu-residues wastes [1] and classification of the waste ions present into four categories - actinides, impurity cations, glass formers and anions. In this work the impacts on waste form performance were

2

Stewart *et* al. 2013

CaF_2 is toxic and a problematic neutron source for (α,n)-reactions:

$$^{19}F + \alpha \rightarrow {}^{22}Na^{*} + n$$
$$^{22}Na^{*} \rightarrow {}^{22}Na + \gamma(1528\,\mathrm{keV})$$

NNL applied an alkali aluminoborosilicate formulation originally developed for K-basin wastes at Hanford.

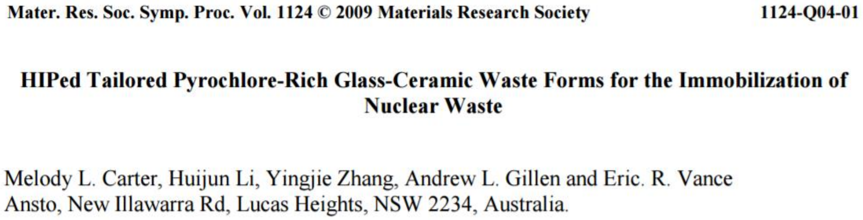

Mater. Res. Soc. Symp. Proc. Vol. 1124 © 2009 Materials Research Society **1124-Q04-01**

HIPed Tailored Pyrochlore-Rich Glass-Ceramic Waste Forms for the Immobilization of Nuclear Waste

Melody L. Carter, Huijun Li, Yingjie Zhang, Andrew L. Gillen and Eric. R. Vance
Ansto, New Illawarra Rd, Lucas Heights, NSW 2234, Australia.

Carter *et* al. (2009)

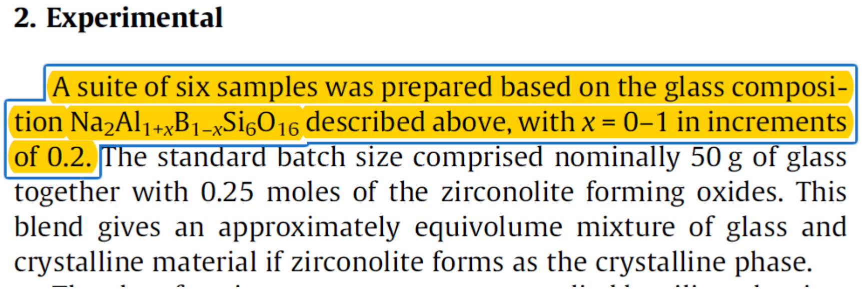

2. Experimental

A suite of six samples was prepared based on the glass composition $Na_2Al_{1+x}B_{1-x}Si_6O_{16}$ described above, with x = 0–1 in increments of 0.2. The standard batch size comprised nominally 50 g of glass together with 0.25 moles of the zirconolite forming oxides. This blend gives an approximately equivolume mixture of glass and crystalline material if zirconolite forms as the crystalline phase.

Maddrell *et* al. 2015

Formulation development

Glass Fraction (wt%)	Glass Composition: $Na_2Al_{1+x}B_{1-x}Si_6O_{16}$					
	X = 0	X = 0.2	X = 0.4	X = 0.6	X = 0.8	X = 1.0
30	$Na_2AlBSi_6O_{16}$	$Na_2Al_{1.2}B_{0.8}Si_6O_{16}$	$Na_2Al_{1.4}B_{0.6}Si_6O_{16}$	$Na_2Al_{1.6}B_{0.4}Si_6O_{16}$	$Na_2Al_{1.8}B_{0.2}Si_6O_{16}$	$Na_2Al_2Si_6O_{16}$
50	$Na_2AlBSi_6O_{16}$	$Na_2Al_{1.2}B_{0.8}Si_6O_{16}$	$Na_2Al_{1.4}B_{0.6}Si_6O_{16}$	$Na_2Al_{1.6}B_{0.4}Si_6O_{16}$	$Na_2Al_{1.8}B_{0.2}Si_6O_{16}$	$Na_2Al_2Si_6O_{16}$
70	$Na_2AlBSi_6O_{16}$	$Na_2Al_{1.2}B_{0.8}Si_6O_{16}$	$Na_2Al_{1.4}B_{0.6}Si_6O_{16}$	$Na_2Al_{1.6}B_{0.4}Si_6O_{16}$	$Na_2Al_{1.8}B_{0.2}Si_6O_{16}$	$Na_2Al_2Si_6O_{16}$

Increased glass fraction reduced the yield of zirconolite

Increased Al, increased zirconolite

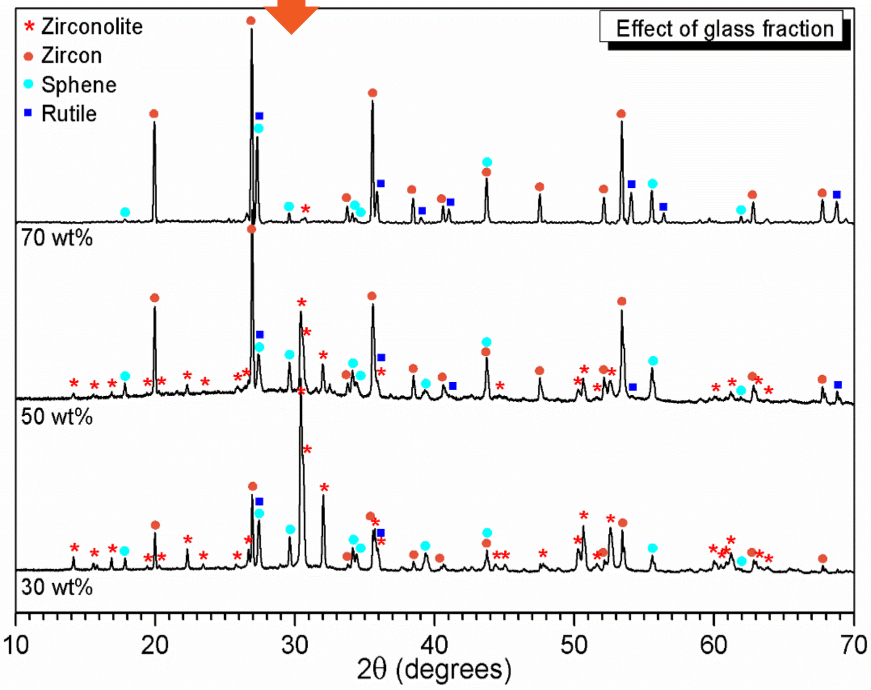

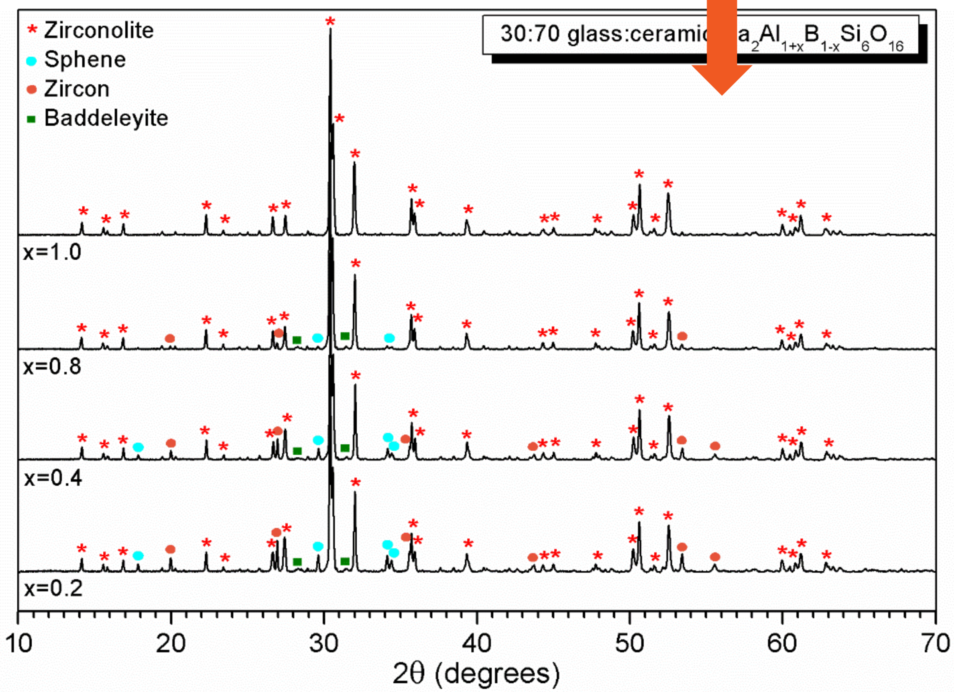

Formulation development

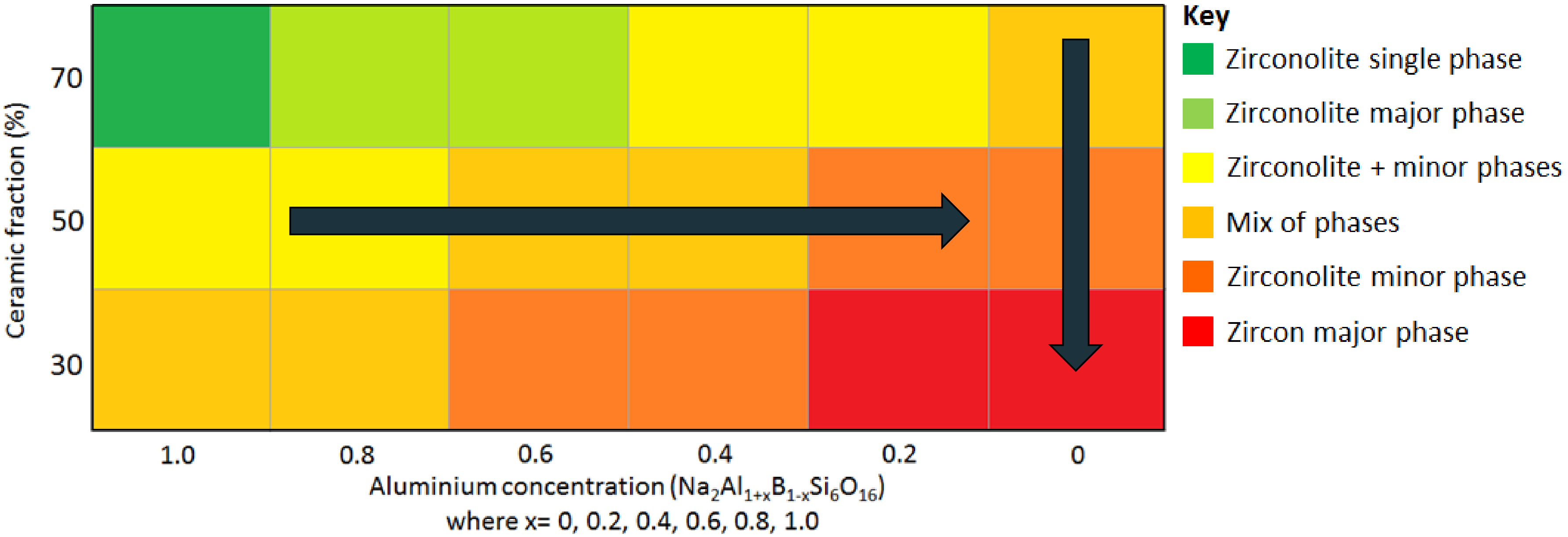

- When $Al_2O_3 \leq Na_2O$ all Al^{3+} is stabilised as tetrahedral units.

- When $Al_2O_3 < Na_2O$ there is excess Na_2O available to stabilise other elemental species and create NBOs.

- Connelly *et* al. predicted the preferential charge compensation of different ions in alkali aluminoborosilicate glasses: **$Al^{3+} > Zr^{4+} > Ti^{4+} > B^{3+} > Si^{4+}$**

↓ Al_2O_3 ↑ Excess Na_2O ↑ Zr^{4+} and Ti^{4+} in glass ↓ Glass connectivity ↑ CaO in glass ↓ $CaZrTi_2O_7$

- SiO_2 acts as the primary glass network former. At low glass fractions all the SiO_2 is consumed within the glass phase, the high glass fraction samples the Si^{4+} is more available to form crystalline phases.

Waste incorporation

Single phase formulation was used for Ce waste incorporation experiments: **30wt% glass phase $Na_2Al_2Si_6O_{16}$**

Sample	Target ceramic composition	Target Ce oxidation state
A	$Ca_{0.8}Ce_{0.2}ZrTi_{1.6}Al_{0.4}O_7$	4+
B	$Ca_{0.9}Ce_{0.1}Zr_{0.9}Ce_{0.1}Ti_2O_7$	3+
C	$CaZr_{0.8}Ce_{0.2}Ti_2O_7$	4+

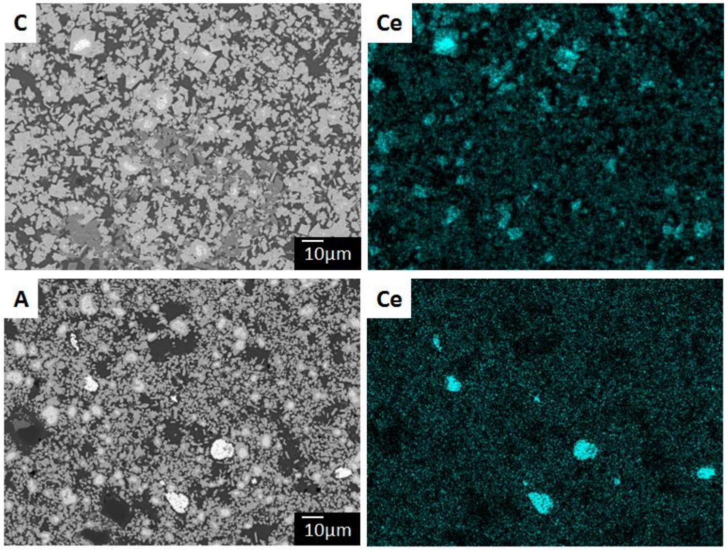

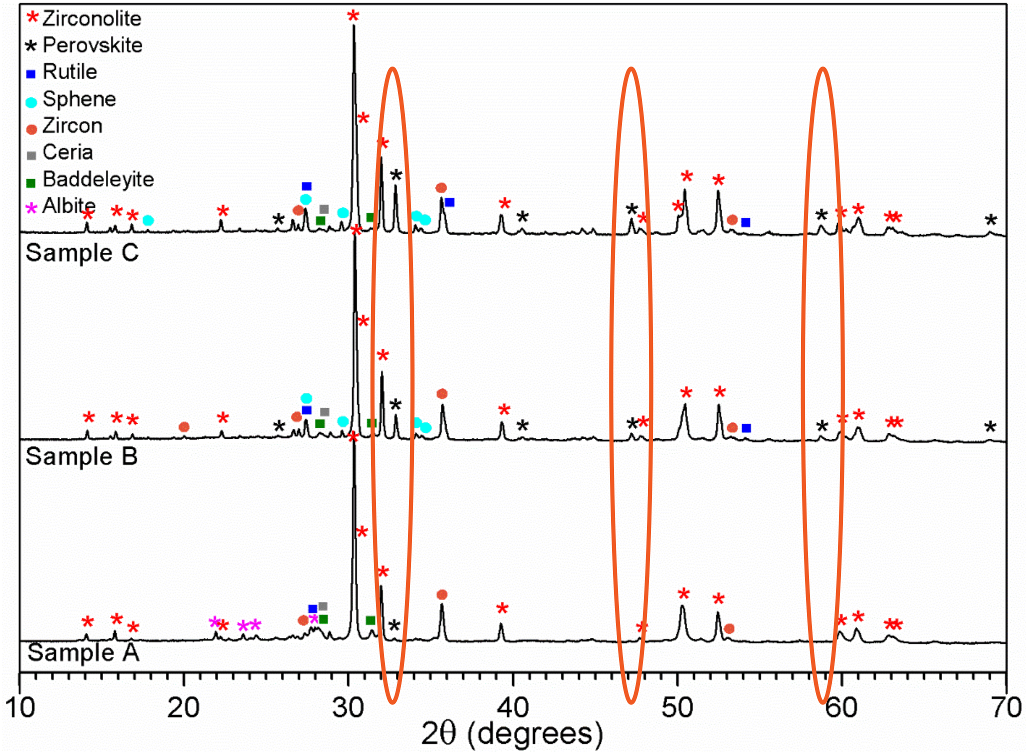

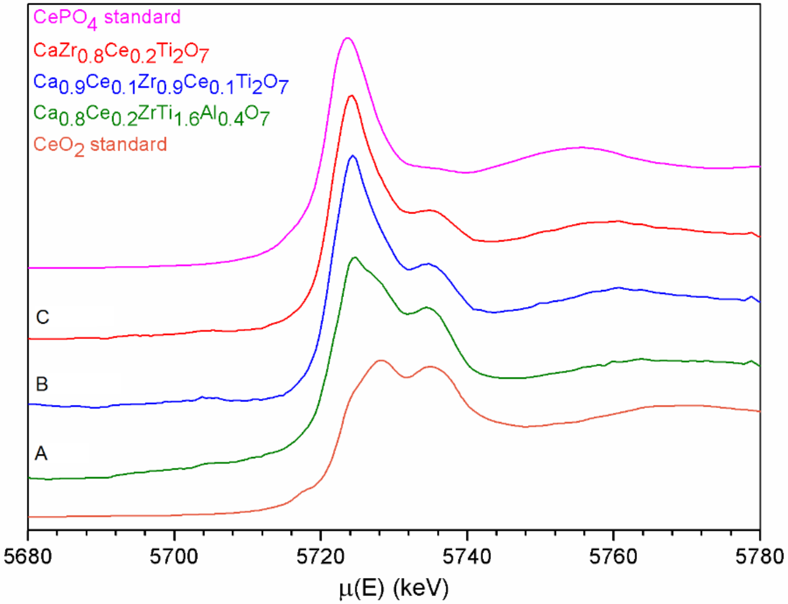

Waste incorporation

Single phase formulation was used for Ce waste incorporation experiments: **30wt% glass phase $Na_2Al_2Si_6O_{16}$**

Sample	Target ceramic composition	Target Ce oxidation state
A	$Ca_{0.8}Ce_{0.2}ZrTi_{1.6}Al_{0.4}O_7$	4+
B	$Ca_{0.9}Ce_{0.1}Zr_{0.9}Ce_{0.1}Ti_2O_7$	3+
C	$CaZr_{0.8}Ce_{0.2}Ti_2O_7$	4+

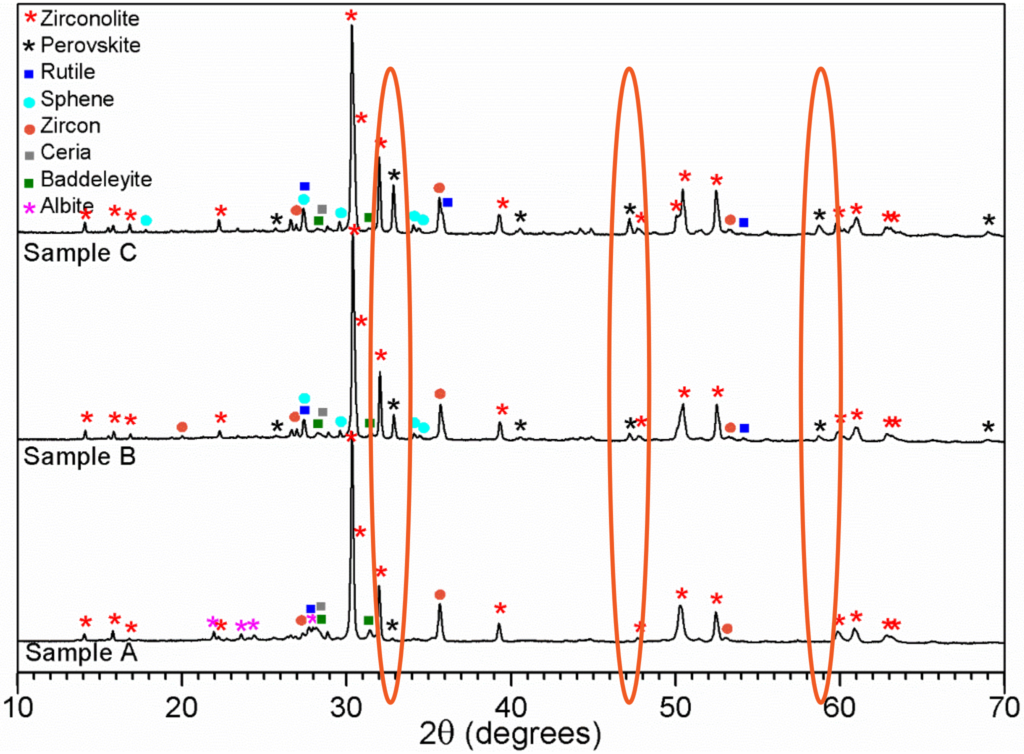

Zirconolite structure:	**Ionic Radii**
Ca^{2+} in 8-fold coordination	1.12Å
Zr^{4+} in 7-fold coordination	**0.78Å**
Ti^{4+} in 5/6- fold coordination	0.51-0.605Å
Perovskite: **Ca^{2+} in 12-fold coordination**	**1.34Å**

Ce^{4+}	**Ionic Radii**
8-fold coordination	0.97Å
7-fold coordination	***0.92Å***
6-fold coordination	0.87Å
Ce^{3+}	
12-fold coordination	**1.34Å**
8-fold coordination	1.14Å
7-fold coordination	1.07Å

Chlorine solubility

Pu-residues stored in PVC packaging are contaminated with Cl.

Can we retain Cl in our HIPed samples?
What is the solubility limit of Cl in our glass-ceramics?
Can we immobilise the Pu (Ce) separately to the Cl?

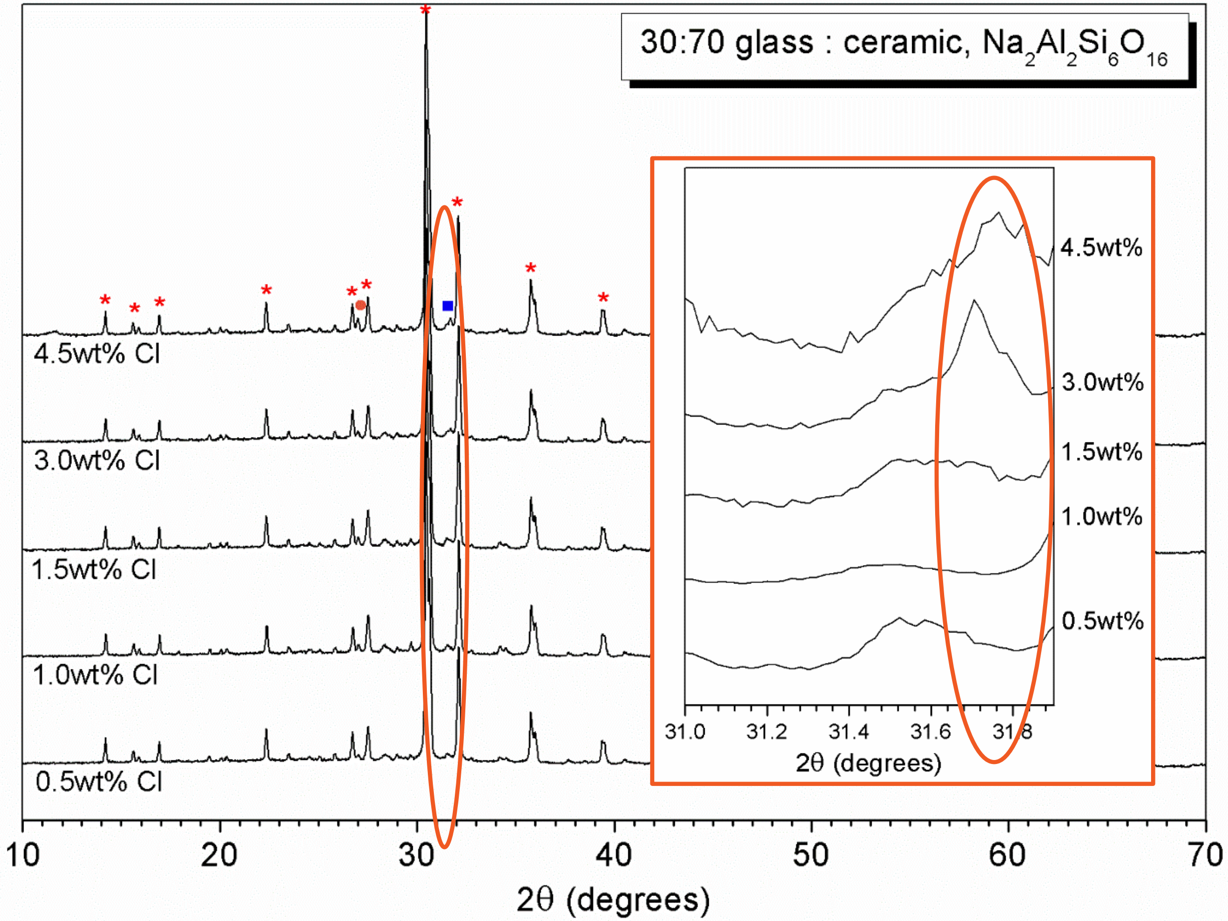

Image courtesy of NNL

Residual NaCl seen between 1.5 – 2.0 wt%

Expected upper limit in Pu-resides is 0.1 wt%.

Stewart *et* al. TMS2013

Chlorine solubility

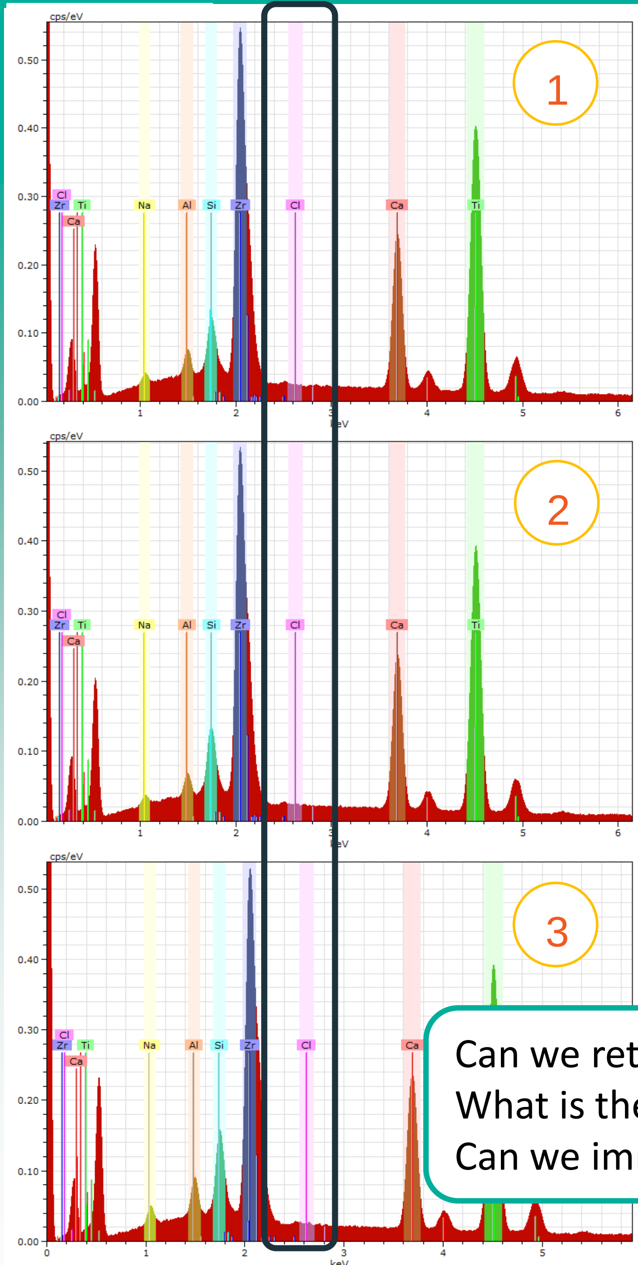

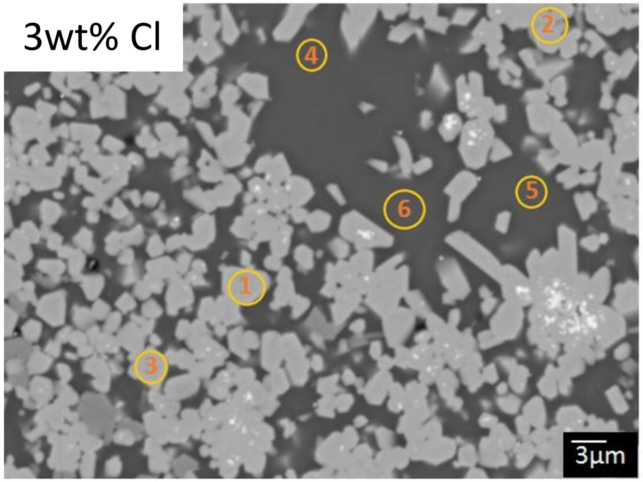

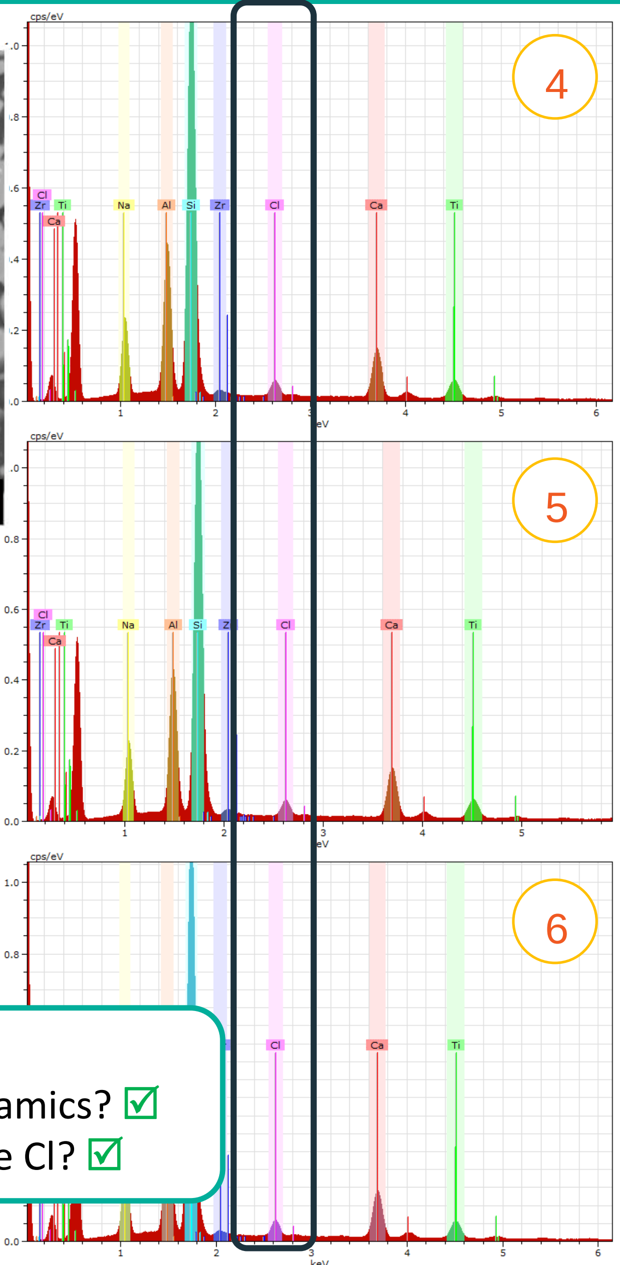

Zirconolite Phase	Glass Phase
Cl = 0.03	Cl = 1.37
Cl = 0.05	Cl = 1.52
Cl = 0.00	Cl = 1.45

Cl preferentially partitioned into the glass phase

Can we retain Cl in our HIPed samples? ☑
What is the solubility limit of Cl in our glass-ceramics? ☑
Can we immobilise the Pu (Ce) separately to the Cl? ☑

Still to come…

- Uranium and Plutonium HIP samples at ANSTO

- U-HIP to support our Ce work
- Pu-HIP to investigate the partitioning of Pu with respect to oxygen fugacity

Nuclear Decommissioning Authority

Australian Government

ansto

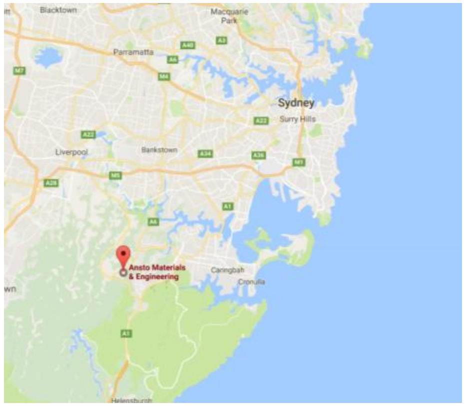

Active HIP facility at University of Sheffield

AIP AMERICAN ISOSTATIC PRESSES, INC.

DISTINCTIVE

Designed and manufactured by AIP as the first official research active HIP facility in the UK.
The first active containment designed for repeated use.

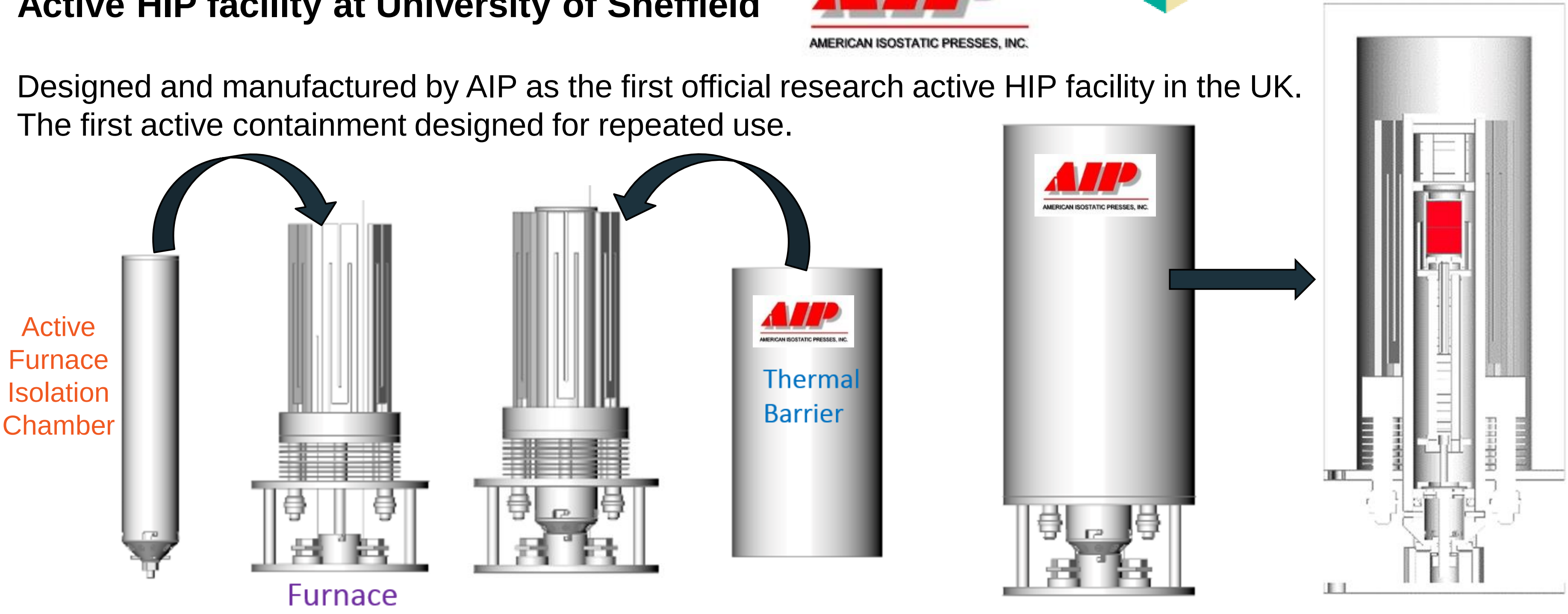

Summary

Process optimisation : the use of a two step heat treatment during sample preparation ensures high quality and reproducible HIPed wasteforms.

Formulation optimisation : a single phase zirconolite glass-ceramic formulation was determined. Increasing Al_2O_3 favours the formation of zirconolite. Changes to the glass composition and fraction effect the glass structure such that a less polymerised glass stabilises more Zr^{4+} and Ti^{4+} in the glass.

Ce incorporation : Ce substitution on either the Ca and / Zr sites showed a limitation of Ce^{4+} on the Zr site resulting in the formation of a Ce-bearing perovskite. When targeting Ce on the Ca site the perovskite yield was reduced and XANES showed better retention of Ce^{4+} in the Al charge compensated sample.

Cl contamination : Cl was successfully retained and incorporated into our HIP glass-ceramics. The Cl was preferentially incorporated in the glass phase therefore separate to Ce / Pu in the wasteform. The solubility limit of Cl in the glass was around 1.5 wt%, which is far above the expected contamination levels in Pu-residues.

Still to come…. U and Pu HIP samples at ANSTO.
Installation of AIP’s active furnace isolation chamber at Sheffield’s HIP facility.

Acknowledgements

Prof Neil Hyatt

Dr Martin Stennett

Dr Ewan Maddrell

Dr Paul Heath

Sam Moricca – AIP

AIP
AMERICAN ISOSTATIC PRESSES, INC.

The University Of Sheffield.

NDA
Nuclear Decommissioning Authority

NucleUS
Immobilisation Science Laboratory

midas

DISTINCTIVE

DELTA

Australian Government
ansto

References

Nuclear Decommissioning Authority, Conditioning of Plutonium Residues by Hot Isostatic Pressing and Options for packaging and Disposal (pre-conceptual stage) Summary of Assessment Report. (2009).

C.R.Scales, E.R.Maddrell, N.Gawthorpe, B.D.Begg, S.Moricca, R.A.Day, M.W.A.Stewart, "Development of a process for the immobilization of actinide containing residues on the Sellafield site," International conference of environmental remediation and radioactive waste management, (2005).

B. D. Begg, E. R. Vance, The incorporation of cerium in zirconolite, Mat. Res. Soc. Symp. **465, (**1997).

B. D. Begg, R. A. Day, A. Brownscombe, Structural effect of Pu substitutions on the Zr-site in zirconolite, Mat. Res. Soc. Symp. **663**, (2001).

M. Gilbert, J. H. Harding, Energetics of Ce and Pu incorporation into zirconolite waste-forms, Phys. Chem. Phys. **13, (**2011).

E.R. Vance, M.W.A. Stewart, and S.A. Moricca, "Progress at ANSTO on SYNROC," J. Aust. Ceram. Soc., **50** [1] 38–48 (2014).

E. Maddrell, S. Thornber, and N. Hyatt, "The influence of glass composition on crystalline phase stability in glass-ceramic wasteforms," J. Nucl. Mater., (2014).

https://www.csun.edu/~hcchm003/321/Ered.pdf accessed on 10/11/2016

M. Carter et al., HIPed Tailored Pyrochlore-rich Glass-ceramic wasteforms for the immobilisation of Nuclear waste, 2009

Stewart *et* al, Glass-Ceramic Waste Forms for Uranium and Plutonium Residues Wastes, WM2013, 2013

Day et. Technical Demonstration of Zirconolite Glass-Ceramics Processed in a Hot Isostatic Press: An Option for Immobilisation of Actinide Containing Residues at Sellafield, ICEM05, 2005

REAL-TIME FAST NEUTRON ASSAY

for plutonium storage and ageing applications

Last Update: November 14, 2016

Rashed Sarwar

PhD Student
Engineering Department
Lancaster University

PROJECT OVERVIEW

THE PROJECT

→ **Objective:**

1. Can plutonium (^{240}Pu) be discerned from curium (^{244}Cm) in the field on the basis of differences in their fast neutron fission multiplicity distributions?
2. Can the relative difference between uncorrelated, 'singles' neutrons derived from americium (^{241}Am) and correlated neutron emissions from plutonium (^{240}Pu) be exploited to infer plutonium ageing?

→ **Motivation:**

1. Small quantity of curium in waste assay can result in severe over-estimation of plutonium and under-estimation of uranium content as well as large uncertainties
2. Can act as intense neutron source, masking signal from plutonium

MULTIPLICITY

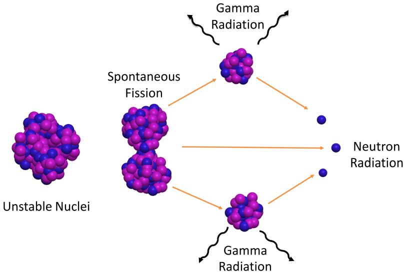

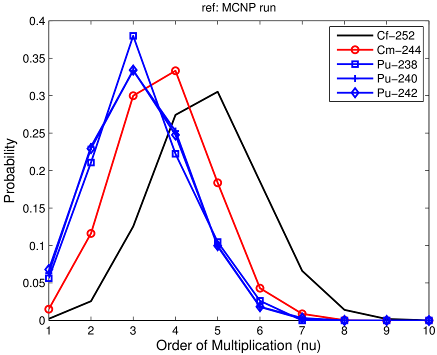

PROGRESS

HARDWARE: MULTIPLICITY REGISTER

Based on Altera DE1-SoC FPGAs

- → Runs linux kernel to allow user to connect monitor and keyboard to use device as a standalone system.
- → Rossi-α & Feynman-Y using shared circuit
- → Time-of-flight analysis

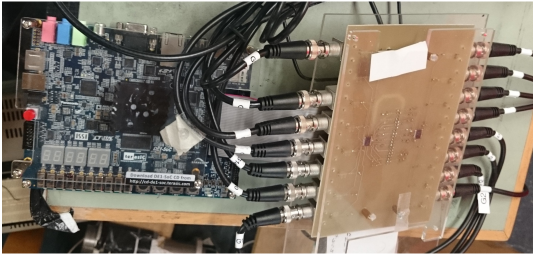

ROSSI-α AND COINCIDENCE DISTRIBUTIONS

- → **Expectation:** Higher order of coincidence for exposed setups compared to secured ones. Higher order of coincidence for joint setups compared to neutron ones.

- → **Exposed:** source at the edge of the tank to expose coincidence events.
- → **Secured:** source at the centre of the tank to hide coincidence events.
- → **Joint:** combined neutron and gamma triggers.

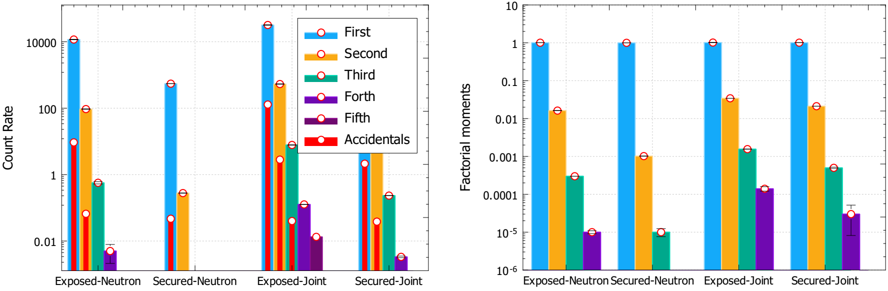

ASSAY

HE3 ASSAY

Modelling He-3 assay in GEANT4 using following physics models:

→ **hadElastic:** Elastic: 4 eV ---> 20 MeV; Model: ThermalScattering: 0 meV ---> 4 eV

→ **Inelastic:** NeutronHPInelastic: 0 meV ---> 20 MeV

→ **nCapture:** NeutronHPCapture: 0 meV ---> 20 MeV

→ **nFission:** NeutronHPFission: 0 meV ---> 20 MeV

→ **Deexcitation model:**
eIoni & eBrem for e- and e+;
annihil for e+;
hIoni, hBrems & hPairProd for γ;
ionIoni & nuclearStopping for Ions;

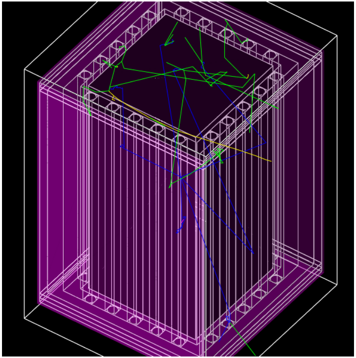

→ **He-3 Density:** 0.0000452*g/cm^3

→ **Efficiency:** 22.94 %

→ **Absolute efficiency:** 7.64 %

LIQUID SCINTILLATION ASSAY

- → **LSD Density:** 0.964*g/cm^3
- → **Efficiency (16-128 detector):** 17.48-35.94 %
- → **Absolute efficiency (16-128 detector):** 5.83-11.98 %

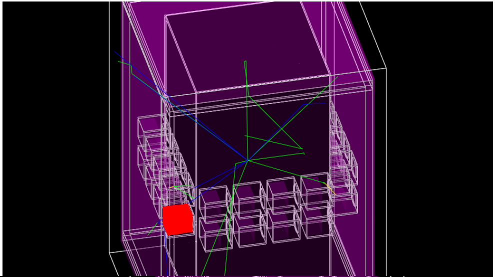

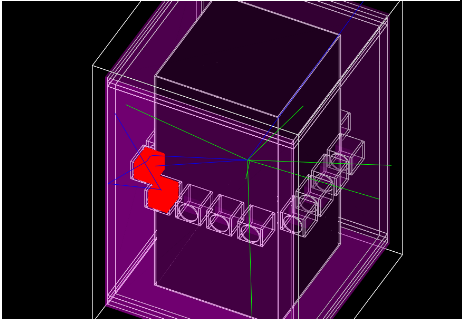

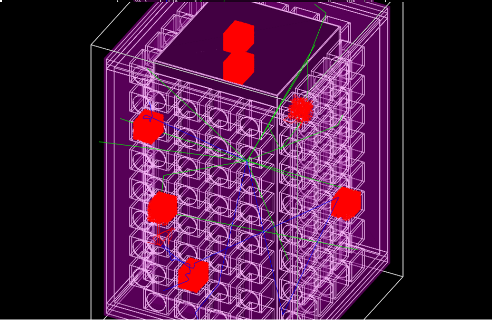

HE3 ASSAY

- → **Detected:** number of neutrons detected from each fission event. this illustrates the efficiency of the He-3.
- → **Foregound distribution:** multiplicity distribution showing close to theoretical multiplicity despite low efficiency due to the large gatewidth.
- → **Background distribution:** very high accidental counts.

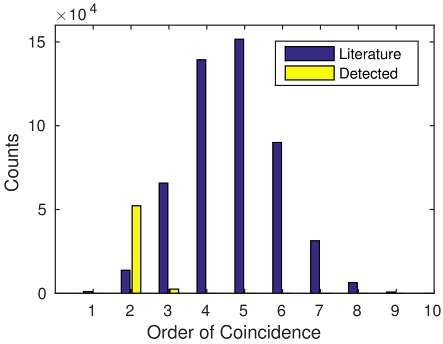

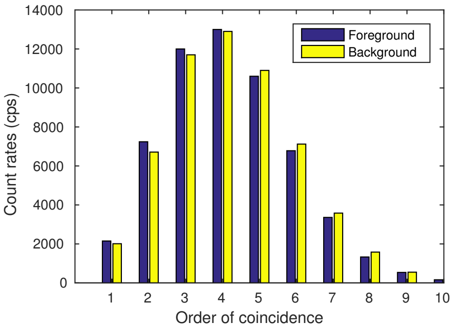

LIQUID SCINTILLATION ASSAY

→ **Detected:** number of neutrons detected from each fission event. this illustrates the efficiency of the LSD.

→ **Foregound distribution:** multiplicity distribution showing close to detected multiplicity reflecting low accidental counts due to the small gatewidth.

→ **Background distribution:** very small accidental counts.

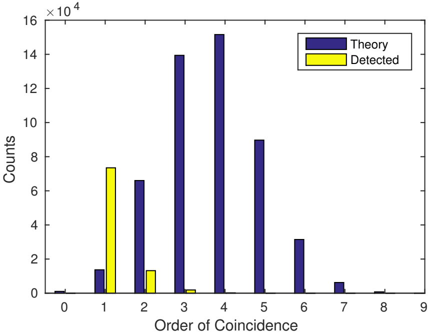

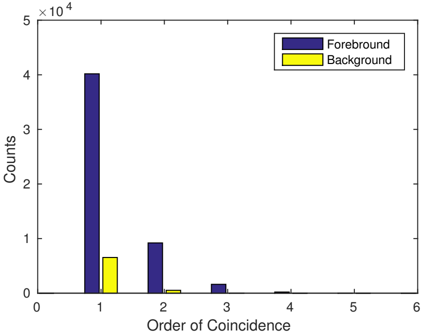

MULTIPLICITY UNFOLDING

METHOD 1: PROBABILITY DISTRIBUTION FUNCTIONS

Using probability distribution functions based transfer function using simulated cases in GEANT4.

- → **We know:** number of particle being generated in each fission event in GEANT4.
- → **We know:** number of particle detected detected during each fission event in GEANT4.
- → **We make:** 2D probability distribution function which can be used as a transfer function.
- → **We transform:** the number of neutron detected in experiment and map it to the theoretical distribution.

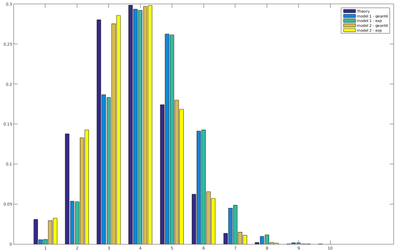

METHOD 2: ARTIFICIAL NEURAL NETWORK

- **Training:** using controlled experiments with known sources.
- **Input:** Detected distribution, runtime, number of detectors, source to detector distance, etc.
- **We make:** Output distribution, factorial moments, uncertainty.

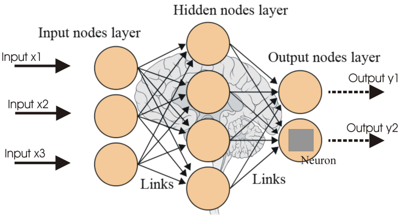

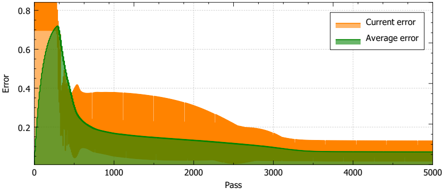

FUTURE WORK

FUTURE WORK

→ Unfolding multiplicity distribution

→ Controlled cross-talk based experiments

→ Semi-empirical model for neutron cross-talk

→ Designing of detection system

END OF FILE

Water Interactions with Actinide Oxide Surfaces

Bengt Tegner
School of Chemistry
The University of Manchester

DISTINCTIVE Theme 2 Meeting
14th November 2016
The Rheged Centre, Penrith

Outline

- Motivation
- Summary of Previous Work (Poster)
    - Water on UO_2(111), (110), and (100) Surfaces
- Results and Discussion
- Conclusions and Future Work
- Acknowledgements

Research Councils UK Energy For a Low Carbon Future

MANCHESTER 1824 The University of Manchester

DISTINCTIVE

Motivation

- The UK's stock of civil plutonium is stored as PuO_2 powder in multi layer steel cans in Sellafield.
- Under certain circumstances, gas generation may occur within the cans, with consequent pressurisation.
- Several proposed routes to gas production, including:

(i) steam produced by H_2O desorption from hygroscopic PuO_2 due to self-heating

(ii) radiolysis of adsorbed water

(iii) generation of H_2 by reaction of PuO_2 with H_2O, producing a "postulated" PuO_{2+x} phase

All involve PuO_2/H_2O interactions and are complex, inter-connected and poorly understood

⇒Model the interaction of water on PuO_2 surfaces at the atomic level

- method development
- initial results

Summary of Previous Work

- Results on the stoichiometric UO_2 (111), (110) and (100) surfaces suggest mixed adsorption on the (111) surface and dissociative adsorption on the (110) and (100) surfaces.
- Using these results we calculate water desorption temperatures for the most stable configurations on each surface at various pressures.
- These results have been written up and submitted for publication to the Journal of Physical Chemistry C.

Results: Desorption Temperatures

Conf. / Pressure	UO$_2$ (111) + 0.5 ML H$_2$O + 0.5 ML (OH + H)	UO$_2$ (110) + 1.0 ML (OH + H)	UO$_2$ (100) + 0.25 ML H$_2$O + 0.75 ML (OH + H)
$p = 10^{-13}$ bar	138	228	271
$p = 10^{-7}$ bar	186	301	356
$p = 1$ bar	300	472	555
$p = 3$ bar	313	490	577
$p = 5$ bar	319	499	587

Desorption temperatures in kelvins.

Results: UO_2 Surface Oxygen Vacancies

Surface	**(111)**	**(110)**	**(100)**
UO_2	6.45	5.69	5.93
UO_2 [3]	5.95 (-0.50)	5.38 (-0.31)	N/A

Oxygen vacancy formation energies in eV.

[3] T. Bo, J-H. Lan, C-Z. Wang, Y-L. Zhao, C-H. He, Y-J. Zhang, Z-F. Chai and W-Q. Shi, *J. Phys. Chem*. *C* **118** (2014) 21935–21944.

Results: Water on Reduced UO_2 (110)

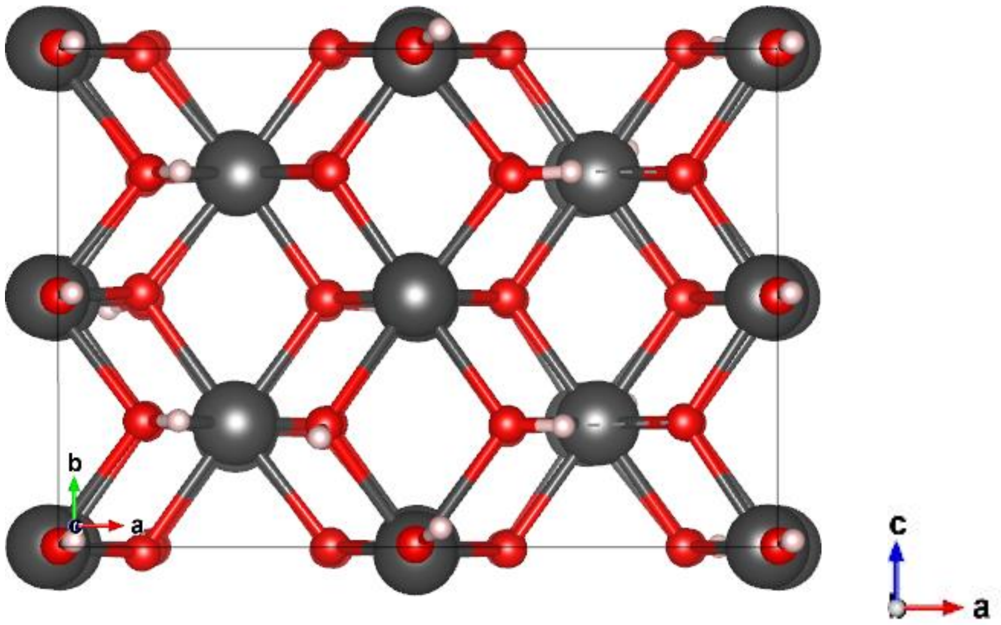

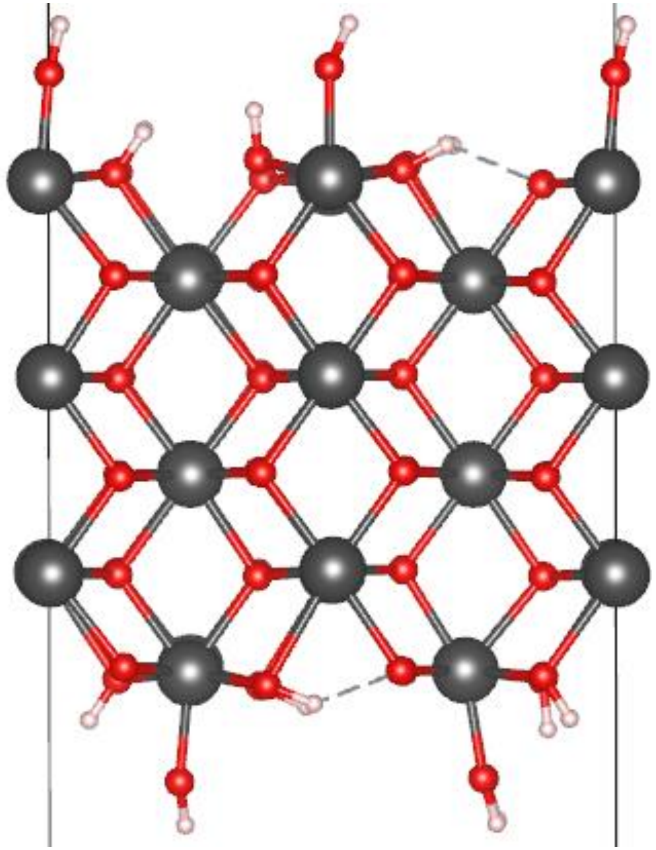

Dissociative

100% Coverage = 1 ML

Results: Water on Reduced UO_2 (110)

System	0.25 ML	1.0 ML
Stoichiometric $UO_2 + H_2O$	-0.93	-0.65
Stoichiometric UO_2 + OH + H	-1.39	-1.00
Reduced $UO_2 + H_2O$	-0.88*	-0.16*
Reduced UO_2 + OH + H	-1.50	-1.01

Adsorption energies in eV per water molecule.

Research Councils UK
Energy
For a Low Carbon Future

MANCHESTER
1824
The University of Manchester

DISTINCTIVE

Results: Water on Reduced UO_2 (100)

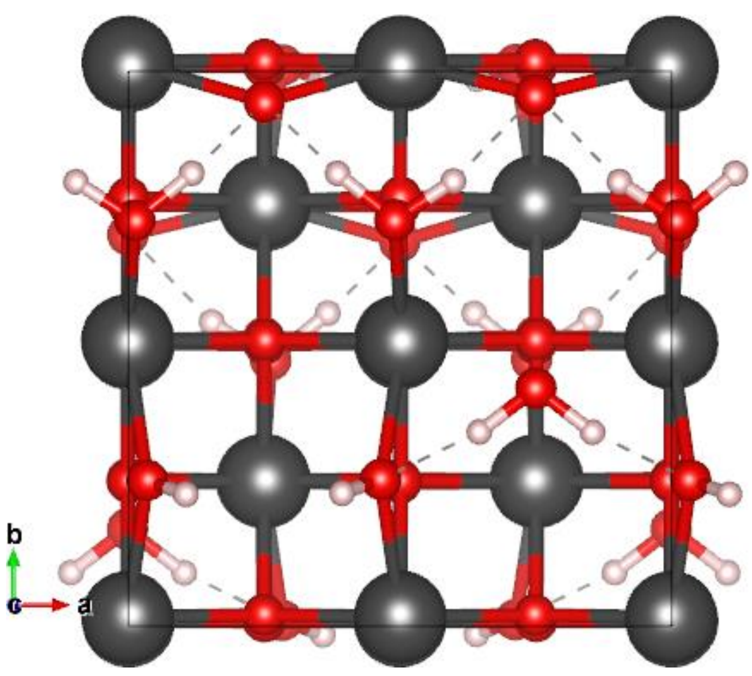

Molecular

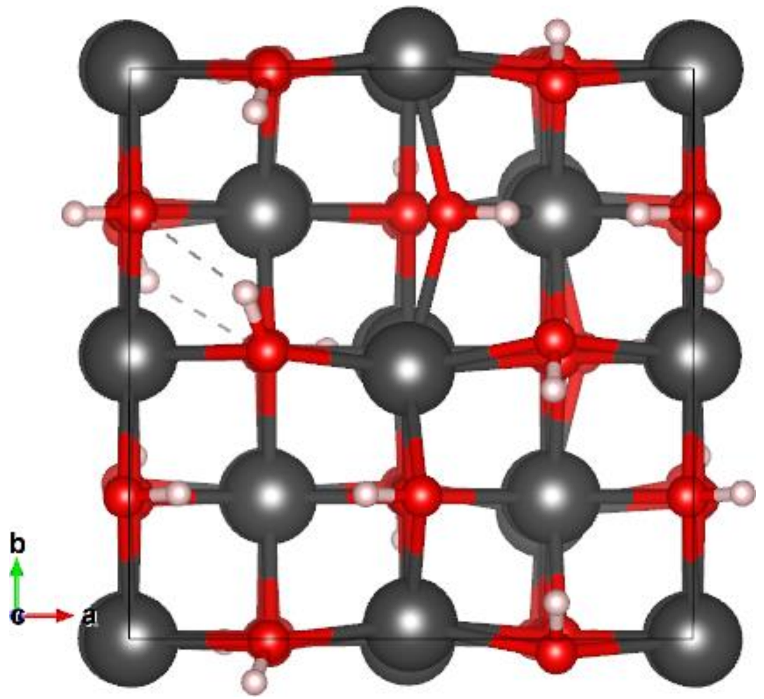

Dissociative

100% coverage = 1 ML

Results: Water on Reduced UO_2 (100)

System	0.25 ML	1.0 ML
Stoichiometric $UO_2 + H_2O$	-0.97	-0.86
Stoichiometric UO_2 + OH + H	-1.55	-1.01
Reduced $UO_2 + H_2O$	-1.62	-1.12
Reduced UO_2 + OH + H	-2.46*	-1.78

Adsorption energies in eV per water molecule.

Results: Extra Water on Wet UO_2 (111)

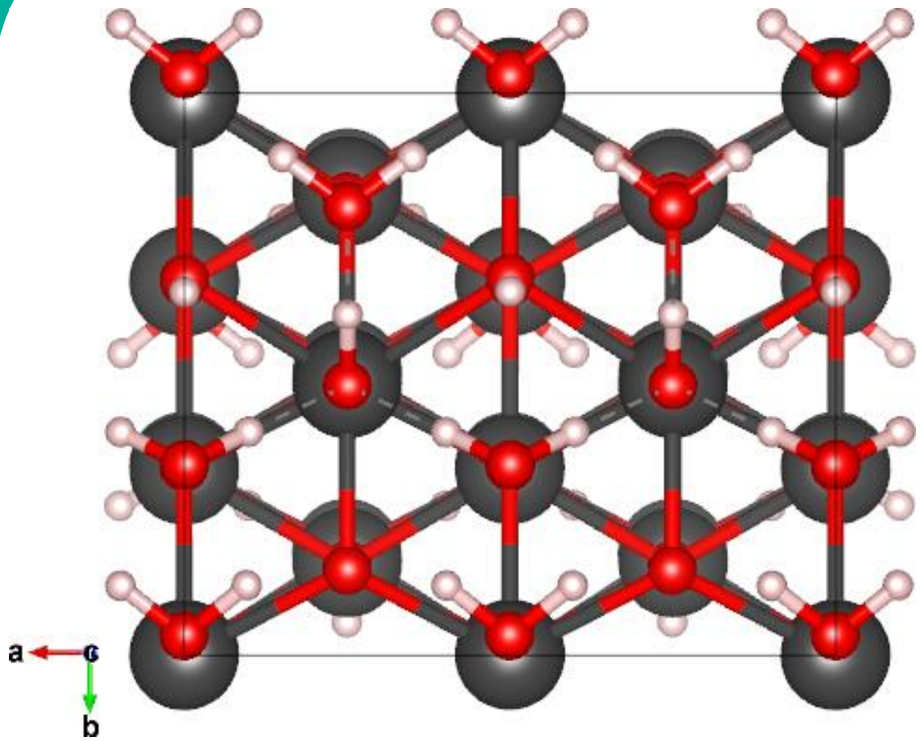

Mixed 50% Molecular and
50% Dissociative + 1 extra ML
Total Coverage = 2 ML

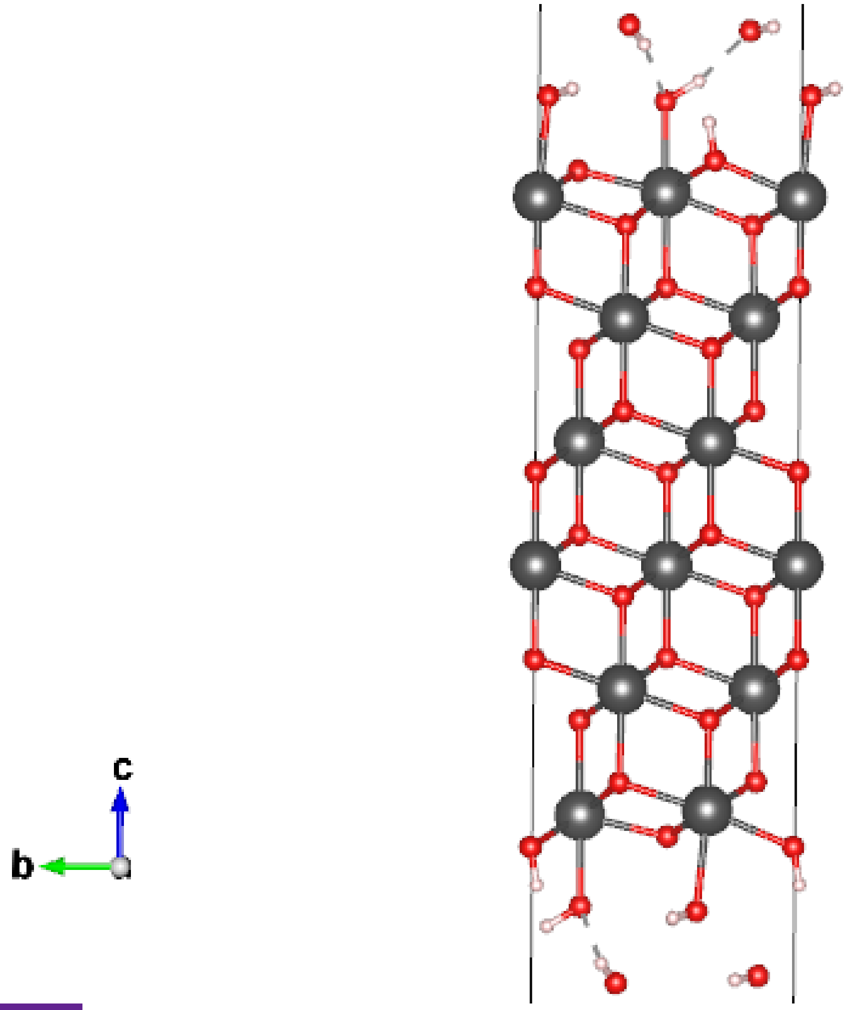

Research Councils UK Energy For a Low Carbon Future

MANCHESTER 1824
The University of Manchester

DISTINCTIVE

Results: Extra Water on Wet UO_2 (111)

System	1st Layer: 100% H_2O or 50% / 50% H_2O / OH + H	2nd Layer: 100% H_2O
$UO_2 + H_2O$	-0.59	N/A
UO_2 + 50% H_2O + 50% OH + H	-0.73	-0.07

Adsorption energies in eV per water molecule.

Results: Extra Water on Hydrox. UO_2 (111)

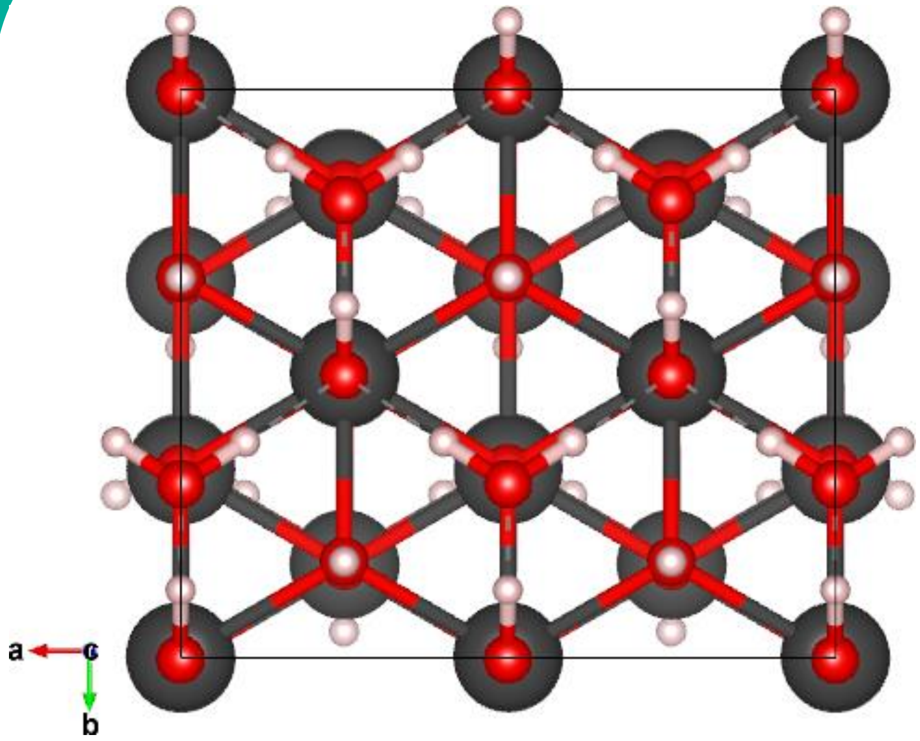

100% Dissociative + 1 extra ML

Total Coverage = 2 ML

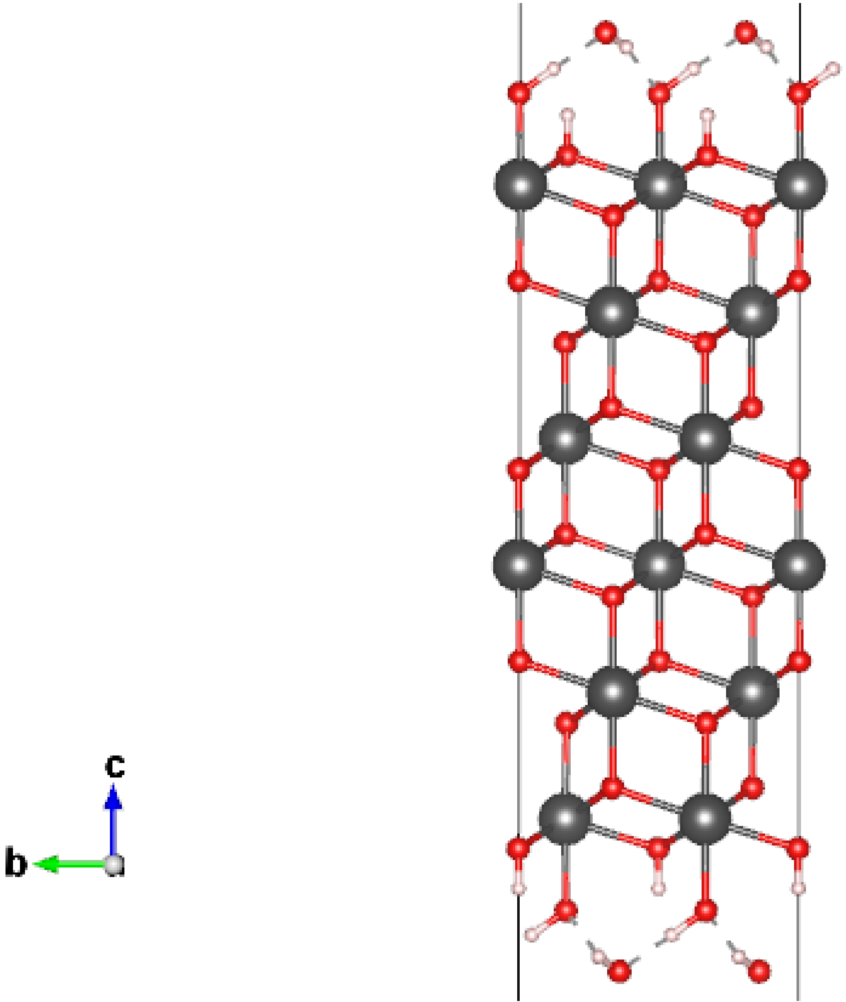

Research Councils UK Energy For a Low Carbon Future

MANCHESTER 1824 The University of Manchester

DISTINCTIVE

Results: Extra Water on Hydrox. UO_2 (111)

System	1st Layer: 100% H_2O or 100% OH + H	2nd Layer: 100% H_2O
$UO_2 + H_2O$	-0.59	N/A
UO_2 + OH + H	-0.32	-0.65

Adsorption energies in eV per water molecule.

Results: Extra Water on Hydrox. UO_2 (110)

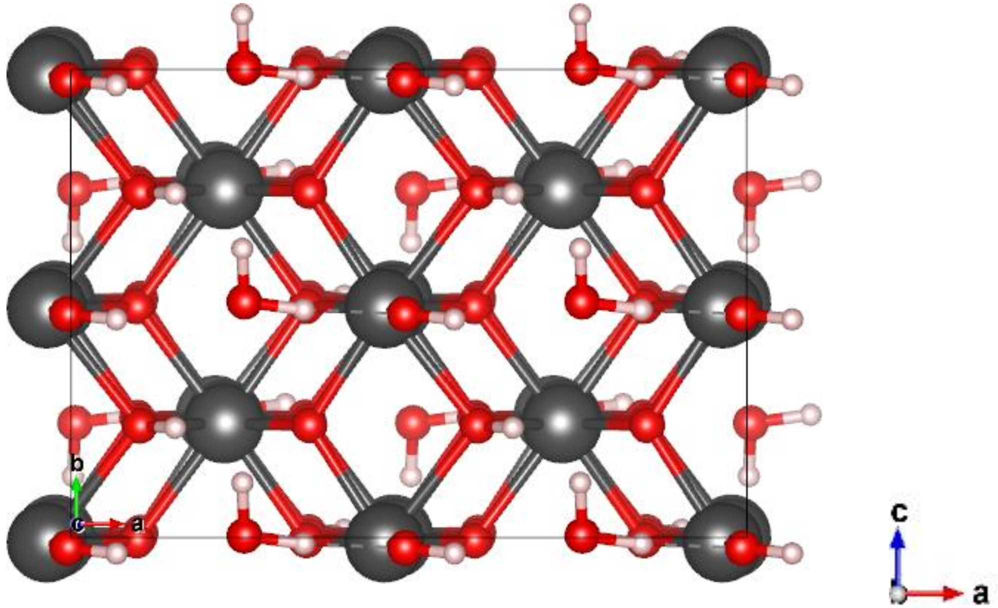

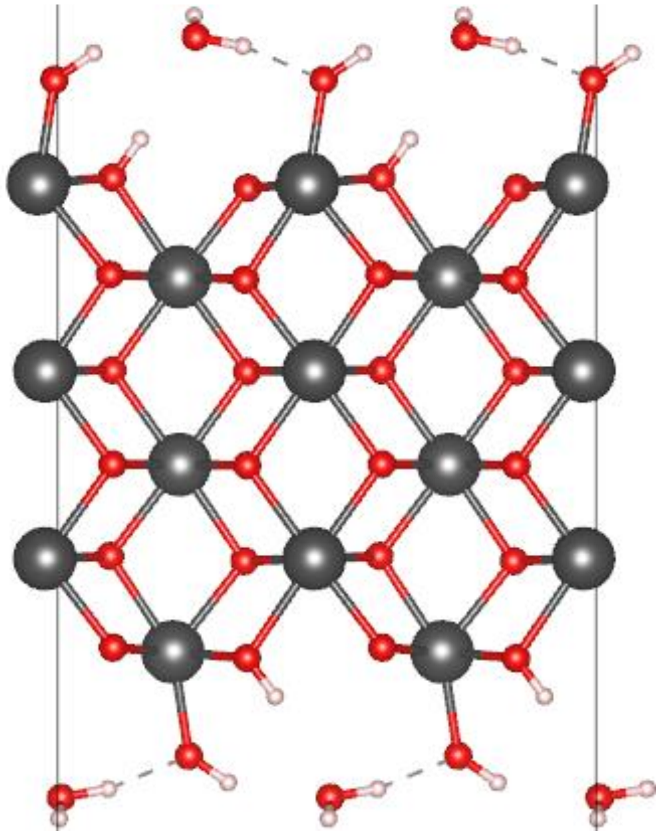

100% Dissociative + 1 extra ML
Total Coverage = 2 ML

Results: Extra Water on Hydrox. UO_2 (110)

System	1st Layer: 100% H_2O or 100% OH + H	2nd Layer: 100% H_2O
$UO_2 + H_2O$	-0.65	N/A
UO_2 + OH + H	-1.00	-0.57

Adsorption energies in eV per water molecule.

Results: Extra Water on Hydrox. UO_2 (100)

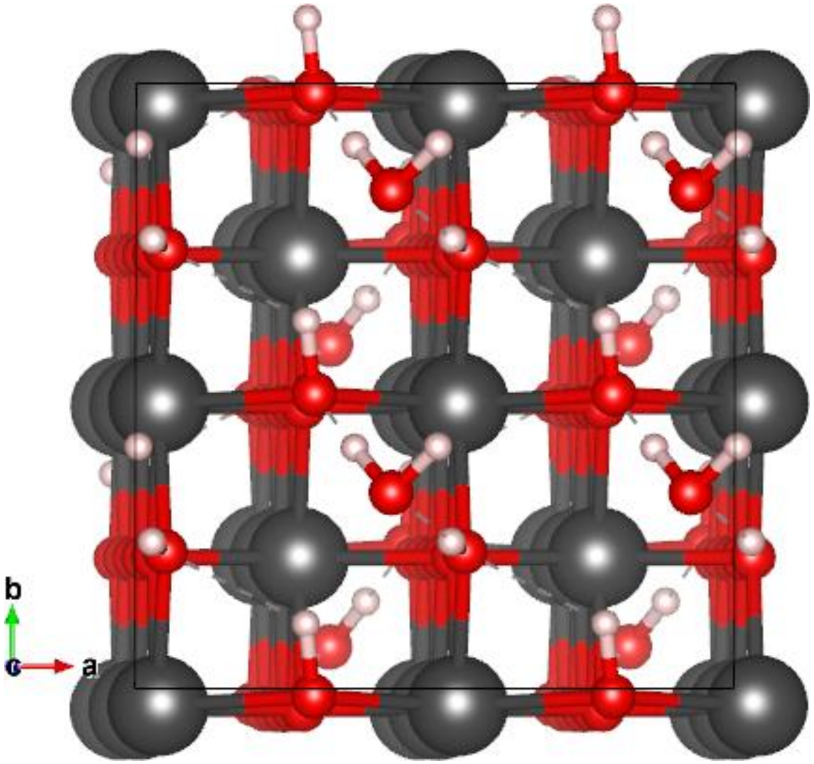

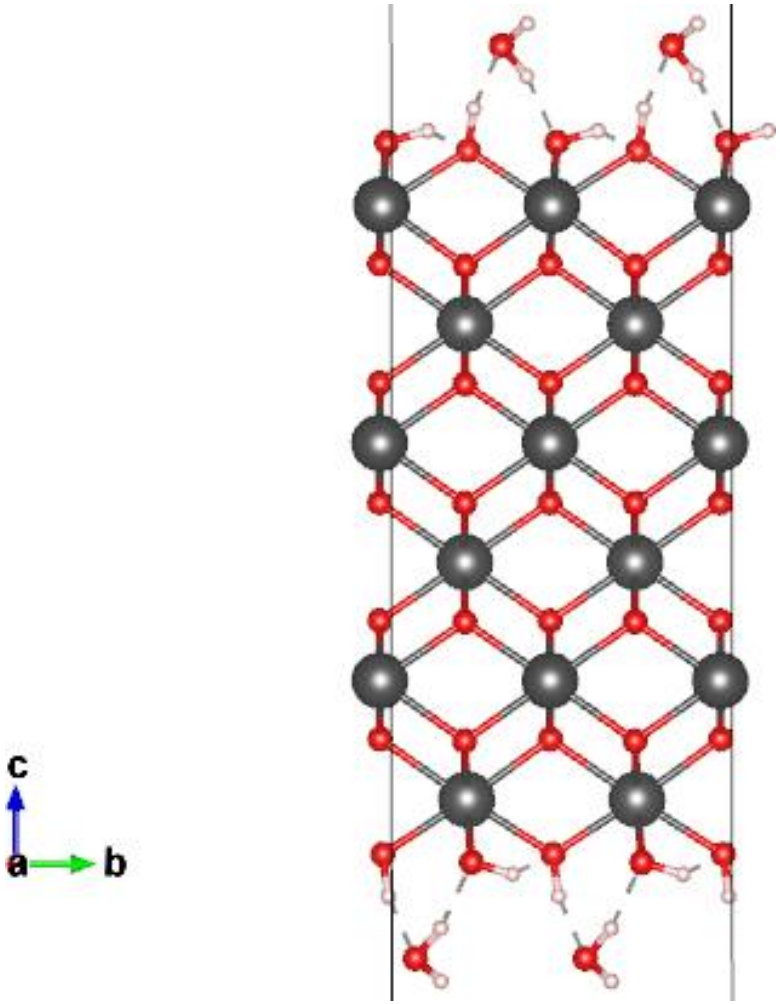

100% Dissociative + 1 extra ML

Total Coverage = 2 ML

Results: Extra Water on Hydrox. UO_2 (100)

System	1st Layer: 100% H_2O or 100% OH + H	2nd Layer: 100% H_2O
$UO_2 + H_2O$	-0.86	N/A
$UO_2 + OH + H$	-1.01	-0.78

Adsorption energies in eV per water molecule.

Research Councils UK Energy For a Low Carbon Future

MANCHESTER 1824 The University of Manchester

DISTINCTIVE

Conclusions and Future Work

- Results on the UO_2(111), (110) and (100) surfaces suggest mixed adsorption on the (111) surface and dissociative adsorption on the (110) and (100) surfaces.
- Using these results we predict the following water desorption temperatures (at p = 1 bar): 275 – 300 K for the (111) surface, 450 – 475 K for the (110) surface and 550 – 600 K for the (100) surface.
- Current and future work will focus on adsorption energies on or near defects followed by adsorption of multiple water layers.

Research Councils UK Energy For a Low Carbon Future

MANCHESTER 1824 The University of Manchester

DISTINCTIVE

Acknowledgements

Nik Kaltsoyannis, The University of Manchester

Andy Kerridge, Lancaster University

Marco Molinari and Steve Parker,
University of Bath

Jeff Hobbs and Helen Steele, Sellafield Ltd

Robin Orr and Howard Sims,
National Nuclear Laboratory

Research Councils UK
Energy
For a Low Carbon Future

MANCHESTER
1824
The University of Manchester

DISTINCTIVE

Computational Method

- Density Functional Theory
- VASP 5.4.1
- PAW-pseudopotentials
- Plane wave basis set
- k-point sampling of 1st BZ
- Spin-polarised
- DFT+*U* = PBE+*U*
- $U_{eff} = (U - J) = 4.0$ eV

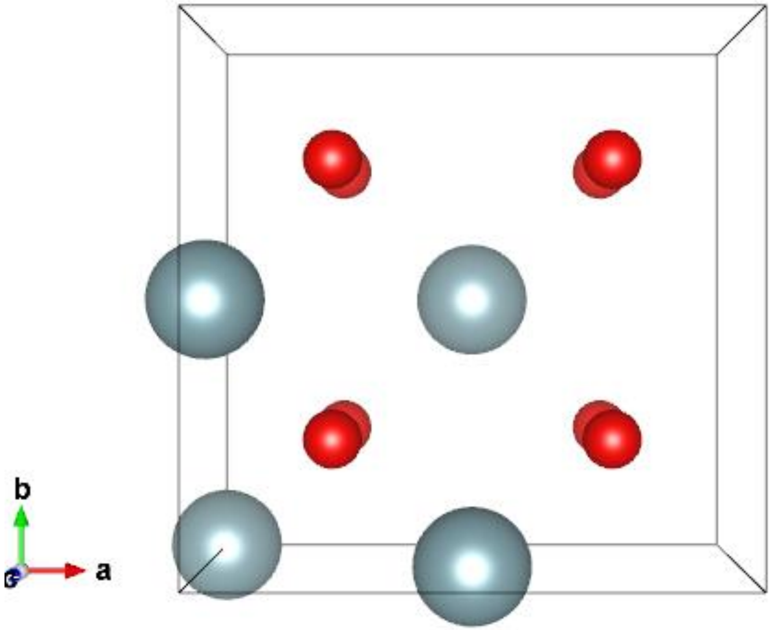

Research Councils UK Energy For a Low Carbon Future

MANCHESTER 1824 The University of Manchester

DISTINCTIVE

Computational Method

- Surfaces are modelled using a repeating slab of 24 UO_2 units with 18 Å of vacuum between each slab.
- Water is adsorbed on both sides of the slab to ensure the system has no net dipole moment.

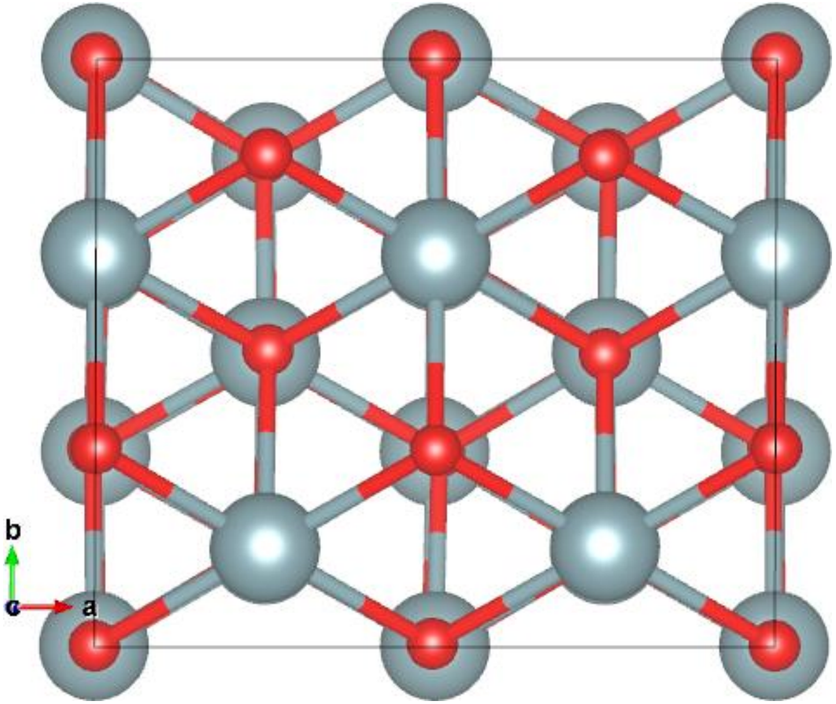

Radiolysis of H_2-O_2 mixtures at the interface with ceramic oxides - update

Luke Jones, Howard Sims, Robin Orr, Simon Pimblott

Luke.jones-2@manchester.ac.uk

Outline

- Update on DCF experimental work
    - ^{60}Co heterogeneous experiments
    - Ongoing accelerator work
    - Water adsorption on CeO_2

- Active work progression

- ARF proposals

Experiment (reminder)

- 3 gas mixtures:
  - 5 : 5 : 90 $H_2 : O_2 : Ar$
  - 5 : 2.5 : 92.5 $H_2 : O_2 : Ar$ (water stoichiometry)
  - 2.5 : 5 : 92.5 $H_2 : O_2 : Ar$ (O_2 excess)
- PuO_2 surrogate oxides – CeO_2 and ZrO_2
- 2 radiation sources – ^{60}Co γ-rays and 5.5 MeV He^{2+} ions
- Irradiations undertaken at atmospheric pressure and ambient temperature

^{60}Co - Gas phase- H_2 depletion

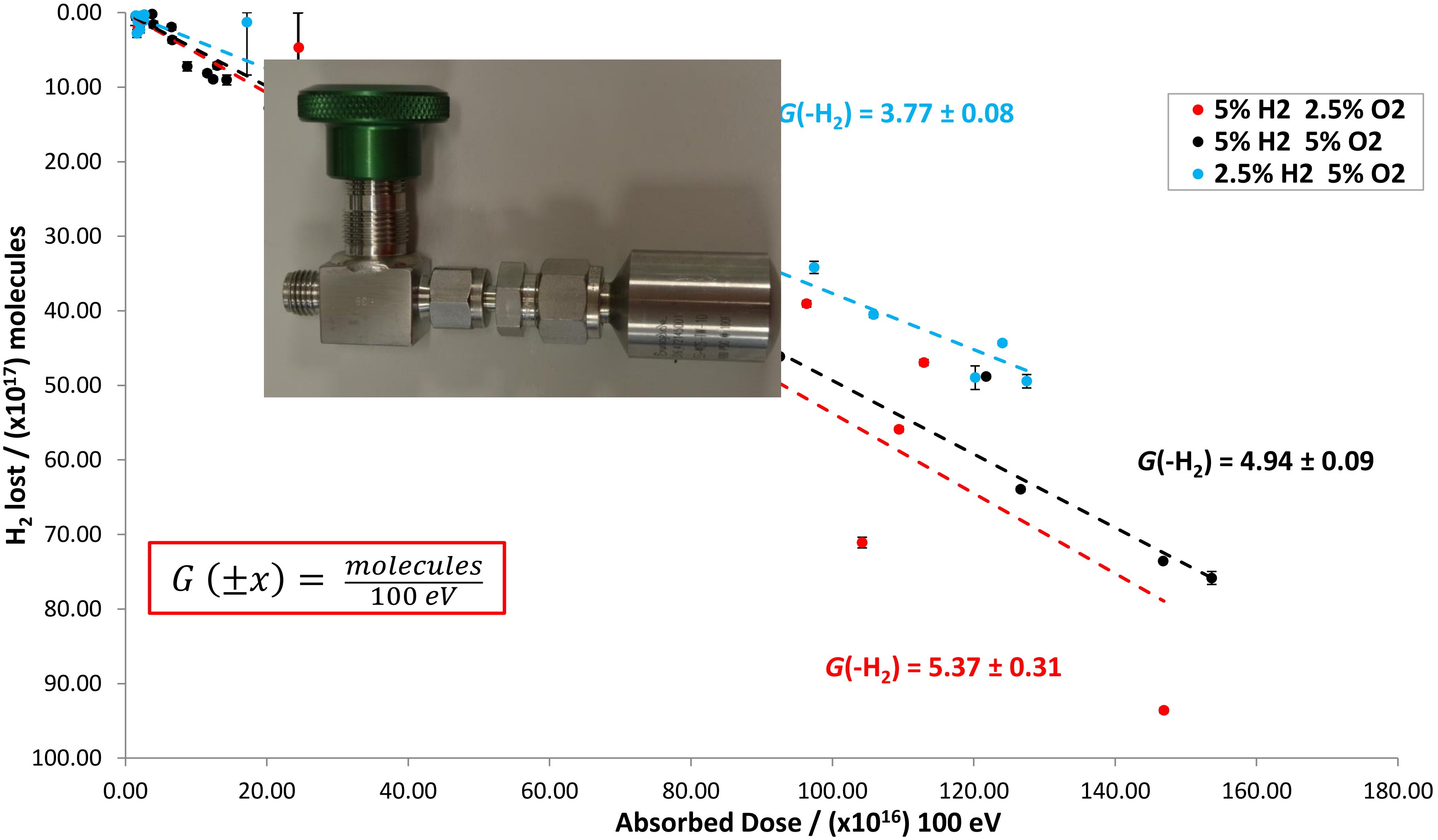

$$G\,(\pm x) = \frac{molecules}{100\ eV}$$

PuO_2 surrogate oxides – CeO_2 and ZrO_2

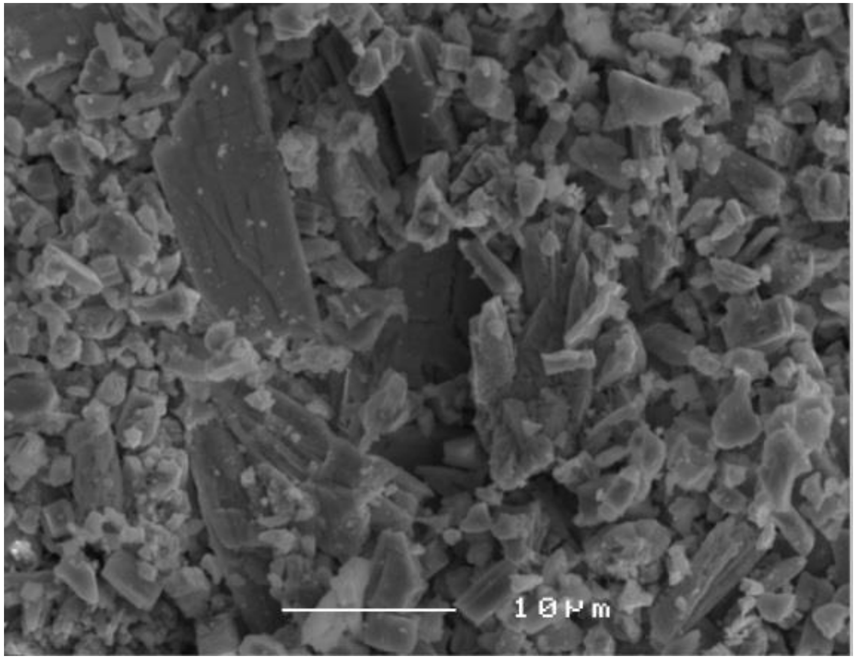

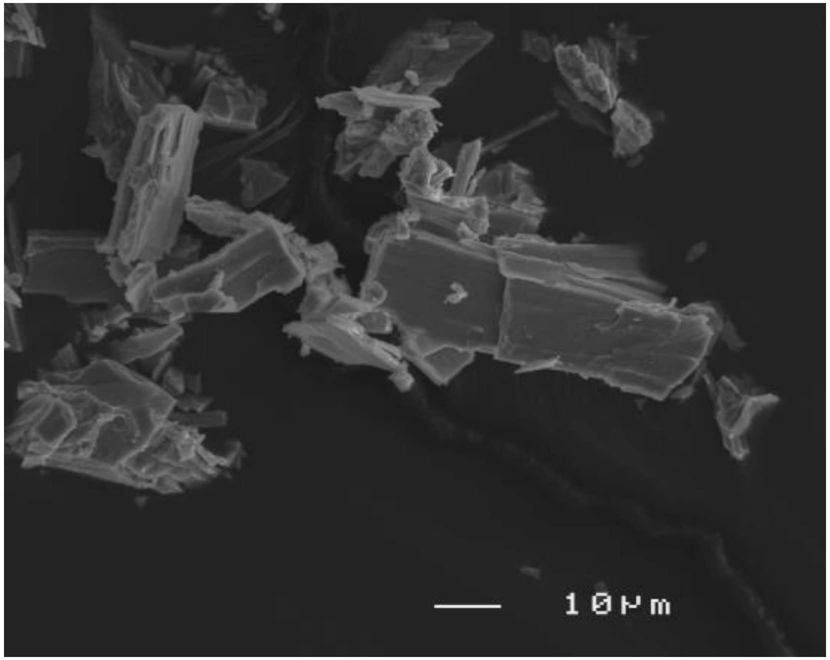

CeO_2
2.52 ± 0.02 $m^2\ g^{-1}$

ZrO_2
9.23 ± 0.03 $m^2\ g^{-1}$

Heterogeneous 5:5:90

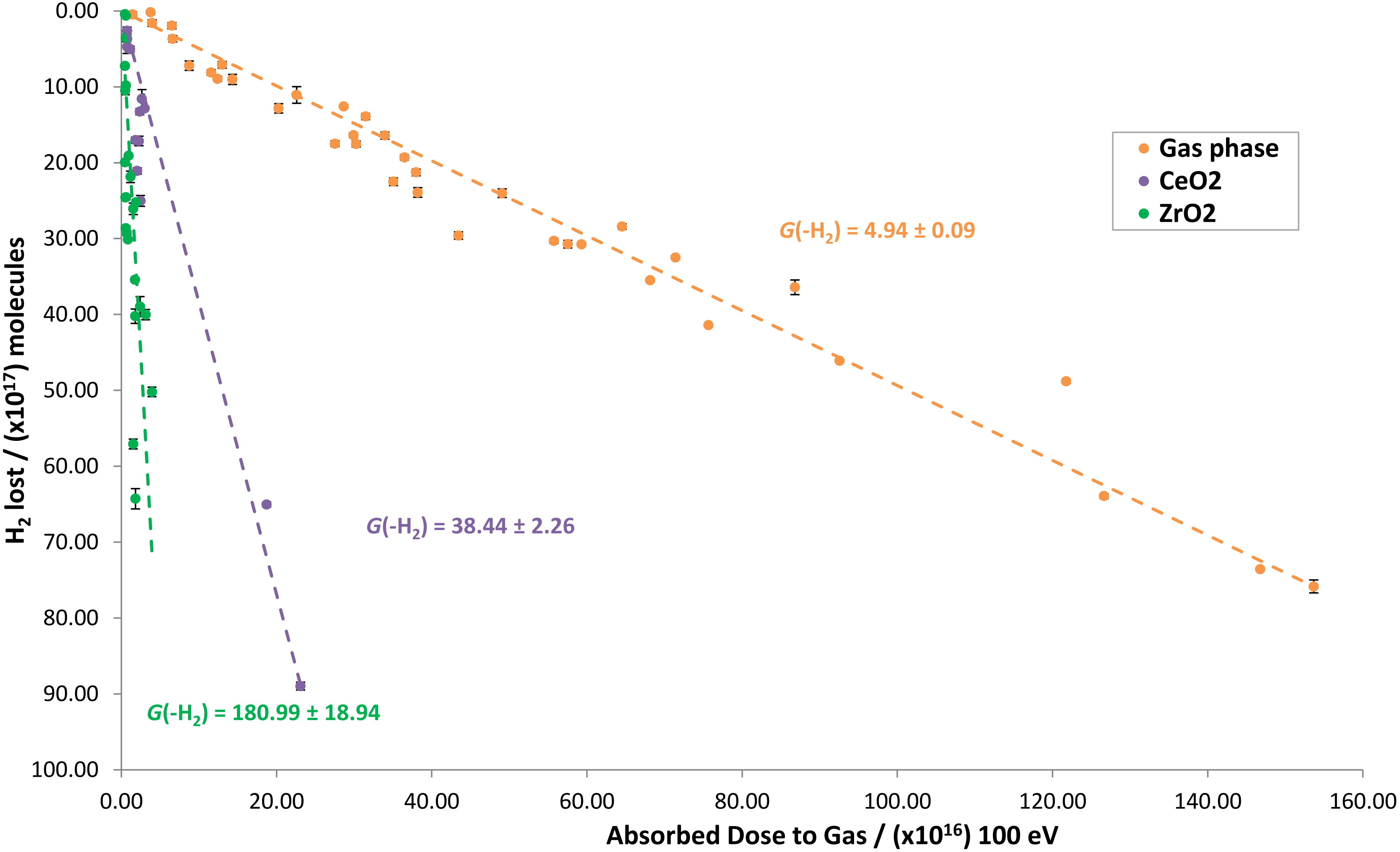

Heterogeneous 5:2.5:92.5

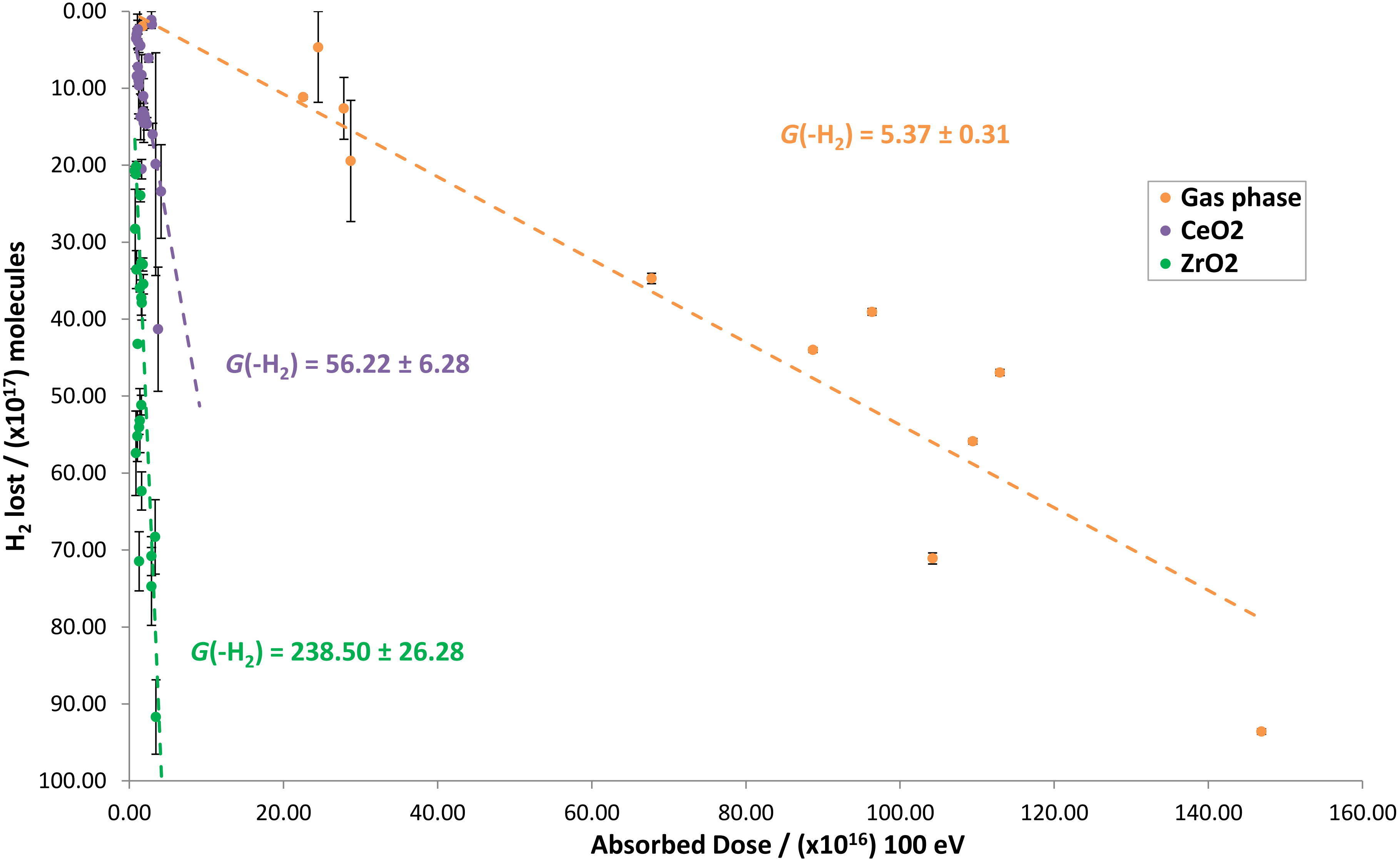

The University of Manchester
Dalton Nuclear Institute

Heterogeneous 2.5:5:92.5

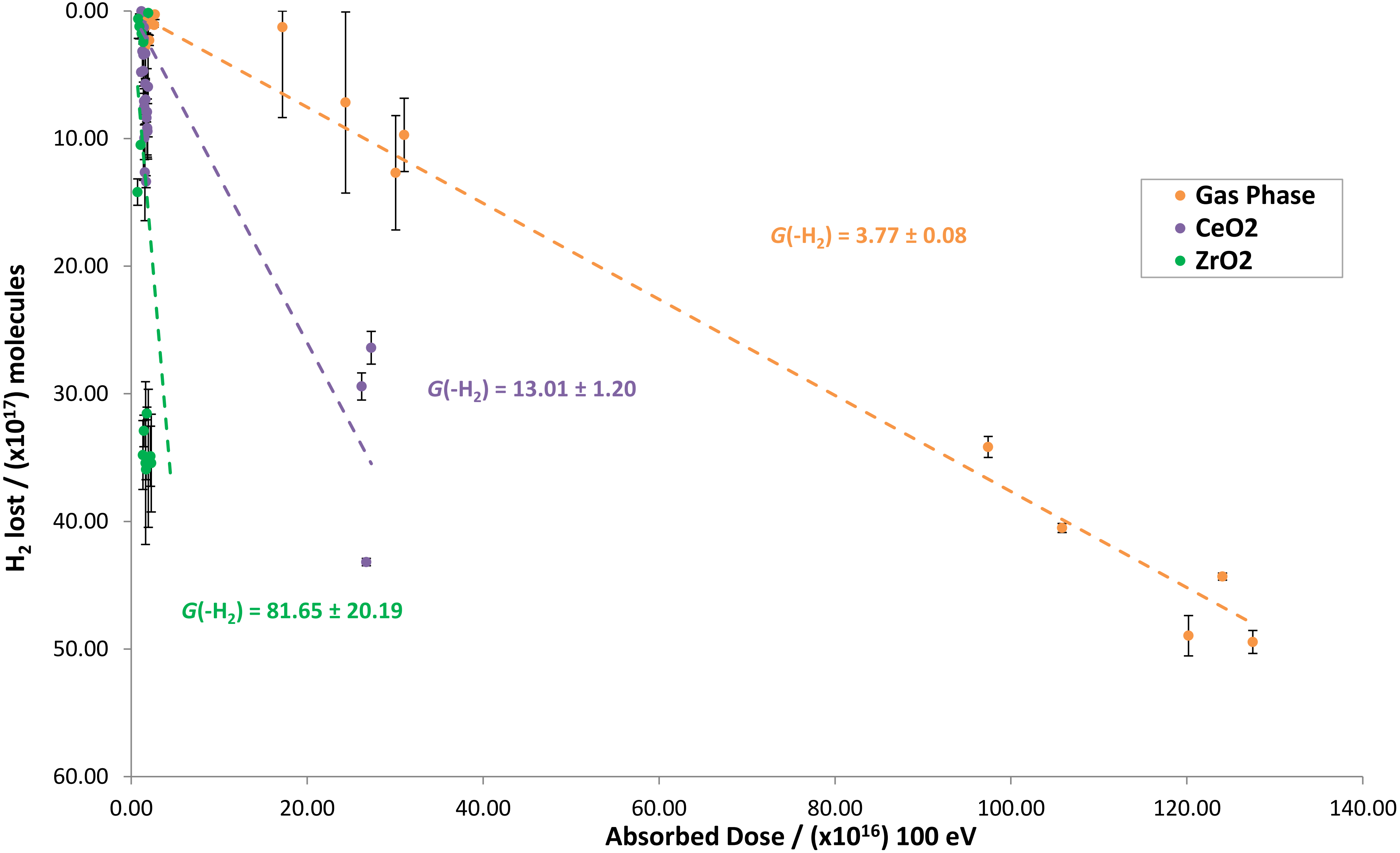

Summary of *G*-values utilising ^{60}Co γ-rays

System Gas Composition (H_2 : O_2 : Ar)	Gas Phase	CeO_2	ZrO_2
🔴 5 : 2.5 : 92.5	5.38 ± 0.31	56.22 ± 6.28	238.50 ± 26.28
● 5 : 5 : 90	4.93 ± 0.09	38.44 ± 2.26	180.99 ± 18.94
🔵 2.5 : 5 : 92.5	3.77 ± 0.08	13.01 ± 1.20	81.65 ± 20.19

Gas phase – He^{2+}

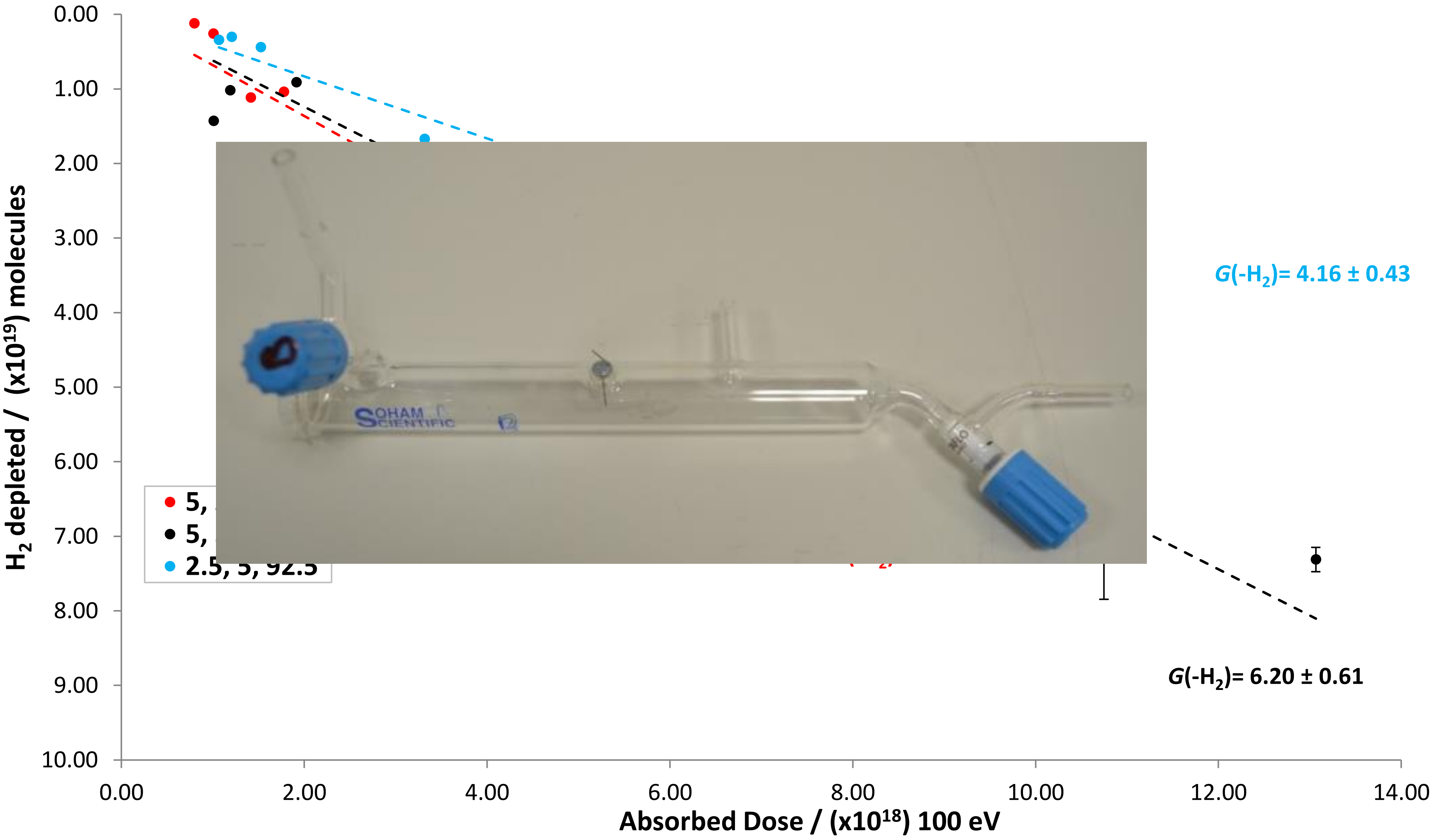

The University of Manchester
Dalton Nuclear Institute

Gas Phase – He^{2+}

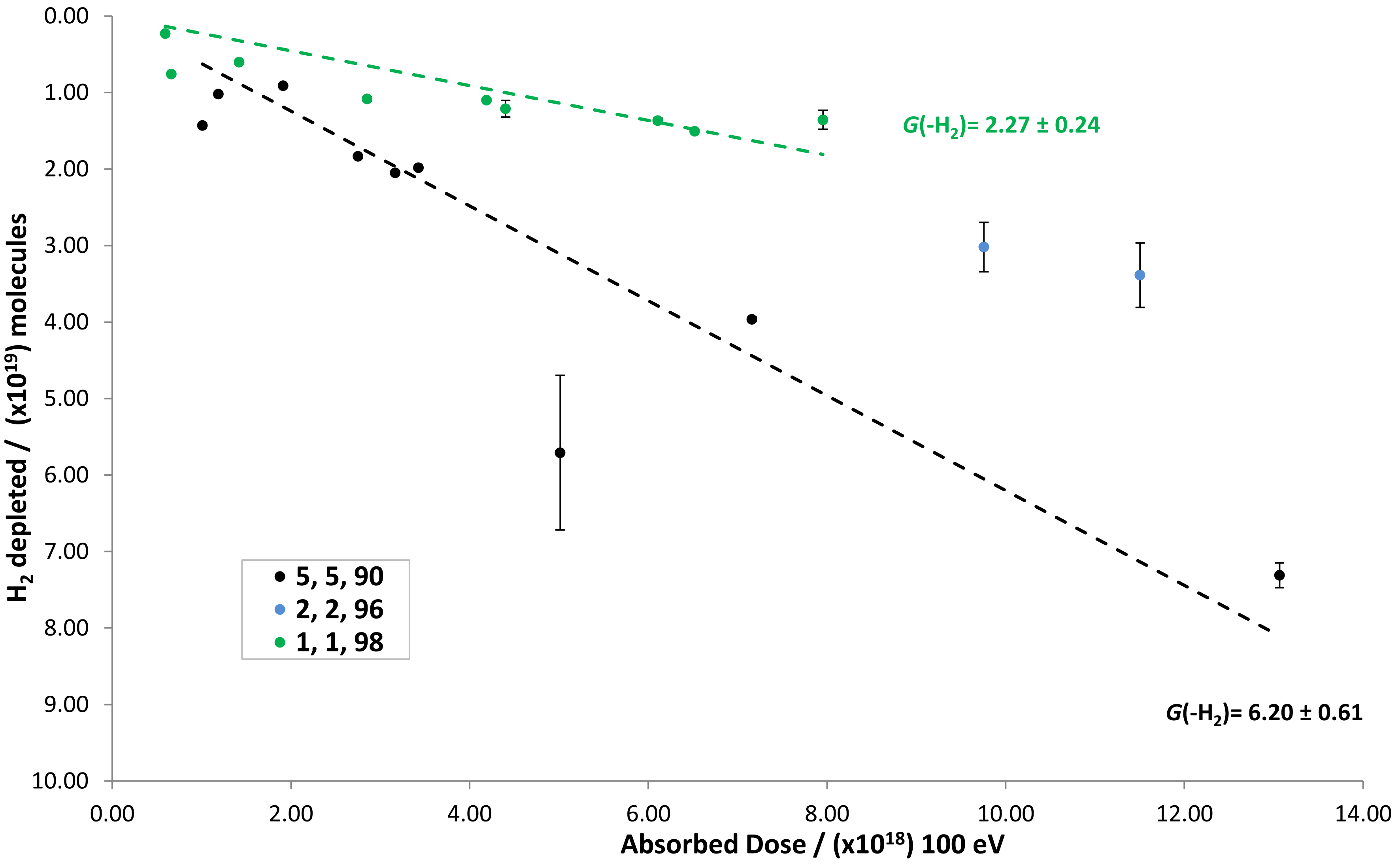

L.E.T. Comparison

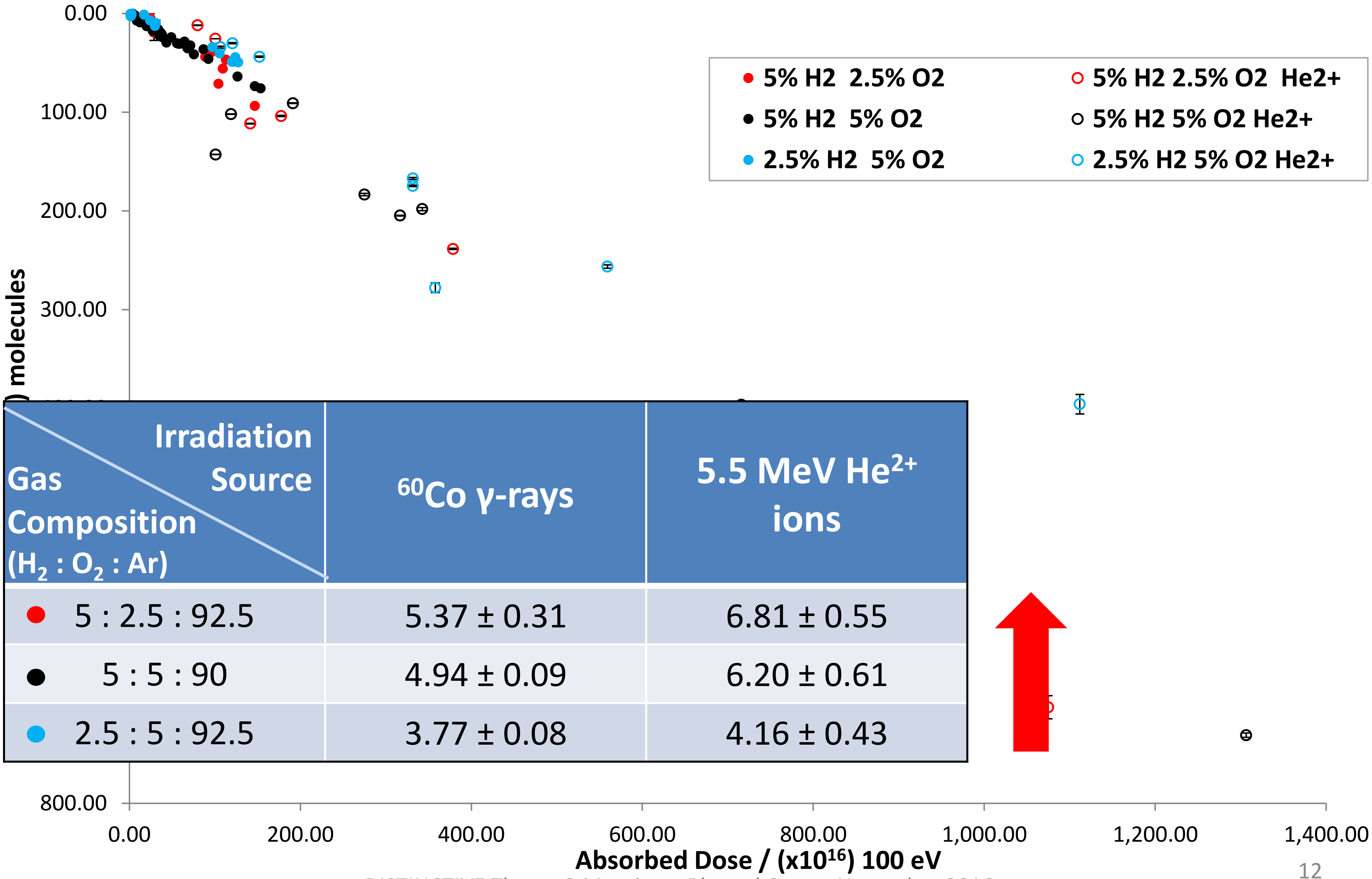

Irradiation Source Gas Composition ($H_2 : O_2 : Ar$)	^{60}Co γ-rays	5.5 MeV He^{2+} ions
🔴 5 : 2.5 : 92.5	5.37 ± 0.31	6.81 ± 0.55
⚫ 5 : 5 : 90	4.94 ± 0.09	6.20 ± 0.61
🔵 2.5 : 5 : 92.5	3.77 ± 0.08	4.16 ± 0.43

Conclusions

- Depletion rate remains constant over time (zero order) utilising ^{60}Co γ-rays
- Presence of an oxide increases depletion of H_2
- No LET effect
- Steady state is not reached
- Depletion rate is dependent of initial H_2 concentration (1st order)

Water uptake on CeO_2

- 4 humidity chambers
- Various molarities of H_2SO_4
- 3x 2 g CeO_2 samples
- Weight and RH monitored
- Assume 1 ML weighs 0.22 mg m^{-2}

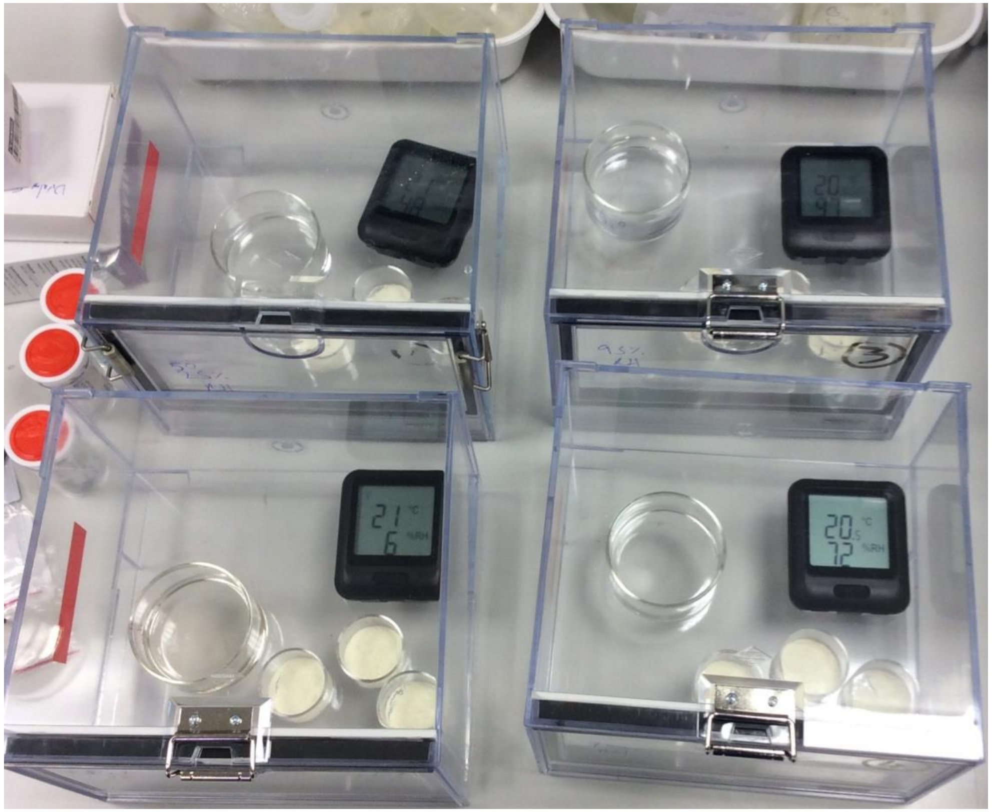

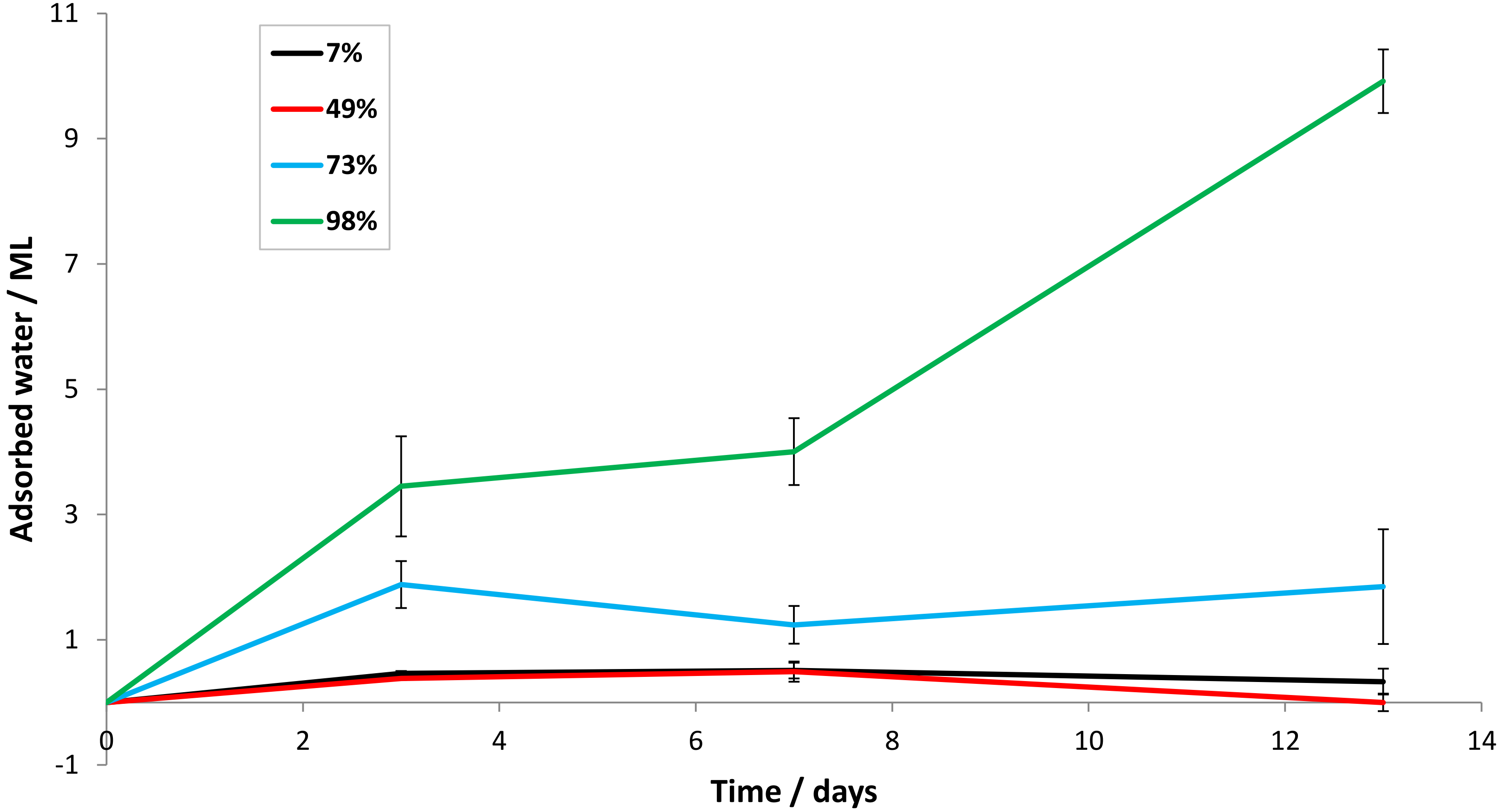
11
9
7
5
3
1
-1
Adsorbed water / ML
0
2
4
6
8
10
12
14
Time / days
7%
49%
73%
98%

NNL Training

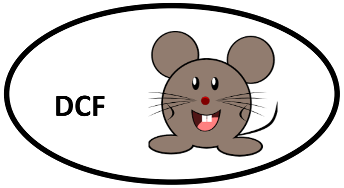

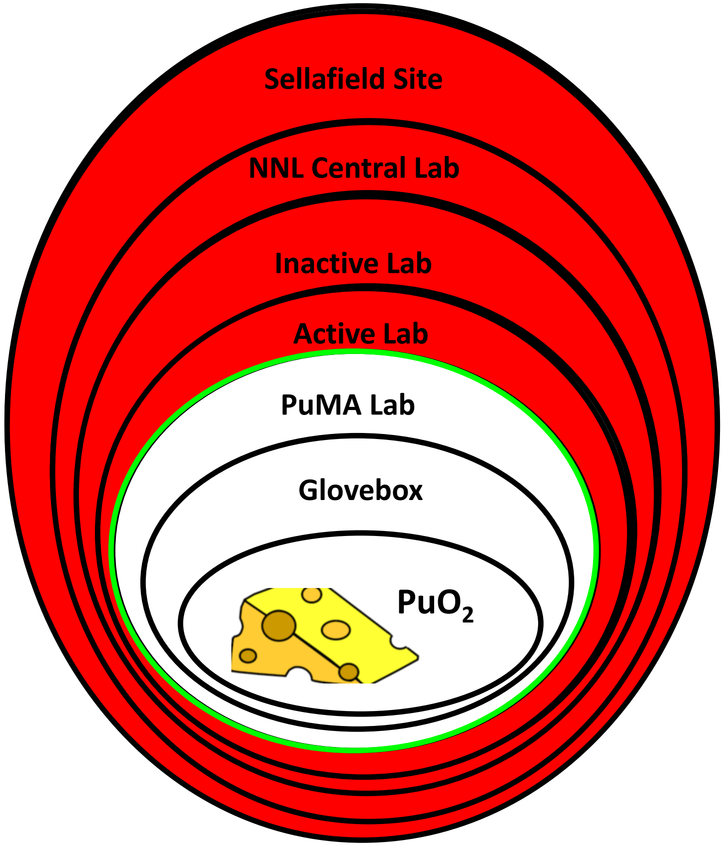

ARF 3rd Round

- Building and Commissioning a Vacuum Sampling System for PuO_2 Glovebox Experiments

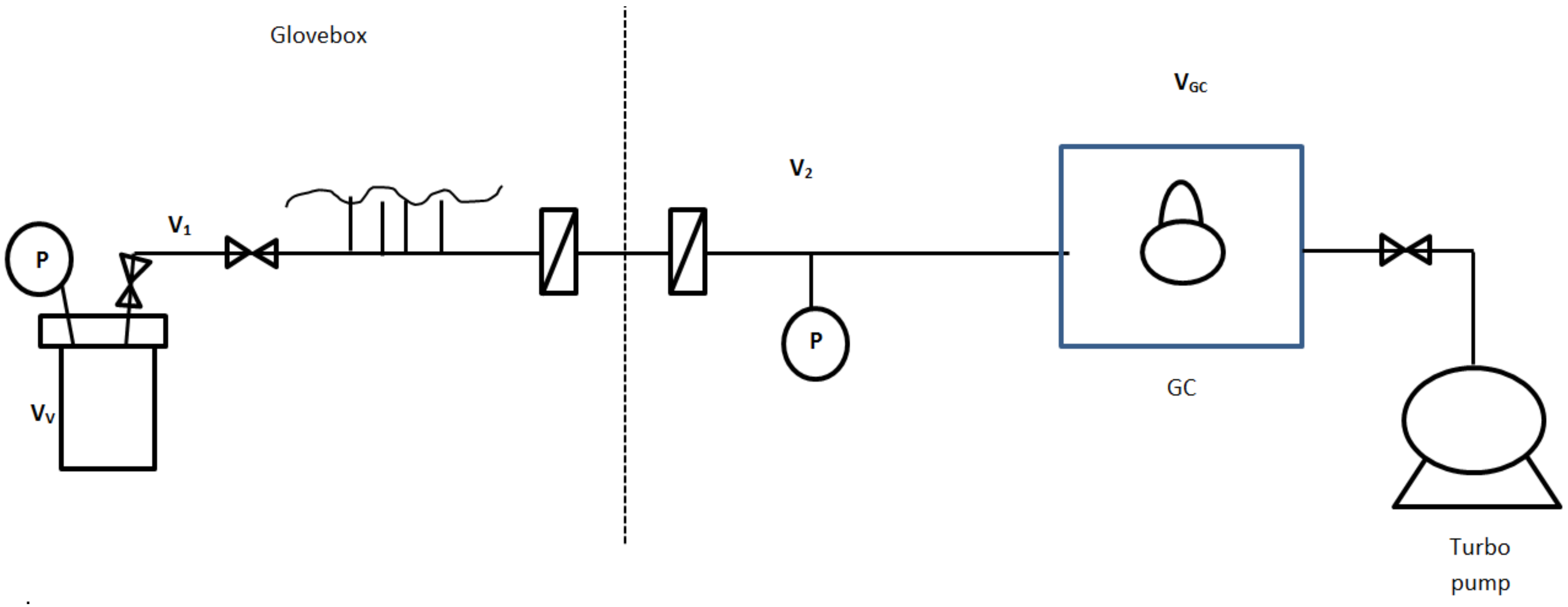

Vessel

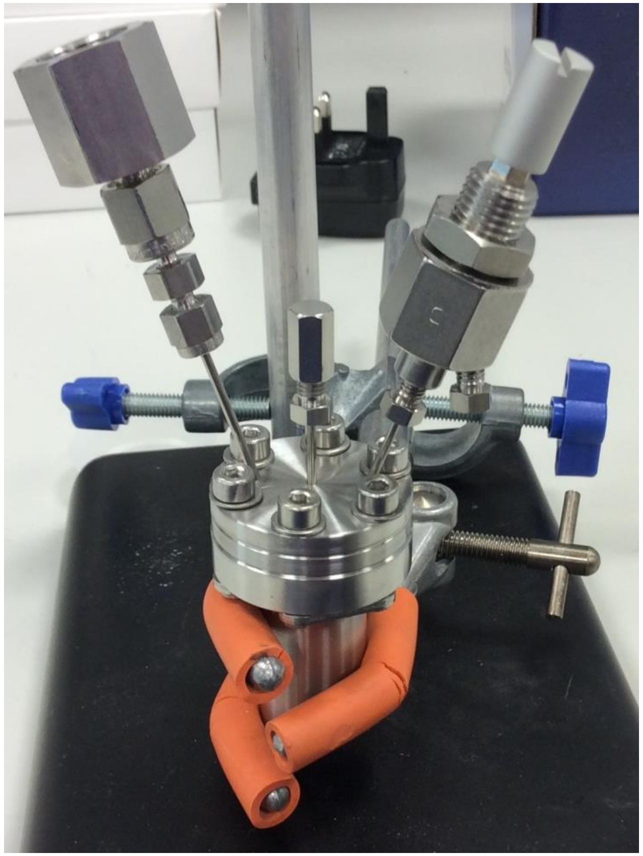

Pressure Testing

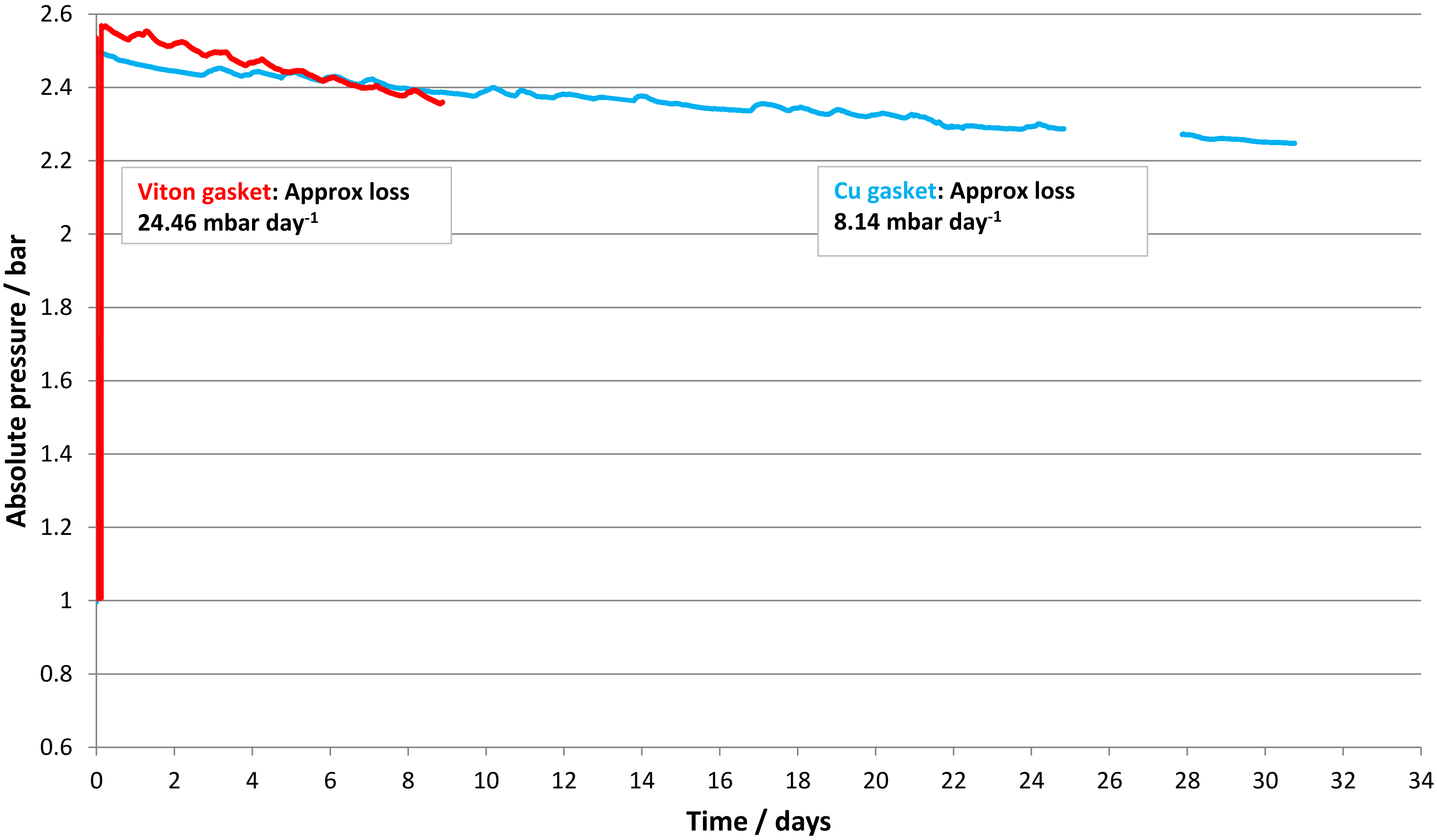

Viton gasket: **Approx loss 24.46 mbar day^{-1}**

Cu gasket: **Approx loss 8.14 mbar day^{-1}**

ARF 4th Round

- A Lab-scale Fixed Bed Reactor to Investigate Gas Phase Kinetics for Long Term PuO_2 storage

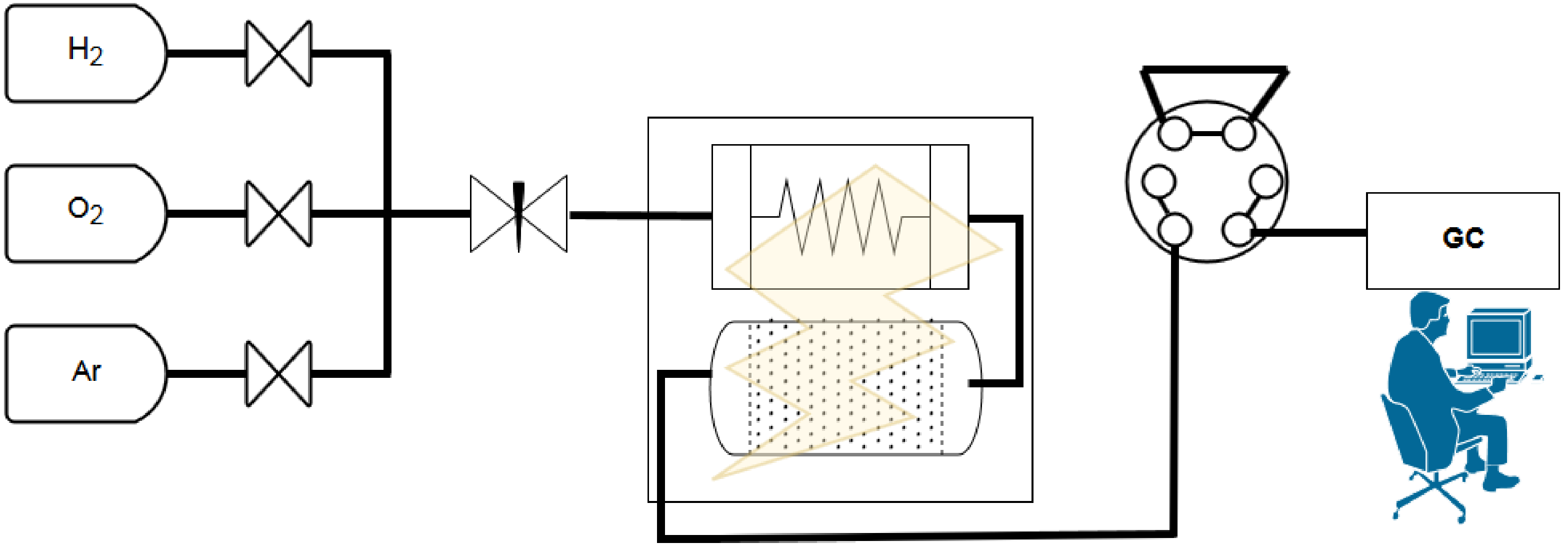

Future Work

- Experiments with PuO_2 (with NNL) investigating:
  - H_2 production
  - H_2/O_2 recombination

- Kinetic modelling of gaseous system
- Heterogeneous experiments utilising He^{2+} ions

Acknowledgements

- Radiation Science Team @ DCF
- Robin Orr and Howard Sims (both NNL)
- Paul Cook, Jeff Hobbs and Helen Steele (all SL)
- Prof. Simon Pimblott

Any Questions

The University Of Sheffield.

Department
Of
Materials Science &
Engineering

NucleUS
Immobilisation Science Laboratory

Understanding radionuclide interactions with cement materials: Synthesis and Characterisation of Calcium-Silicate-Hydrate phases

Antonia Yorkshire, Dr Claire Corkhill, Prof John Provis, Prof Neil Hyatt

DISTINCTIVE

EPSRC
Engineering and Physical Sciences
Research Council

NATIONAL NUCLEAR
LABORATORY

midas

THE 1ST STUDENT EXPERIENCE SURVEY 2014-15

ILW: Plutonium contaminated materials

Supercompacted PCM wasteform of PPE, metals, masonry…

Encapsulation of ILW in cement grouts

Pu sorption and incorporation into cement hydrate phases?

Cement encapsulation of ILW

1:1 FA/PC
28 days curing
w/s = 0.33

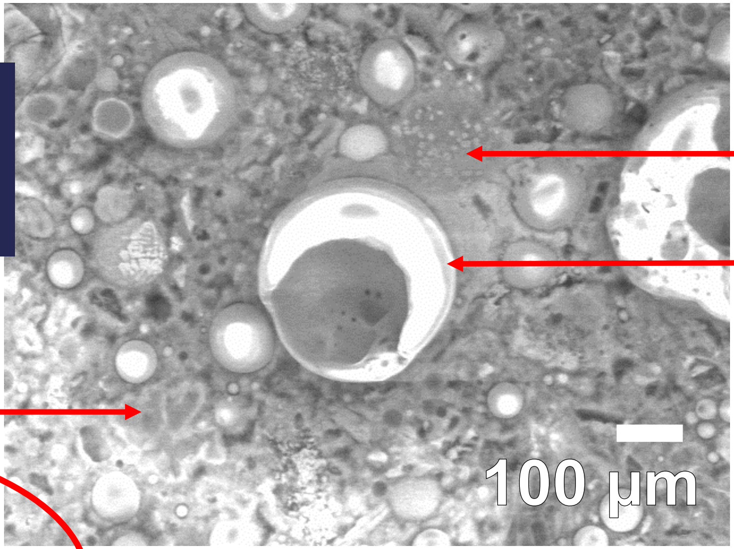

Portlandite: Ca(OH)$_2$

Fly ash particle

C-S-H: bulk of the cement matrix

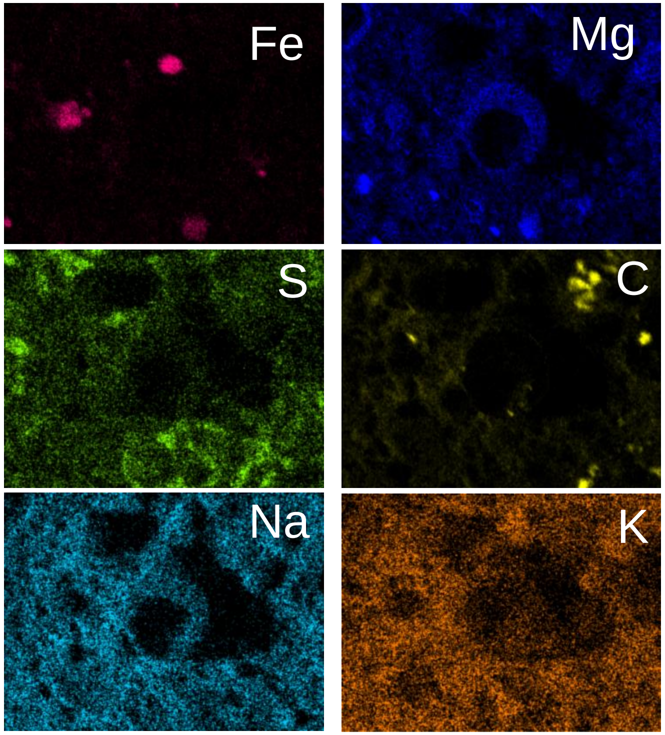

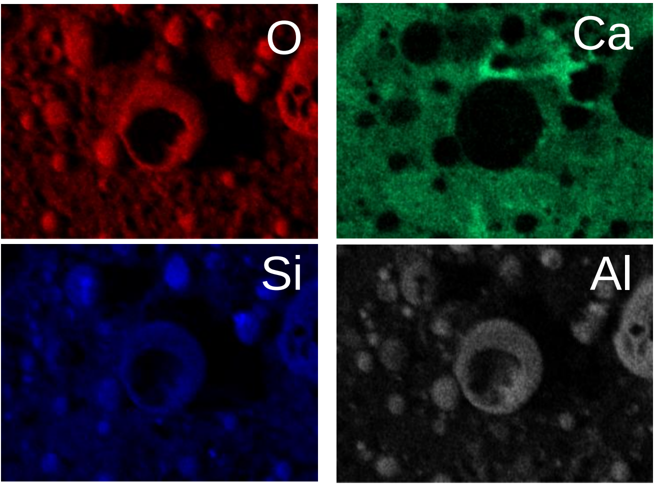

Ettringite:
$Ca_6(Al_2O_6)(SO_4)_3.32H_2O$

Monosulfate:
$Ca_4(Al_2O_6)(SO_4).12H_2O$

Calcium-Silicate-Hydrates

Structure based on 14 Å tobermorite

~ 50 wt% in PC

Important for radionuclide retention; UO_2 moiety

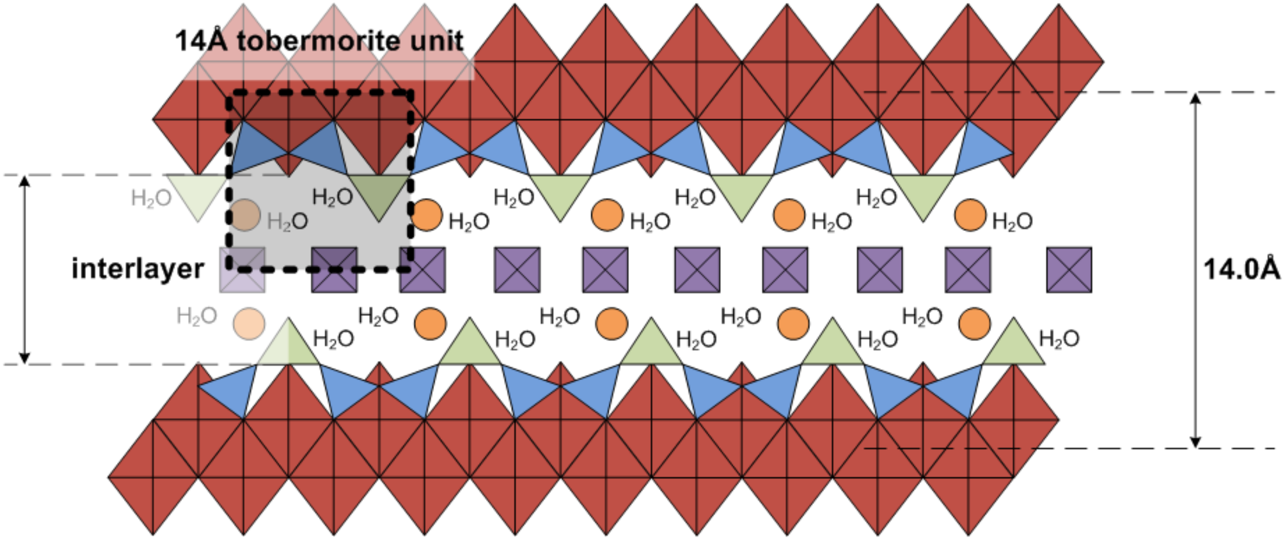

R.J. Myers, S. A. Bernal, R. San Nicolas, J. L. Provis, *Langmuir*, 2013, 29, pp 5294–5306

Synthesis

- 1:1 wt% $CaO:SiO_2$
- w/s = 15
- Theoretical Ca/Si = 1.07
- Constant agitation of the slurry at 40 rpm to prevent solidification / gel-formation
- Filtration of the solid after equilibration with drying, in air
- Conducted first in air on a benchtop…

CO_2 exposed sample

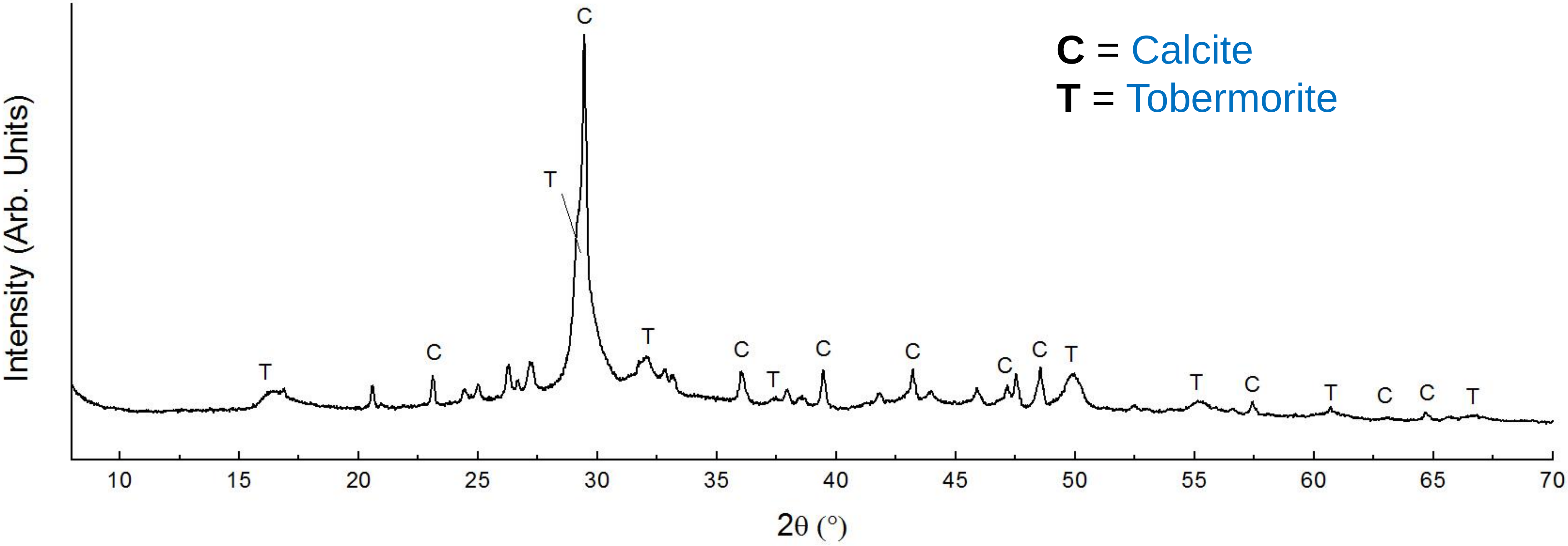

C = Calcite

T = Tobermorite

- See the conversion off calcium hydroxide components into calcite in the presence of air → inert atmosphere required

CO_2 free sample

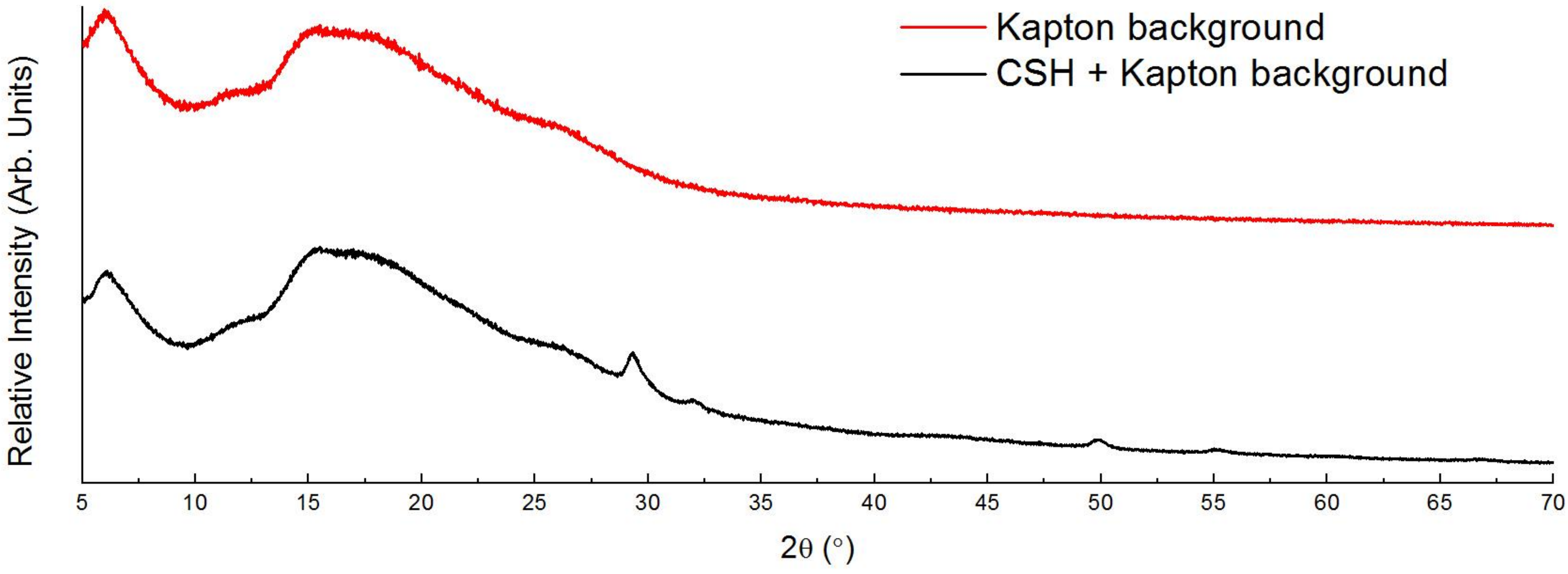

- XRD samples covered with Kapton tape to prevent exposure to air → background subtracted

CO_2 free sample

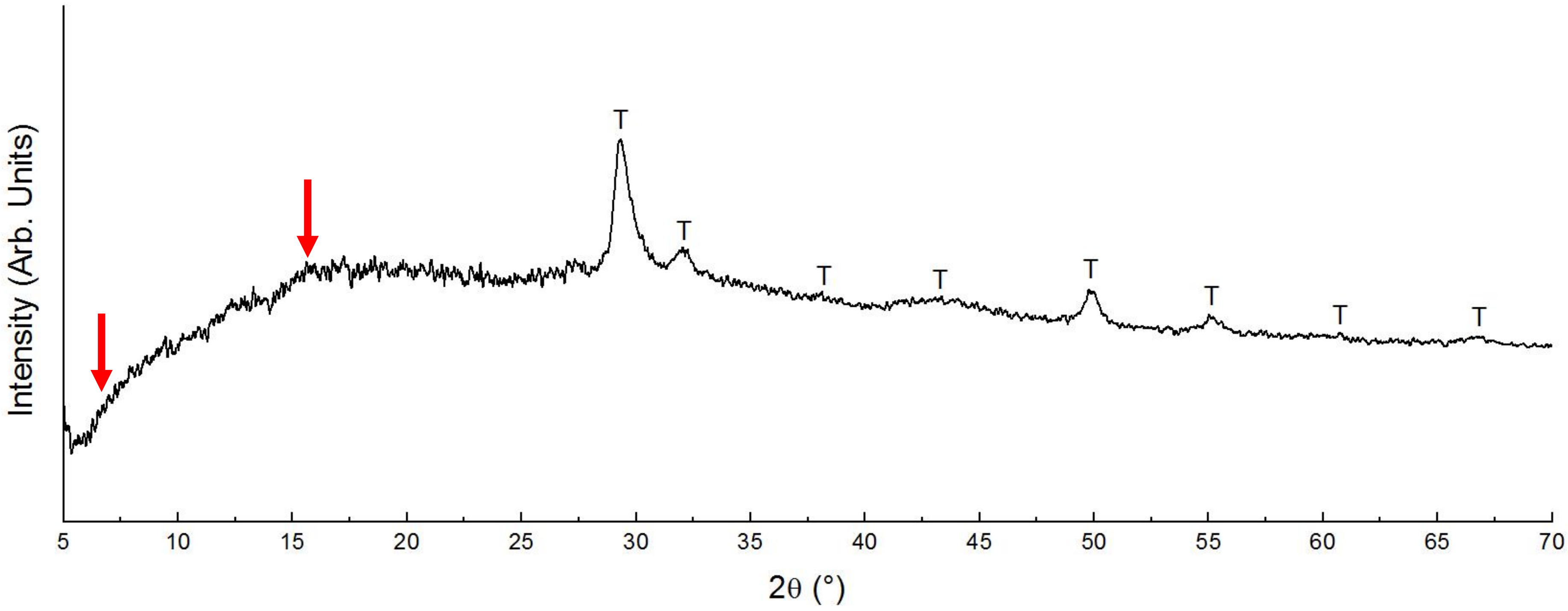

- Peaks at 7.1° and 16.2° 2θ are not easily identifiable due to Kapton tape background interference

Carbonation consequences

- Carbonation of cements leads to formation of $CaCO_3$
- Leads to cracking and expansion of the cement microstructure
- Decreases the alkalinity and may affect the cement's affinity for radionuclides …

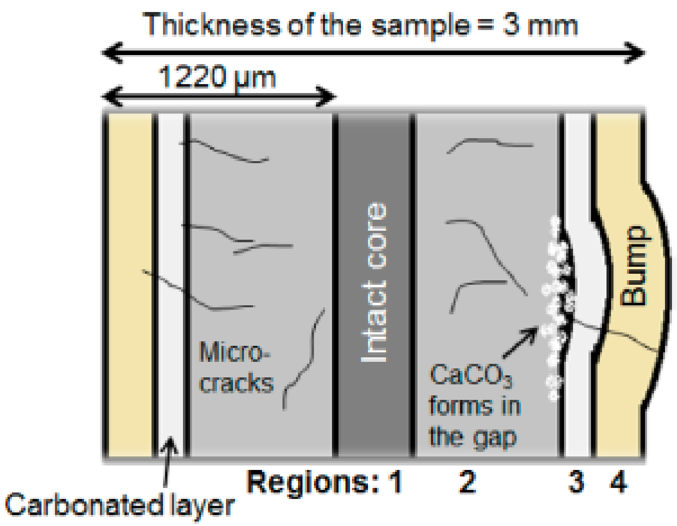

Q. Li, Y.M. Lim, K.M. Flores, K. Kranjc & Y. Jun, *Env. Sci. Technol.*, 2015, 49, pp 6335–6343

Considering uranium-CSH interactions

- 0.1 M $UO_2(NO_3)_2$ solution replacing water

<u>Observations</u>

- Instant agglomeration seen – perhaps formation of uranyl silicate
- On filtration, a yellow solid was seen and the mix solution had turned colourless

The University Of Sheffield.

Further work…

NucleUS
Immobilisation Science Laboratory

NATIONAL NUCLEAR LABORATORY

PuO_2 containing cement samples

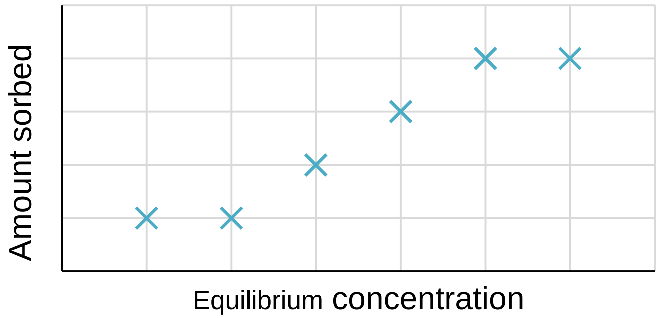

Solid State characterisation

- μ-XAS: coordination environment of radionuclides
- Solid state NMR: Al-27 & Si-29

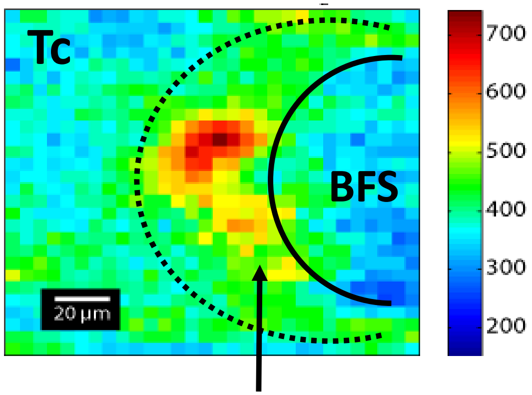

Cement hydrate phase?

In depth dynamic sorption tests

A range of hydrate phases to synthesise and consider…

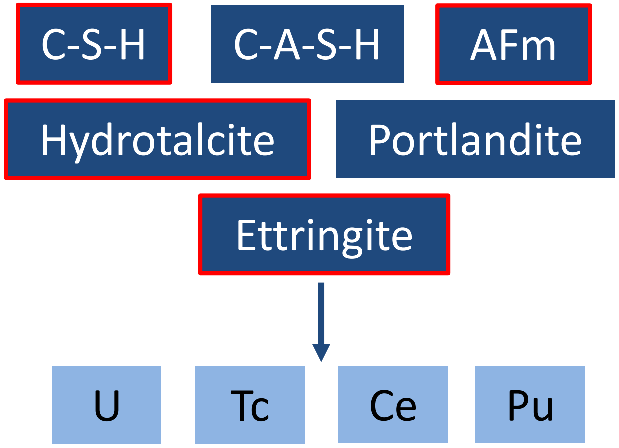

Conclusions

- Tobermorite successfully synthesised, can be used as an analogue to the C-S-H phase found in Portland cements
- An inert atmosphere is required for preparation to prevent carbonation
- The UO_2 moiety shows potential for incorporation into the C-S-H phase – how does this happen? Further investigation needed…

Acknowledgements

Claire Corkhill
John Provis
Oday Hussein

This research was conducted in part at the MIDAS facility at the University of Sheffield, which was established with support from the department of Energy and Climate Change.

Thanks go to the NDA for sponsorship and to NNL for industrial supervision.

DISTINCTIVE

EPSRC
Engineering and Physical Sciences Research Council

midas

NATIONAL NUCLEAR LABORATORY

Cement hydration

$$\boxed{C_3S + H_2O \rightarrow C\text{-}S\text{-}H + CH}$$

- Two processes:
  1. Dissolution
  2. Precipitation

C_3S = Alite, Ca_3SiO_5

C-S-H = Calcium silicate hydrate

CH = Portlandite, $Ca(OH)_2$

- Dissolution and reaction of the *calcium silicates* that are present in cement clinker with H_2O
- Precipitation of *calcium silicate hydrates* (C-S-H) and *portlandite* ($Ca(OH)_2$) in hardened cement paste

Hydrotalcite: BFS hydrate phase

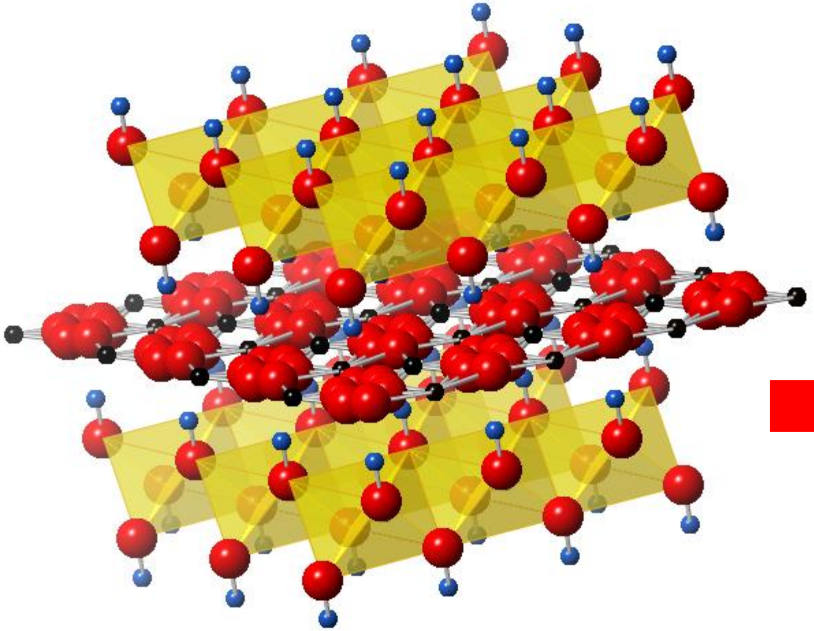

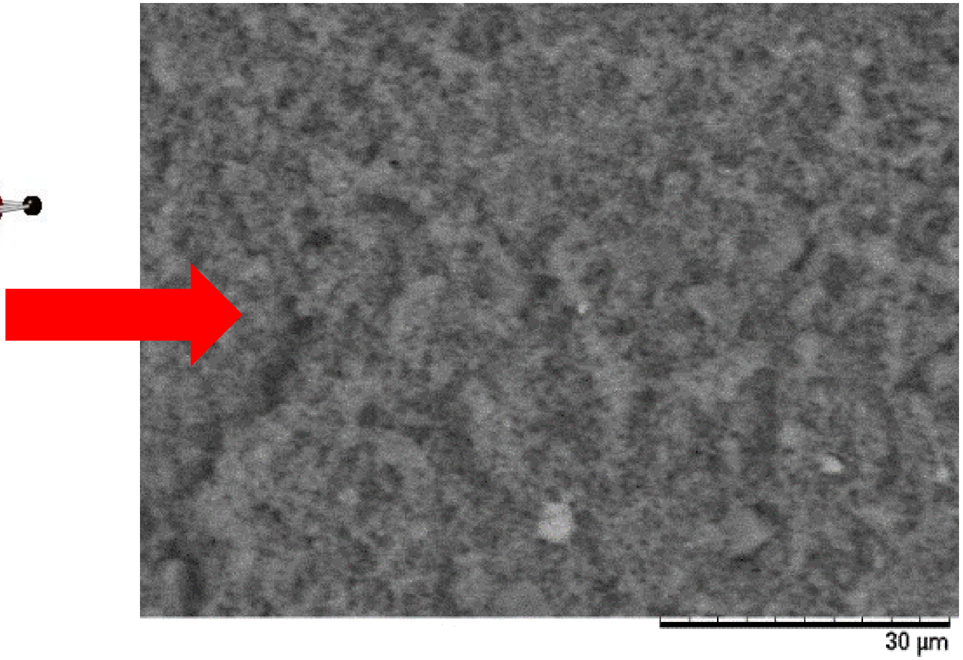

$Mg_6Al_2CO_3(OH)_{16}.4(H_2O)$

Hydrotalcite: BFS hydrate phase

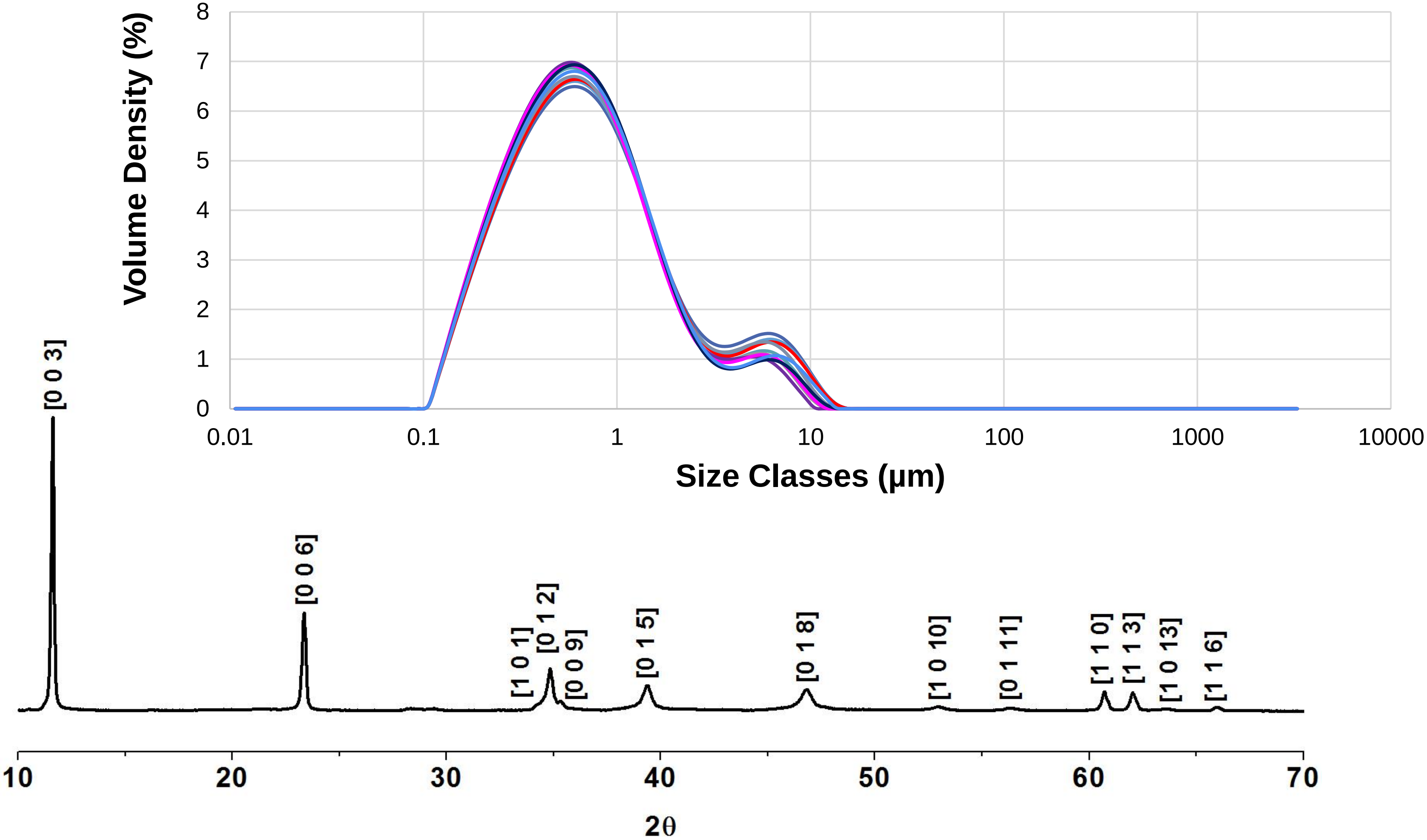

Immobilisation of ^{99}Tc by BFS/PC (9:1)

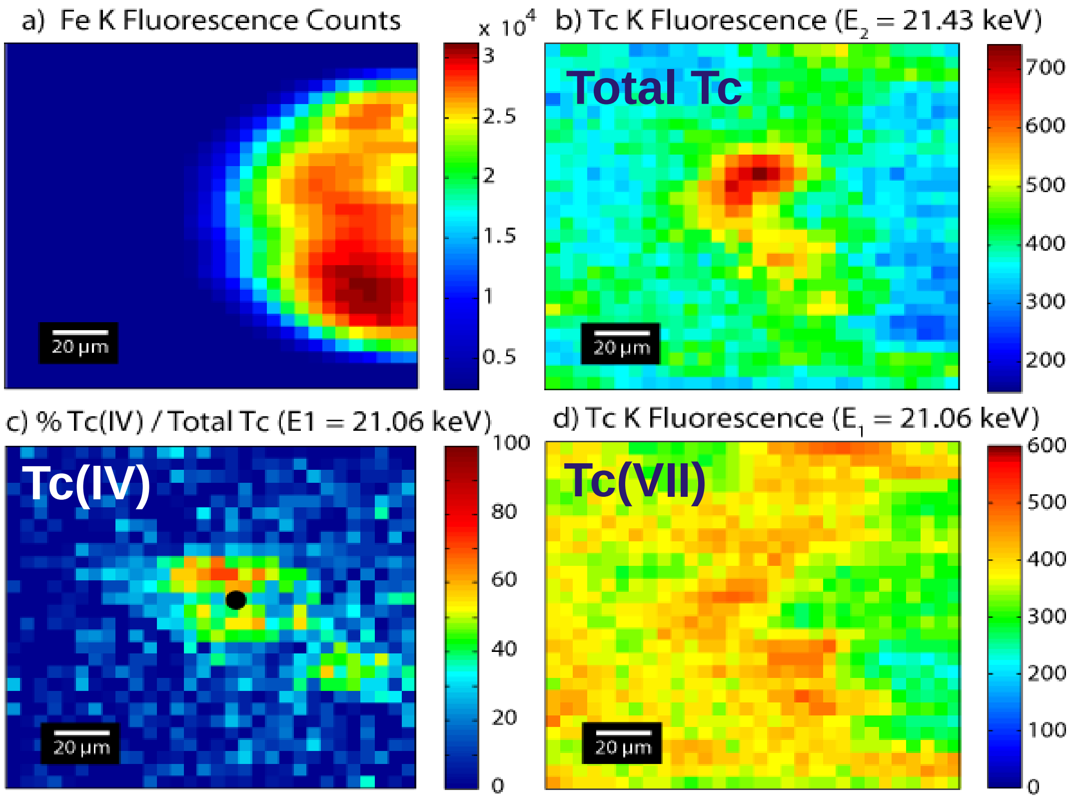

Courtesy of C. Corkhill

- ^{99}Tc mobility is controlled by its oxidation state: reduction of Tc(VII) to Tc(IV) results in insoluble, poorly mobile TcO_2-like phases.
- ^{99}Tc(IV) is present only on the edge of BFS particles
  - possibly incorporated in hydration products OR as a reduced TcO_2 or TcS_2-like phase.

S. Grangeon et. al., Structure of nanocrystalline calcium silicate hydrates: insights from X-ray diffraction, synchrotron X-ray absorption and nuclear magnetic resonance, *J. Appl. Crystallogr*., 2016, **49**, 771-783

M. Harfouche et. al., EXAFS study of U(VI) uptake by calcium silicate hydrates, *J. Colloid Interface Sci*., 2006, **303**, 195-204

X. Gaona et. al., Aqueous-solid solution thermodynamic model of U(VI) uptake in C-S-H phases, *Appl. Geochem*., 2012, **27**, 81-95

Direct mass analysis of water absorption onto ceria and urania thin films

Dominic Laventine
Colin Boxall
Lancaster University

14th November, 2016
Penrith

Plutonium storage

- ~250 tonnes of separated Pu currently stockpiled worldwide.
- ~50% in long-term storage in UK whilst the Government develops its options
- Interim storage of PuO_2 involves sealing in inert steel containers.

- Under certain circumstances, these gas cans may pressurise; this must be avoided in practice.
- Need to understand how the structure and properties of PuO_2 change with time under storage conditions (e.g. in the presence of H_2O).

Plutonia interaction with water

- 5 routes to gas production have been suggested:
  - (i) Helium accumulation from α decay
  - (ii) Decomposition of polymeric packing material;
  - (iii) H_2O desorption (steam) from hygroscopic PuO_2
  - (iv) Radiolysis of adsorbed water
  - (v) Generation of H_2 by chemical reaction of PuO_2 with H_2O, producing a postulated PuO_{2+x} phase.

- The last 3 processes all involve PuO_2/H_2O interactions and are complex, inter-connected & poorly understood.

- Haschke has suggested a reaction: $PuO_2 + H_2O \rightarrow PuO_{2+x} + H_2$
  This has been disputed on thermodynamic grounds.

- Experimental methods have been employed to determine extent of H_2O adsorption, typically through measurement of pressure changes and use of the ideal gas equation to indirectly determine water adsorption at the plutonium oxide surface.

Aims

Current models suggest water is initially absorbed onto metal oxides as a chemi-absorbed monolayer followed by multiple, physi-sorbed layers (with possible intermediate layers of differing binding energies).

- Study the interactions of plutonium oxide and analogues with water.
  - Ceria
  - Urania
  - Thoria
  - Plutonium oxide
- Use of quartz crystal microbalance methodology to experimentally determine:
  - The number of monolayers of water bound to the surface
  - The enthalpy of binding of the different layers.

Quartz crystal microbalance (QCM)

- The QCM measures in-situ mass changes at the surface of a piezoelectrode. Changes in mass, due to oxide formation or dissolution at the electrode surface or adsorption/desorption of gases, result in resonant frequency changes of the quartz crystal.
- Changes in frequency can be related to changes in mass through the Sauerbrey equation:

$$\Delta f = -\left(\frac{n{f_0}^2}{A\sqrt{\rho_q \mu_q}}\right)\Delta m$$

- Knowing the surface area of the metal oxide layer and the mass of water absorbed allows the number of layers to be accurately calculated.
- The differences in temperature at which water absorption/desorption occurs allows the thermodynamics to be determined, indicating which layers are chemi- or physio-sorbed.

Ceria films on quartz crystals: SEM

Thin films of ceria were coated onto QCM crystals *via* spin-coating of a cerium(III) nitrate precursor solution followed by calcination at 300°C.

Layers of differing depth and porosity could be produced by altering the spin-coating duration and precursor / surfactant concentration.

A

40 nm thick

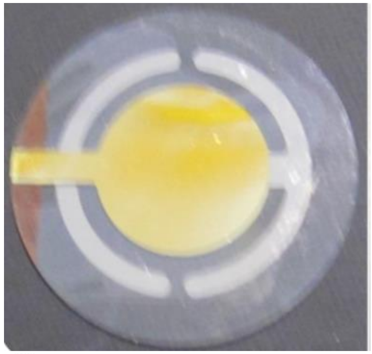

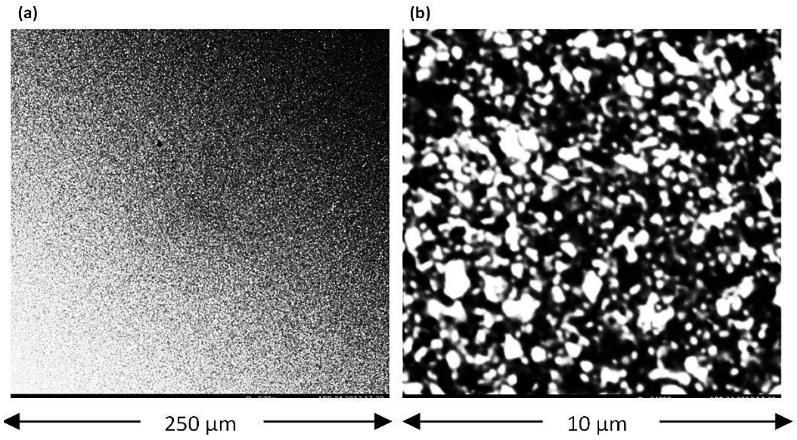

B

400 nm thick

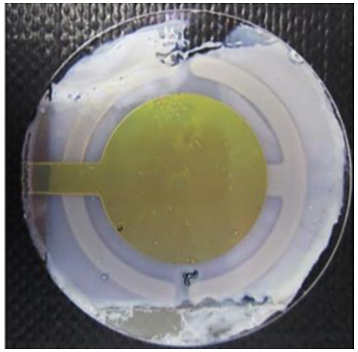

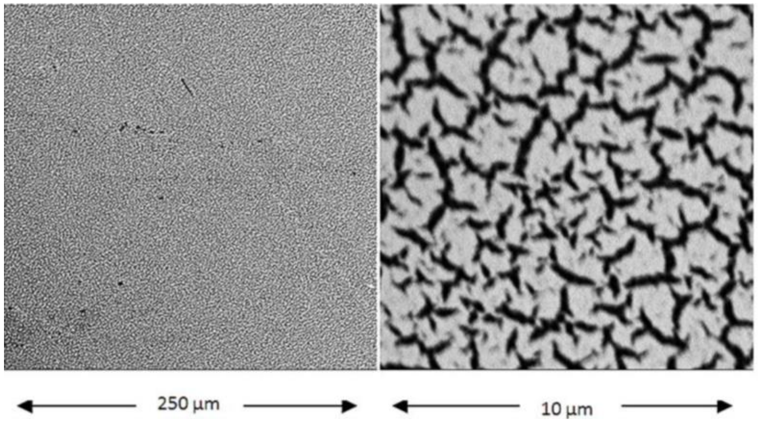

Ceria films on quartz crystals: XRD and Raman

The films were confirmed to be crystalline CeO_2 by XRD and Raman spectroscopy, which showed characteristic peaks.

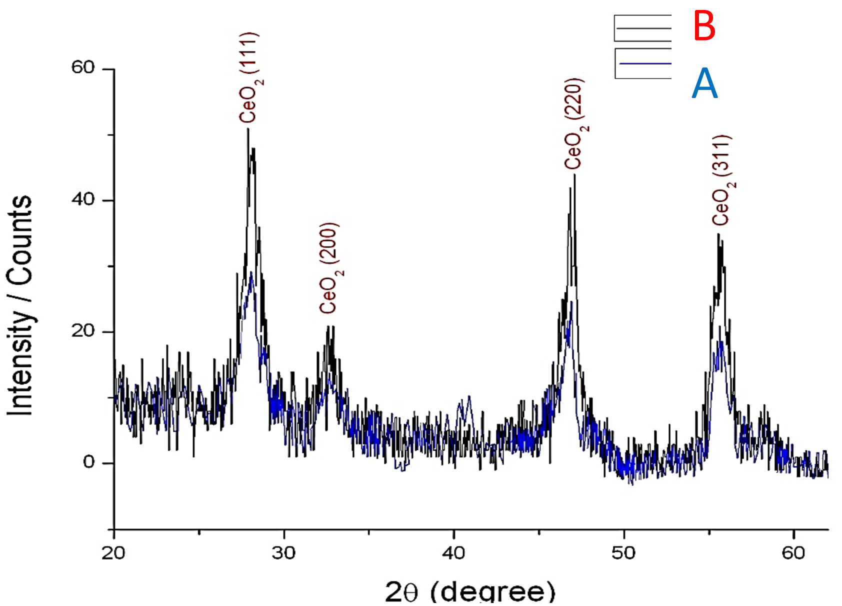

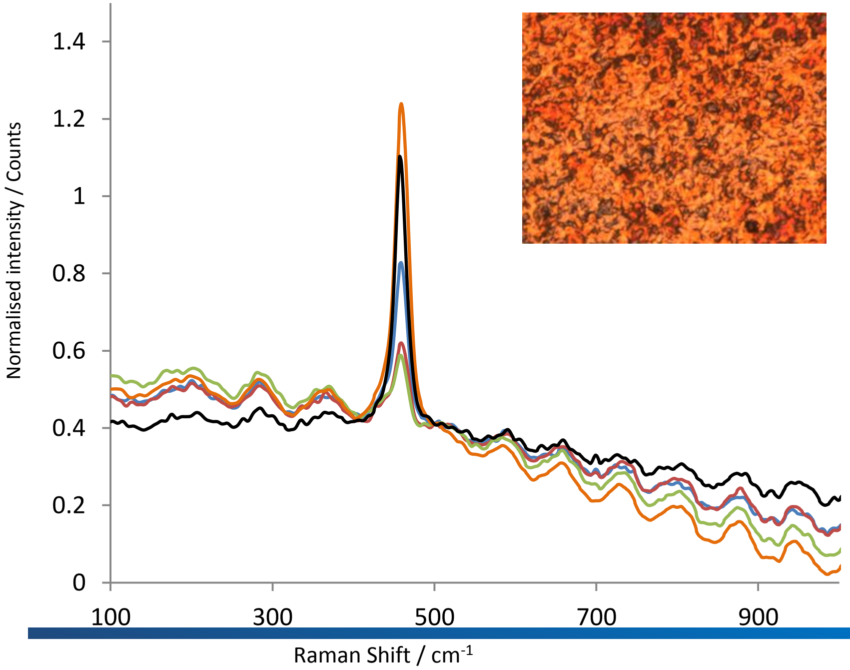

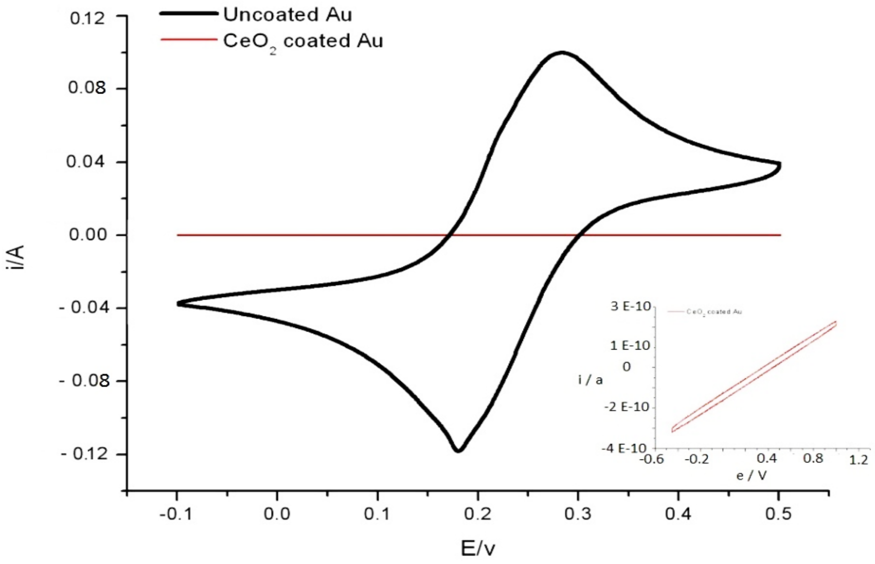

Ceria films on quartz crystals: QCM and AFM

Application of the Sauerbrey to the change in frequency after coating allows the mass of ceria to be calculated:

$$\Delta f = -\left(\frac{n{f_0}^2}{A\sqrt{\rho_q \mu_q}}\right)\Delta m$$

ρ_q = 3.570 g.cm^{-1} n = 1
μ_q = 2.147 x 10^{11} g.cm^{-1}s^{-2}
Coated area = 1.54 cm^2
Active area = 0.342 cm^2
d_{CeO_2} = 7.65 g.cm^{-3}

A

Δ F$_{25^oC}$ = –1180Hz
Δ m = 7.25 μg
h (QCM) = 28 nm

B

Δ F$_{25^oC}$ = –7130 Hz
Δ m = 43 μg
h (QCM) = 164 nm

Atomic force microscopy was used to measure the film thickness experimentally:

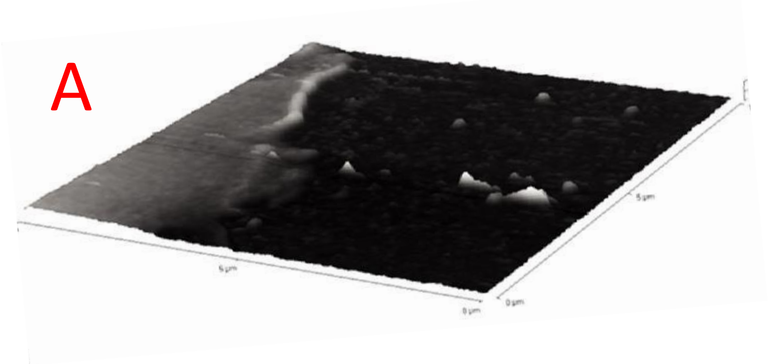

h (AFM) = 40-45 nm
porosity = 30%

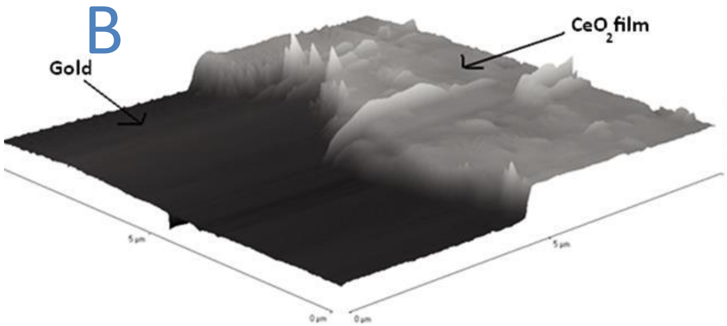

h (AFM) = 400-420nm
porosity = 60%

Water absorption: Pilot experiments

Frequency changes due water adsorption onto quartz crystals at 25°C, 100% humidity.

Uncoated crystals showed no appreciable water absorption.

Ceria coated crystals showed a reduction in frequency due to absorption of water.

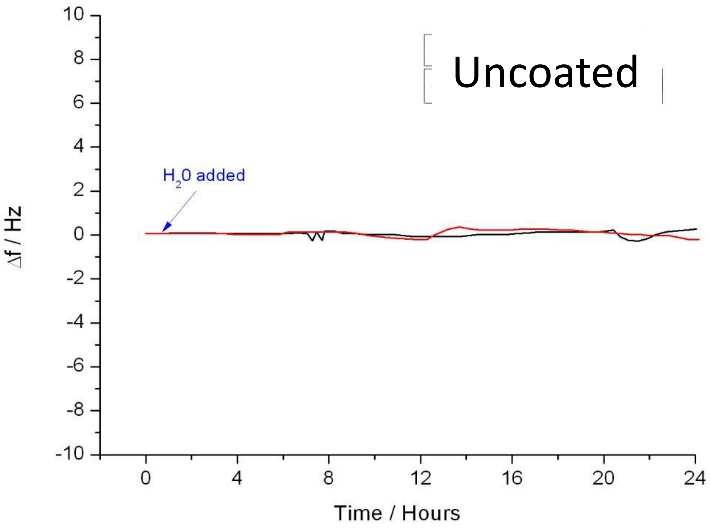

A

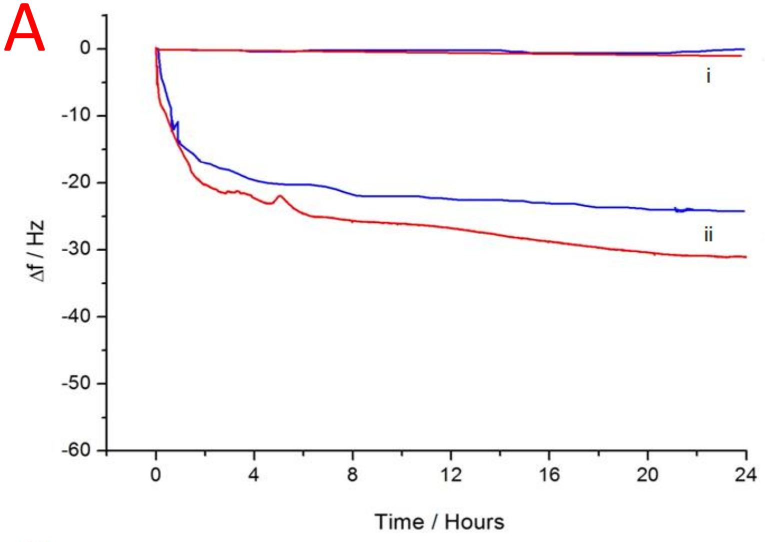

B

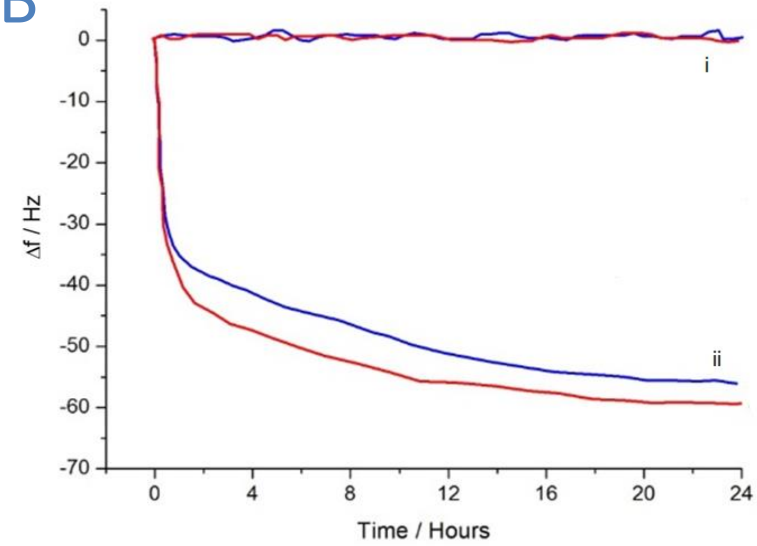

Water absorption: Humidity variation

The amount of water added to the system was varied, allowing the variation in water absorption as a function of water partial pressure / humidity to be determined.

As expected, more water was absorbed onto the ceria at higher partial pressures. At all humidities the more porous later was found to absorb more water.

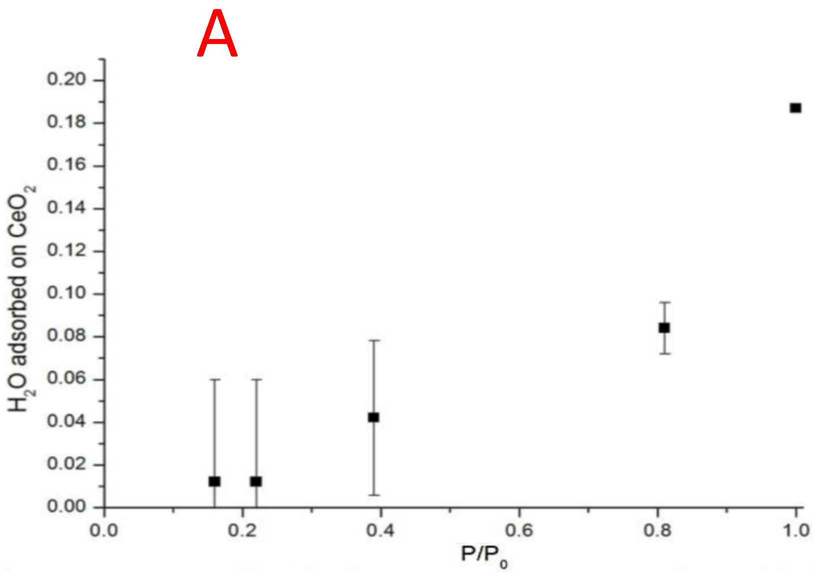

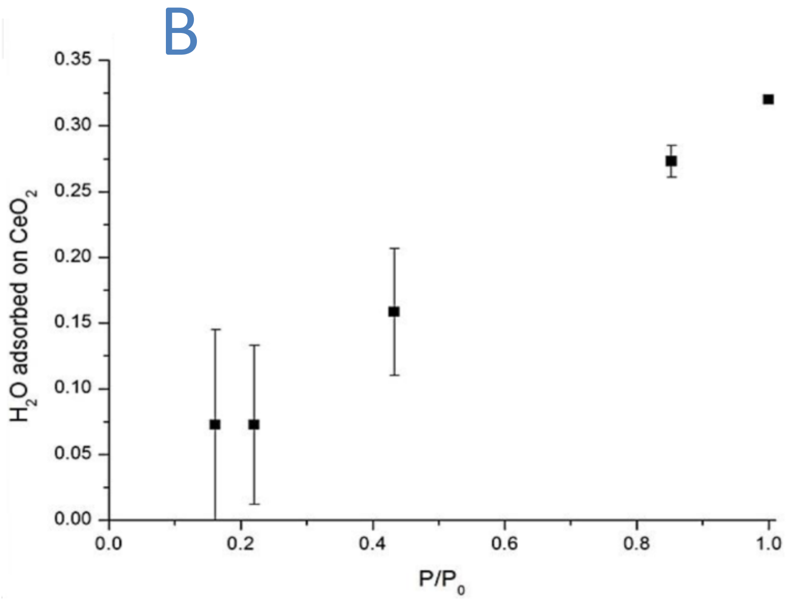

Water absorption: Surface area calculation

The BET equation can be used to calculate the enthalpy of absorption (ΔH_{ads}) and the volume of a monolayer of molecular water adsorbed onto a surface

$$1/\left[Va\left(\frac{P0}{P}-1\right)\right]=\left(\frac{C-1}{V_M C}\right)\left(\frac{P}{P_0}\right)+\frac{1}{VmC}$$

$C = \exp(\Delta H_{ads} - \Delta H_{liq} / RT)$
V_m = monolayer volume

A

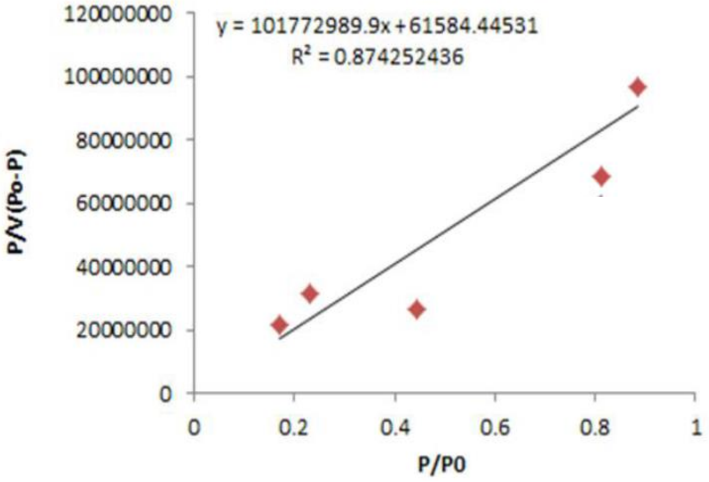

B

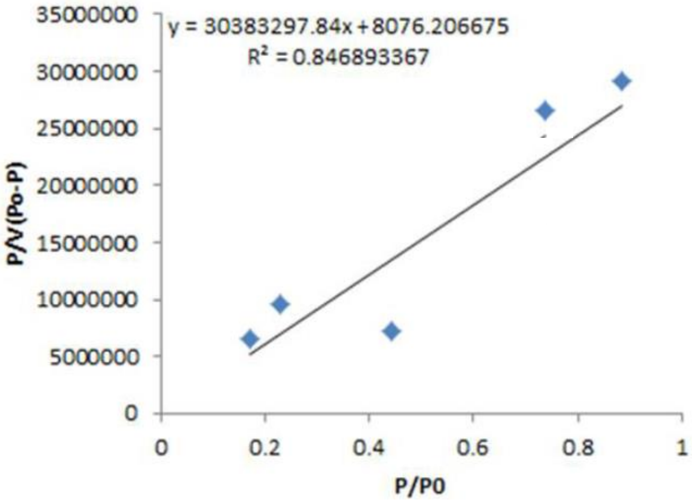

$\Delta H_{ads} = 62\ kJmol^{-1}$
$V_m = 9.8 \times 10^{-9}\ cm^3$
$SA = 5.25 \times 10^{-5}\ m^2$
No. monolayers = 18

$\Delta H_{ads} = 64\ kJmol^{-1}$
$V_m = 33 \times 10^{-9}\ cm^3$
$SA = 17.6 \times 10^{-5}\ m^2$
No. monolayers = 10

Water absorption: Temperature variation

The temperature of the system was increased, while maintaining a fixed amount of added water.

As the temperature increased, the amount of water absorbed onto the surface decreased.

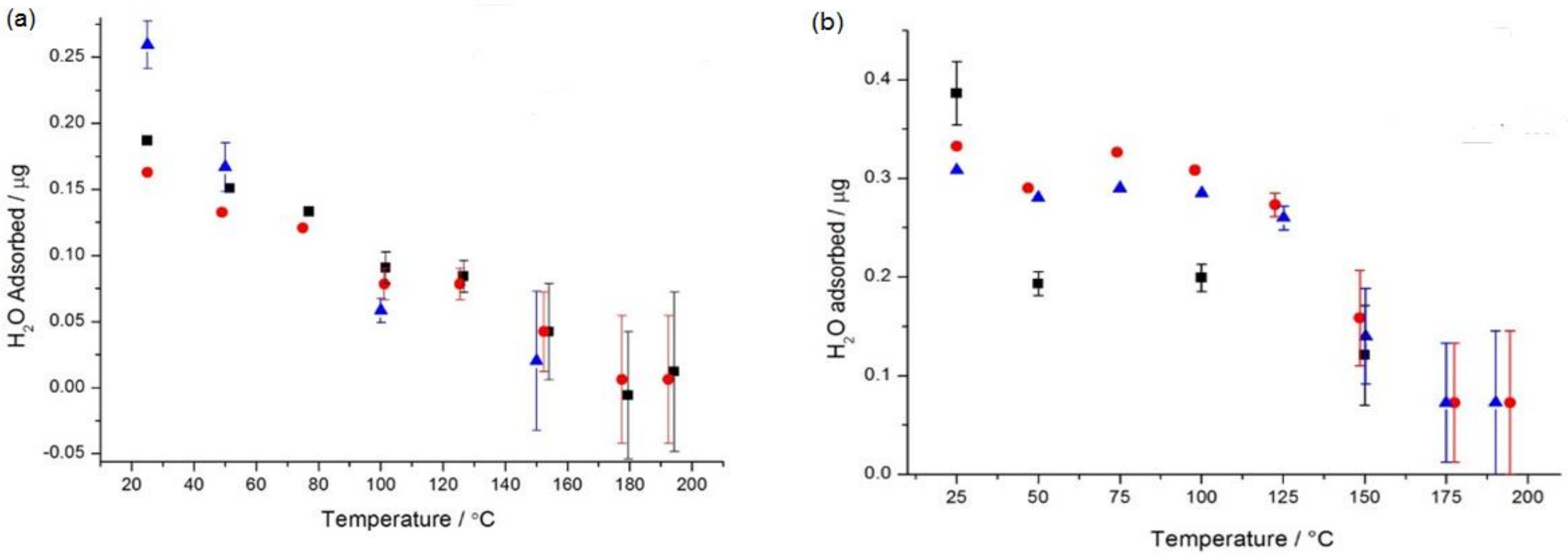

The maximum operating temperatures was approximately 200°C. At this temperature, a significant amount of water of water was still absorbed onto the ceria surface. For the 400 nm thick ceria layer, this equates to ~90 ng, the equivalent of ~3 monolayers of water.

$GaPO_4$

$GaPO_4$ crystals have a higher piezoelectric limiting temperature, allowing for higher calcination temperatures of metal oxide coatings (up to ~900ºC), reducing porosity.

Redesign of system to use metal sensor head in place of teflon.

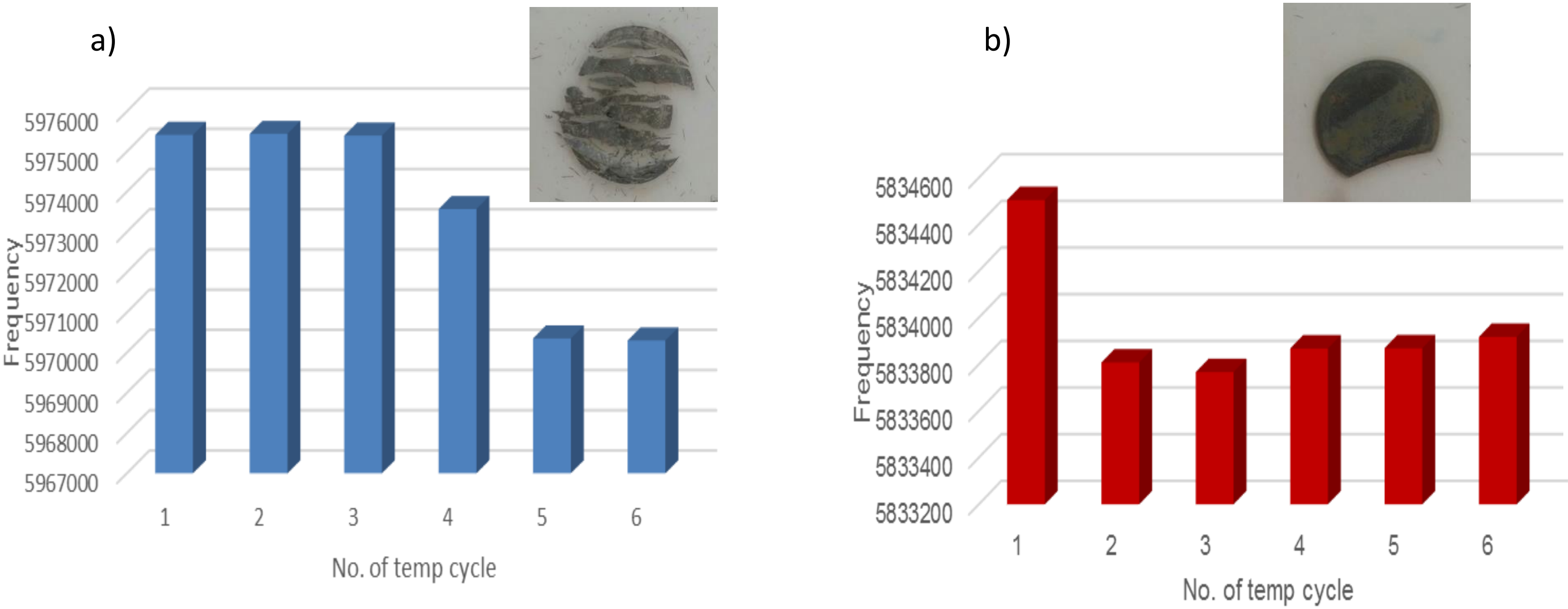

Frequency of uncoated a) Quartz and b) Galium phosphate crystals at room temperature after repeated temperaturecycling to 550ºC. Inset: photographs of crystals after heating to 950°C.

$GaPO_4$ crystals

Use of $GaPO_4$ crystals, which have a linear temperature-frequency dependence, making higher temperature measurements much more accurate.

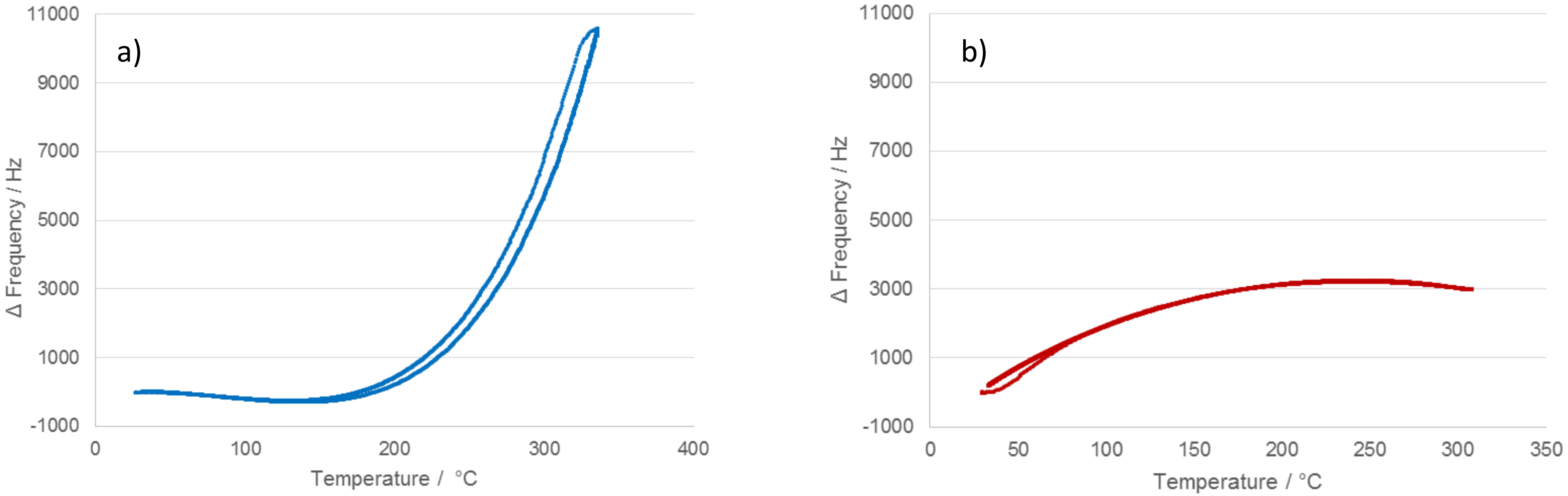

Temperature dependence of uncoated a) Quartz and b) Galium phosphate crystals, between 30 and 300°C, using high temperature QCM probe.

Ceria films on high temperature crystals: QCM

Uncoated crystal $F_{21ºC}$ = 5833918 Hz

Coated crystal $F_{25ºC}$ = 5826468 Hz

$\Delta F_{25ºC} = -7450$ Hz

$\Delta m = 42\ \mu g$

vol = 5.5×10^{-6} cm^3

Thickness = 125 nm

$$\Delta f = -\left(\frac{n{f_0}^2}{A\sqrt{\rho_q \mu_q}}\right)\Delta m$$

$\rho_q = 3.570$ g.cm^{-1} n = 1

$\mu_q = 2.147 \times 10^{11}$ g.cm^{-1}s^{-2}

Coated area = 1.33 cm^2

Active area = 0.46 cm^2

$d_{CeO_2} = 7.65$ g.cm^{-3}

$nF_0^2 = 3.409\text{x } 10^{13\ Hz2}$

$(Pgxug^{0.5}) = 8.755 \times 10^{5\ gcm\text{-}1s\text{-}1}$

$Cf = 3.89 \times 10^7$

A_{Pu239} = 210 KBq

A_{Pu240} = 768 KBq

(A_{Pu241} = 350 MBq)

$A_{Pu239\text{-}240(70:30)}$ = 377 MBq

$$A = N_A \frac{M}{m_r} \cdot \frac{\ln(2)}{t_{1/2}}$$

$N_A = 6.022 \times 10^{23}$ mol^{-1}

Pu^{239} $t_{1/2}$ = 24100 yrs = 760×10^9 s

Pu^{240} $t_{1/2}$ = 6560 yrs = 207×10^9 s

Pu^{241} $t_{1/2}$ = 14.4 yrs = 0.454×10^9 s

Ceria films on $GaPO_4$ crystals: SEM and XRF

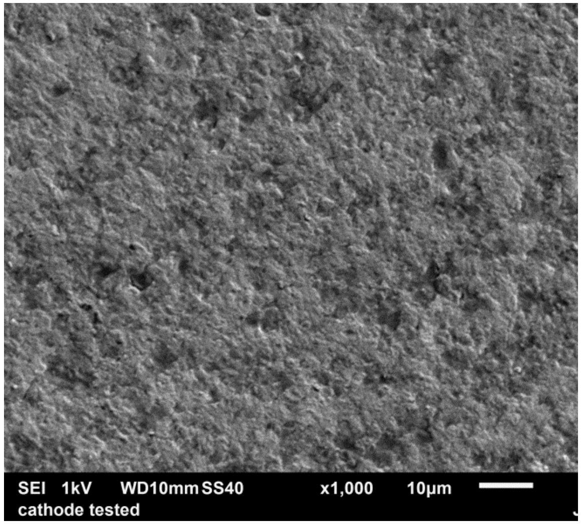

$\Delta F_{25ºC} = -7450$ Hz

$\Delta m = 33$ µg

h (QCM) = 71 nm

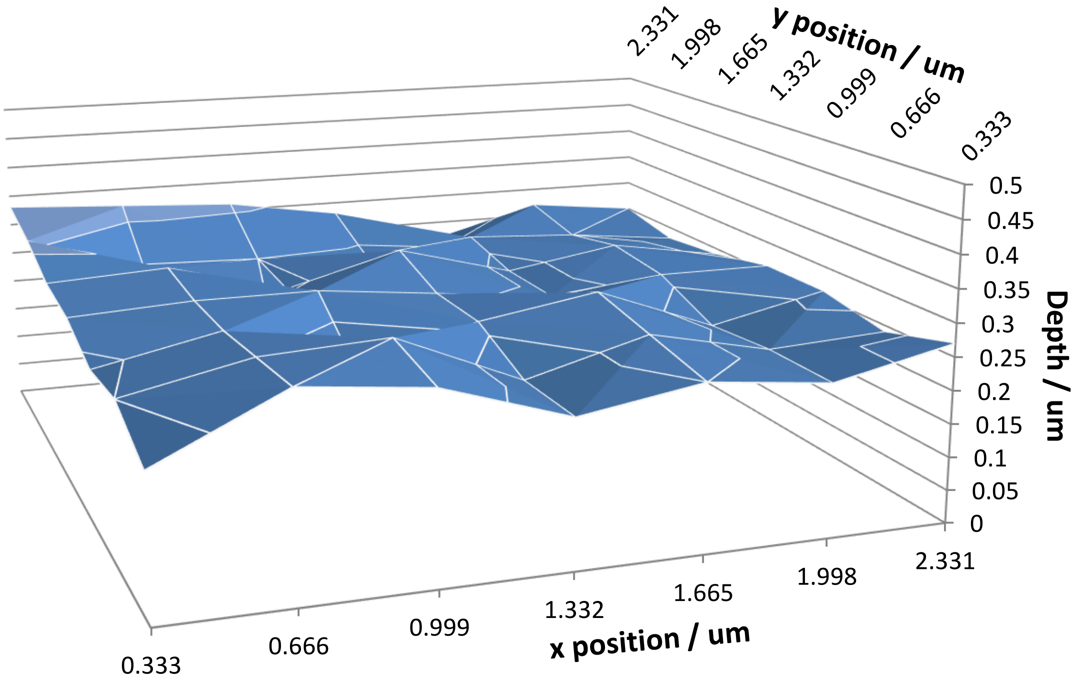

XRF map in a 7 x 7 grid (49 points) gives a average ceria thickness of 261 nm (SE = 29 nm).

This gives a piezoactive volume of 8.9×10^{-6} cm^3 and therefore a porosity of 54%.

Ceria films on $GaPO_4$ crystals: BET

The BET equation allows the volume of a monolayer and the enthalpy of absorption to be calculated:

$$1/\left[Va\left(\frac{P0}{P}-1\right)\right] = \left(\frac{C-1}{V_M C}\right)\left(\frac{P}{P_0}\right) + \frac{1}{VmC} \qquad C = e^{(\Delta H_{ads} - \Delta H_{liq} /RT)}.$$

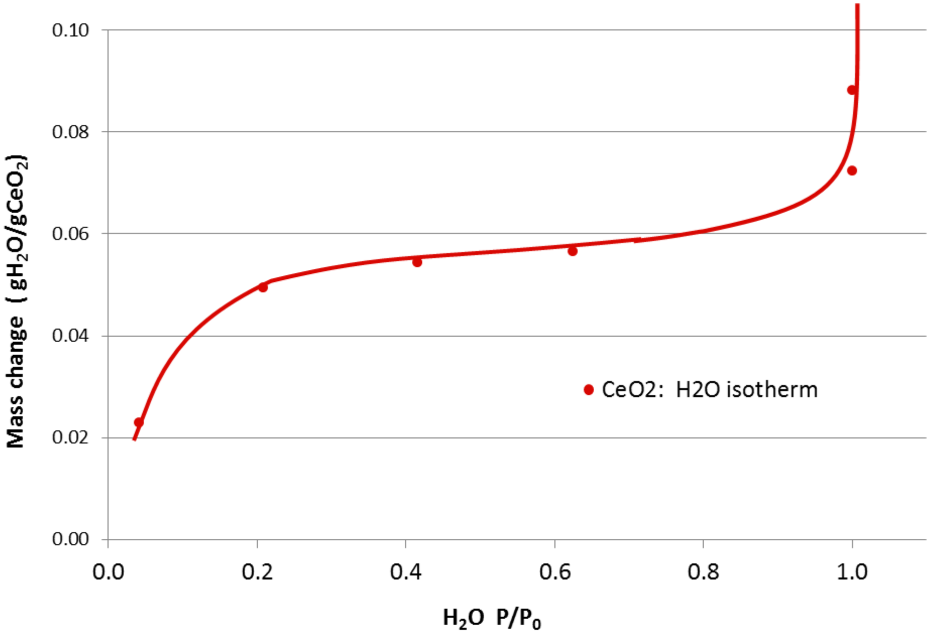

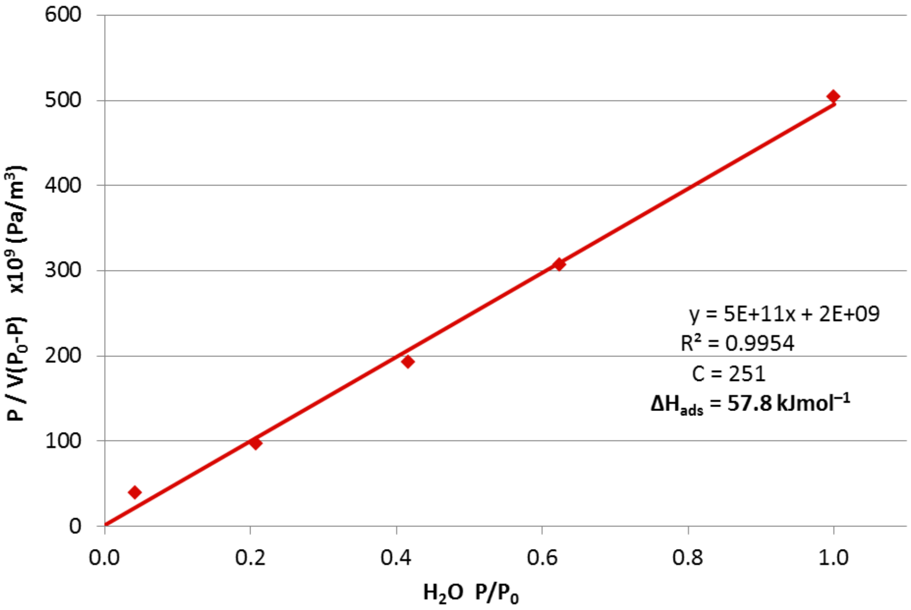

A plot of $P/V(P_0\text{-}P)$ against P/P_0 gives an intercept of 1/VmC and a gradient of $(C-1)/(V_M C)$, therefore we can calculate:

$V_m = 2.0 \times 10^{-12}\ m^3$ $\qquad$ $SA = 600\ m^2g^{-1}$

$\Delta H_{abs} = 57.8\ kJmol^{-1}$ $\qquad$ $\Delta H_{bind} = 16.1\ kJmol^{-1}$

Ceria films on $GaPO_4$ crystals: High temperature

The BET equation allows the volume of a monolayer and the enthalpy of absorption to be calculated:

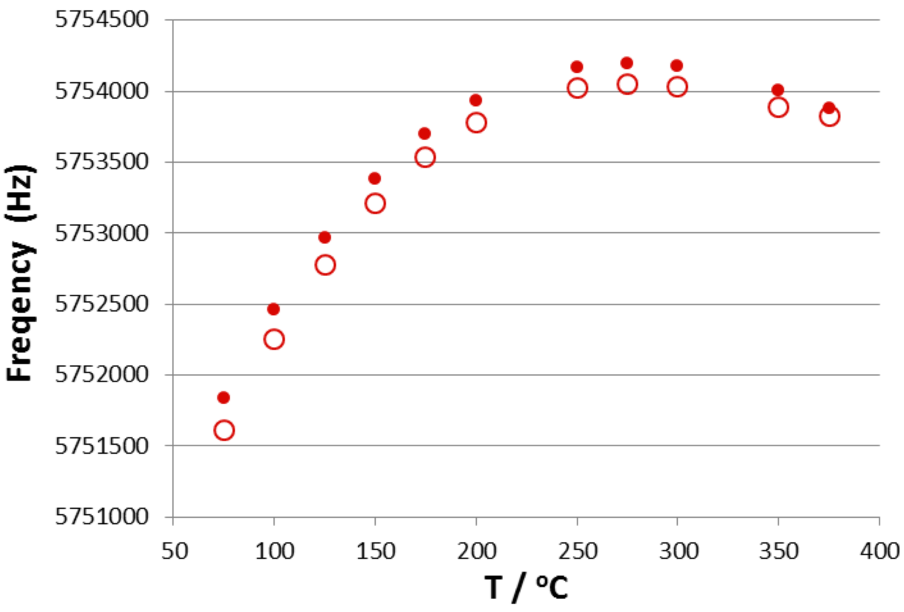

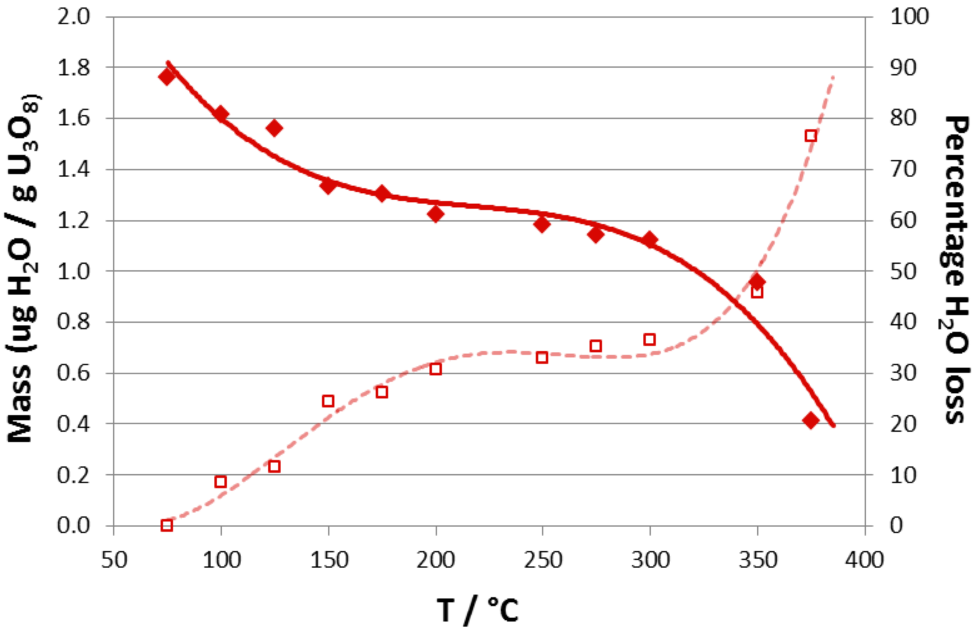

Urania films on $GaPO_4$ crystals: SEM and XRF

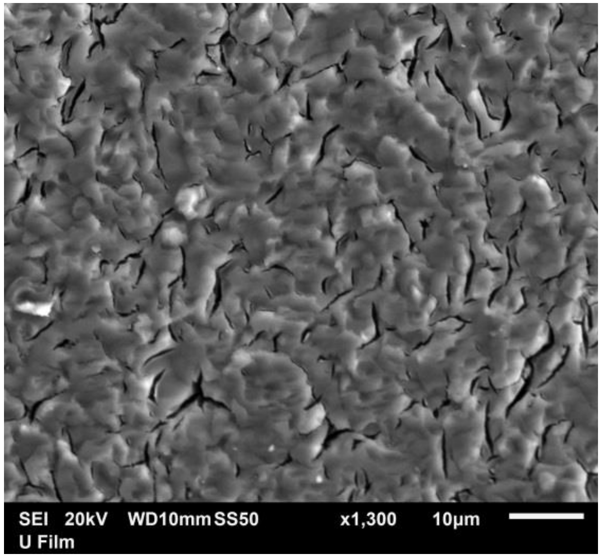

$\Delta F_{25ºC} = -2352$ Hz

$\Delta m = 18\ \mu g$

h (QCM) = 27 nm

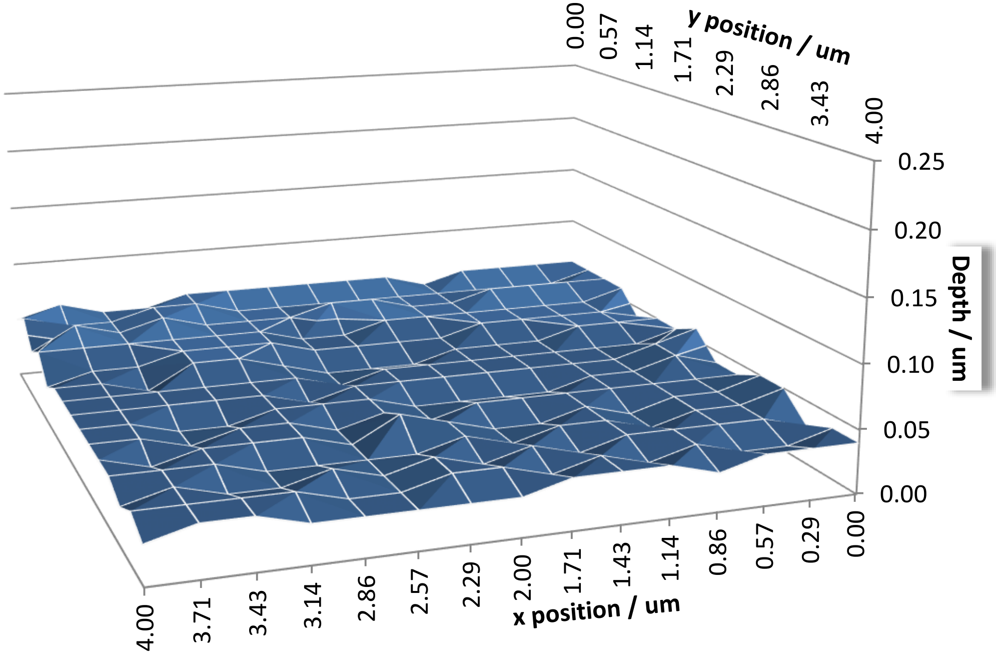

XRF map in a 15 x 15 grid (225 points) gives an average urania thickness of 42 nm (SD = 9 nm).

This gives a volume of 2.52×10^{-6} cm^3 and therefore a porosity of 35%.

Urania films on $GaPO_4$ crystals: BET

The BET equation allows the volume of a monolayer and the enthalpy of absorption to be calculated:

$$1/\left[Va\left(\frac{P0}{P}-1\right)\right] = \left(\frac{C-1}{V_M C}\right)\left(\frac{P}{P_0}\right)+\frac{1}{VmC} \qquad C = e^{(\Delta H_{ads} - \Delta H_{liq}/RT)}.$$

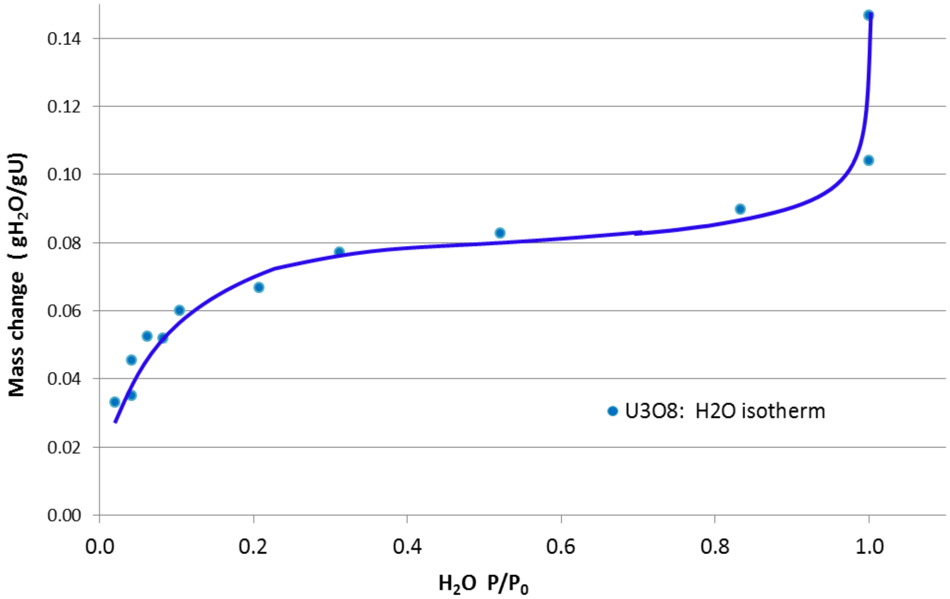

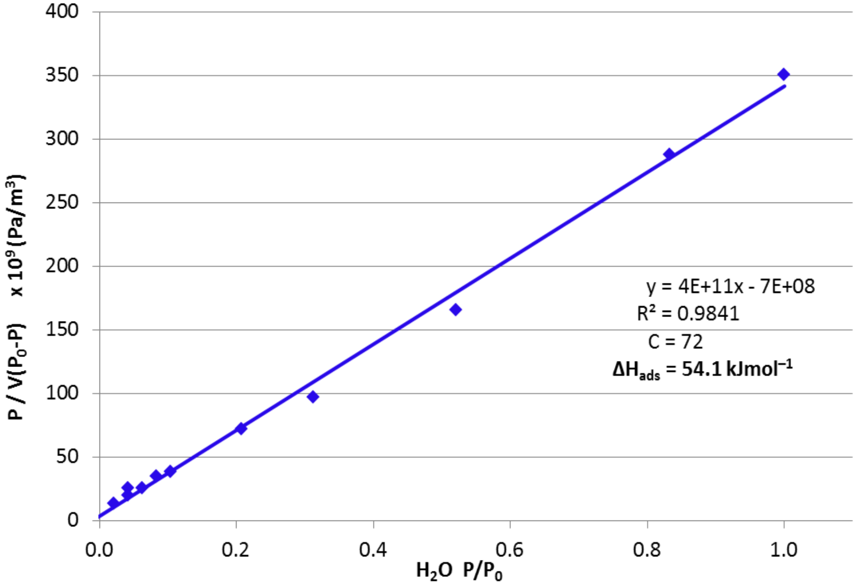

A plot of $P/V(P_0-P)$ against P/P_0 gives an intercept of 1/VmC and a gradient of $(C-1)/(V_M C)$, therefore we can calculate:

V_m = 3.0 x 10^{-12} m³ SA = 890 m^2g^{-1}

ΔH_{abs} = 54.1 $kJmol^{-1}$ ΔH_{bind} = 12.4 $kJmol^{-1}$

Urania films on $GaPO_4$ crystals: High Temperature

The BET equation allows the volume of a monolayer and the enthalpy of absorption to be calculated:

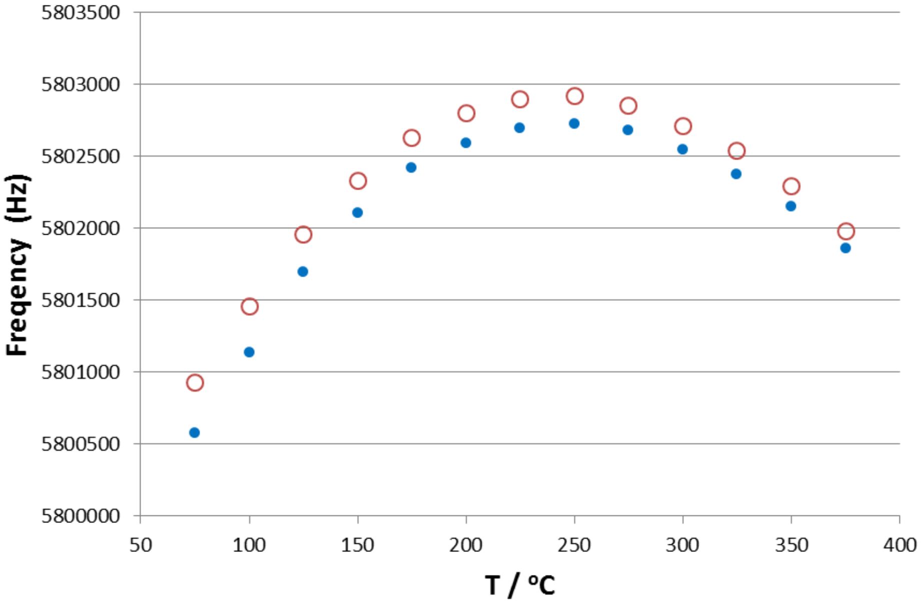

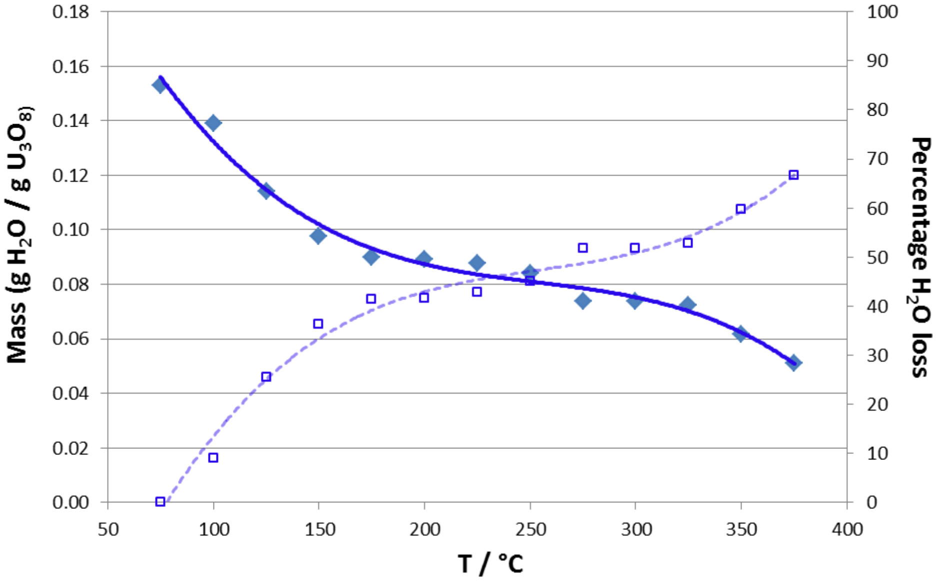

Conclusions

- Coated quartz piezocrystals with ceria and urania layers of different porosities. Analysed the morphology and thickness by SEM, AFM, XRF.

- Measured the absorption of water onto the ceria and urania films by direct mass analysis at different humidities.

- Calculated the surface area of the ceria and urania films, and the volume and number of absorbed monolayers at room temperature.

- Varied the temperature of the ceria- and urania-water systems, showing the desorprtion of water up to 375°C.

- Thoria-coated $GaPO_4$ crystals.
- Oxalate precursor.
- Increase the temperature of the systems, showing the desorprtion of water up to 500°C.

Acknowledgments

Lancaster University

- Pat Murphy
- Richard Wilbraham
- Fabrice Andrieux

NNL

- Robin Taylor
- Dave Woodhead
- Robin Orr

Thanks for your attention

Saturated vapour pressure water